The Use of Reversible Addition-Fragmentation Chain Transfer (RAFT) Polymerization, Supercritical Carbon Dioxide and New Heterocycle-Containing Monomers in Polymer Chemistry

Gerard Hawkins, M.Sc (Hons)

Thesis presented for the qualification of Ph.D degree to the National University of Ireland, Galway.

School of Chemistry,

National University of Ireland, Galway

August 2017

Supervisor: Dr. Fawaz Aldabbagh

Head of School: Professor Paul V. Murphy

TABLE OF CONTENTS

Acknowledgements

I would first like to thank my supervisor Dr. Fawaz Aldabbagh for giving me the opportunity to do this PhD and for all his guidance and advice throughout the course of my research.

I would like to thank Prof Per B. Zetterlund (CAMD, UNSW, Australia) for his input into the work related to supercritical carbon dioxide.

I would also like to thank Dr. Benjamin A. Chalmers and Abdullah Alzahrani for their contributions to the work presented in chapter 4.

I would also like to thank Dr. Pádraig O'Connor for training me in the use of the supercritical CO_2 reactor.

I would like to thank fellow members of the Aldabbagh group for their advice and support throughout the years.

Finally, I would like to thank my friends and family for their continuous support and encouragement throughout the course of my PhD.

Abstract

Chapter 1 is a general introduction with a description of conventional radical polymerization and reversible deactivation radical polymerizations for controlled/living techniques. In particular, the use of Reversible Addition Fragmentation Chain Transfer (RAFT) polymerization and benign supercritical carbon dioxide ($scCO_2$) are included.

Chapter 2 describes a new controlled/living heterogeneous polymerization in $scCO_2$. Poly(2-ethoxyethyl methacrylate) macroRAFT agent is insoluble in $scCO_2$ and forms a whitish emulsion at the polymerization conditions of 65 °C and 30 MPa. The precipitated macroRAFT agent is used in controlled/living polymerizations with *N*,*N*-dimethylacrylamide and 4-acryloylmorpholine (4AM) with induced precipitation polymerizations in $scCO_2$ compared with solution polymerizations. The faster RAFT of 4AM was taken to ≥70% conversion in $scCO_2$ to give powders that were washed with $scCO_2$ to remove traces of monomer, offering a green large scale route to the synthesis of poly(2-ethoxymethyl methacrylate)-*b*-(acrylamides) useful for potential biomedical applications. This work is published in *J. Polym. Sci., Part A: Polym Chem.* **2015**, *53*, 2351-2356.

Chapter 3 describes Polymerization Induced Self-Assembly (PISA) and examines the possibility of its use to form higher order objects in heterogeneous controlled/living radical polymerizations in $scCO_2$. After reviewing literature PISA using emulsion/dispersion polymerizations in conventional solvents, an attempt at Atom Transfer Radical Polymerization (ATRP) of benzyl methacrylate (BzMA) using a dispersion polymerization from poly(dimethylsiloxane) bromide in $scCO_2$ is described. Some non-spherical morphologies were apparent, but further work is required, including altering the size of the solvophobic poly(BzMA) block.

Chapter 4 describes the first efficient synthesis of the *N*-[(cycloalkylamino)methyl]acrylamide monomer class. The monomer synthesis involves addition of acrylamide onto *in situ* generated methylene Schiff Base salts with monomer hydrochloride salt intermediates also isolated on multi-gram scale. The macroRAFT agent of the morpholine monomer was extended with *tert*-butylacrylamide to give amphiphilic block copolymers that self-assembled into large rod-like vesicles. For the triblock of similar hydrophobic monomer content, but incorporating the piperidine monomer, a very different aggregation was observed with pH-expandable nanoparticle spheres observed. Part of this chapter is published in *J. Polym. Sci., Part A: Polym Chem.* **2017**, *55*, 2123-2128.

Abbreviations

AA	acrylic acid
4AM	4-acryoylmorpholine
ACP	allyl 2-chloropropionate
AIBN	2,2’-azobisisobutyronitrile
α	fractional monomer conversion
ARGET	Activator Regenerated Electron Transfer
ATRP	atom transfer radical polymerization
b	block
BIS	*N,N’*-methylenebisacrylamide
b.p	boiling point
bpy	2’2’-bypyridine
BMA	butyl methacrylate
BzMA	benzyl methacrylate
CLRP	controlled/living radical polymerization
Conv.	conversion
DDMAT	2-(dodecylthiocarbonothioylthio)-2-methylpropionic acid
DLS	dynamic light scattering
DMA	*N*,*N*-dimethylacrylamide
DMAEMA	2-(dimethylamino)ethyl methacrylate
DMF	*N*,*N*-dimethylformamide
dNdpy	4,4’-dinonyl-2,2’-dipyridyl
DP	degree of polymerization
Et	ethyl
f	initiator efficiency
g	gram
GMA	glycerol monomethacrylate
GPC	gel permeation chromatography
h	hour
HEL	homogeneous expansion limit

HEMA	2-hydroxyethyl methacrylate
HMPA	2-hydroxypropyl methacrylate
HMTETA	1,1,4,7,10,10-hexamethyltriethylenetetramine
HPLC	high performance liquid chromatography
Hz	hertz
[I]	initiator concentration
$I^{\bullet}$	initiating radical
ICAR	initiator for continuous activator regeneration
inistab	macroinitiator and stabilizer combined
ITP	iodine transfer polymerization
J_{crit}	number average degree of polymerization at which precipitation occurs
K	equilibrium constant
k_{act}	rate coefficient for activation
k_{deact}	rate coefficient for deactivation
k_p	rate coefficient for propagation
k_t	rate coefficient for termination
L	litre
LCST	lower critical solution temperature
[M]	monomer concentration
MAA	methacrylic acid
MADIX	Macromolecular design via the interchange of xanthates
Me	methyl
Me_6CyClam	5,5,7,12,12,14-hexamethyl-1,4,8,11-tetraazacyclotetradecane
mg	milligram
µm	micrometer
MMA	methyl methacrylate
mmol	millimole
M_n	number average molecular weight
M_n(GPC)	number average molecular weight calculated by GPC
$M_{n,th}$	theoretical number average molecular weight
mol	mole

MPa	megapascal
MPC	2-(methacryloyloxy)ethyl phosphorylcholine
M_t^n	transition metal
MW	molecular weight
M_w	weight average molecular weight
MWD	molecular weight distribution
M_w/M_n	polydispersity
*n*BA	*n*-butyl acrylate
NIPAM	*N*-isopropylacrylamide
nm	nanometer
NMP	nitroxide mediated polymerization
NMR	nuclear magnetic resonance
$P^\bullet$	propagating radical
PDMS	poly(dimethylsiloxane)
PEG	poly(ethylene glycol)
PEO	poly(ethylene oxide)
PGMA	poly(glycerol monomethacrylate)
Ph	phenyl
PISA	polymerization induced self assembly
PLP	pulsed laser polymerization
POEOMA	poly(oligo(ethylene oxide) methyl ether methacrylate
ppm	parts per million
PS	poly(styrene)
P-T	polymeric alkoxyamine
$R^\bullet$	radical
RAFT	reversible addition fragmentation chain transfer
RDRP	reversible deactivation radical polymerization
R_p	rate of polymerization
rpm	revolutions per minute
R_{pr}	rate of radical production
RTCP	reversible chain transfer catalyzed polymerization

R-X	alkyl halide
s	second
$scCO_2$	supercritical carbon dioxide
SEM	scanning electron microscopy
SG1	*N*-*tert*-butyl-*N*- [1-diethylphosphono-(2,2-dimethylpropyl)] nitroxide
SNH	saturated nitrogen heterocycle
t	time
$T^{\bullet}$	nitroxide trap
TBAM	*N*-*tert*-butylacrylamide
TEM	transmission electron microscopy
TEMPO	2,2,6,6-tetramethylpiperidine-1-oxyl
T_g	glass transition temperature
THF	tetrahydrofuran
TIPNO	2,2,5-trimethyl-4-phenyl-3-azahexane-3-aminoxyl
VA-044	2,2′-azobis[2-(2-imidazolin-2-yl)propane]dihydrochloride
4VP	4-vinylpyridine
wt%	weight percent
w/w	weight per weight

Appendix of ATRP Ligands

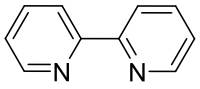

2'2'-Bypyridine
(bpy)

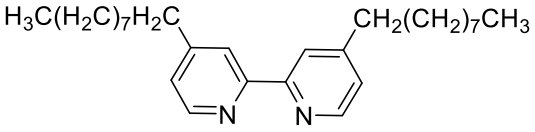

4,4'-Dinonyl-2,2'-dipyridyl
(dNdpy)

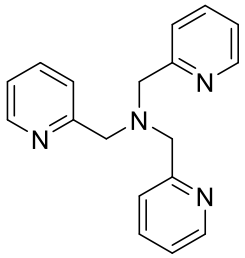

Tris(pyridin-2-yl methyl)-amine
(TPMA)

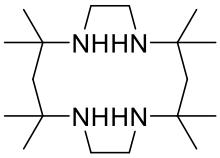

5,5,7,12,12,14-Hexamethyl-1,4,8,11-tetraazacyclotetradecane
(Me_6CyClam)

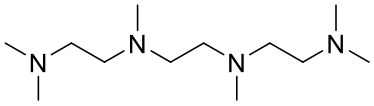

1,1,4,7,10,10-Hexamethyltriethyltetramine
(HMTETA)

CHAPTER 1

GENERAL INTRODUCTION

1.1 Significance of Radical Polymerization

Radical polymerization is the most widely used polymerization by academia and industry.[1] It has fundamental advantages over ionic polymerizations, including being applicable to nearly all vinyl monomers, and requiring relatively undemanding conditions. In comparison, anionic polymerization requires scrupulous purification of reagents, inert atmospheres, low temperatures, and in the case of vinyl monomers the presence of electron-withdrawing substituents (e.g. as in vinylpyridine and alkyl methacrylates).[2] In the 1950s, Szwarc carried out the first living (free of termination) polymerizations of styrene,[3-4] but this anionic polymerization is now rarely used, and is superseded by the more robust and versatile radical polymerization alternatives. Cationic polymerization is applicable to only electron-rich monomers (e.g. isobutene, vinyl ether, *N*-vinylcarbazole), however disadvantages include the need for rigorous purification of reagents and side reactions such as β-proton elimination.[5] Styrene is one of the few vinyl monomers that can be polymerized by all three addition polymerization techniques.[6]

Radical polymerization can be carried out in a variety of reaction media, most importantly in water. As such, radical polymerizations can be performed in bulk, emulsion, solution, precipitation, dispersion, and suspension. Therefore it is not surprising that it accounts for the production of approximately 50% of all commercial polymers.[7]

1.2 Conventional Radical Polymerization

Conventional radical polymerization proceeds *via* a chain reaction mechanism whereby monomer sequentially adds onto a propagating radical chain to generate high molecular weight polymer. The conventional radical polymerization mechanism consists of initiation, propagation, chain transfer and termination steps (Scheme 1.1). Initiation is a two-step process in which the initiator first decomposes thermally to yield two initiating radicals ($I^{\bullet}$) with the decomposition of the initiator having a rate constant k_d. The rate of radical production R_{pr} is expressed by the equation 1.1,

$$R_{pr} = 2fk_d[I] \qquad (1.1)$$

where [I] is the initiator concentration, the factor of 2 accounts for the decomposition of the initiator molecule into two initiating radicals, and *f* is the initiator efficiency which is less than 1 due to side reactions of the initiator derived radicals.[8]

The second step involves addition of these initiating radicals onto monomer, producing a propagating radical ($P^{\bullet}$). Propagation involves the successive addition of monomer units onto the propagating radical species, producing growing radical chains. The rate of polymerization is given by equation 1.2, it varies from monomer to monomer depending on the relative stability of the adduct radical. Table 1.1 shows the propagation rate coefficients (k_ps) of various monomers. The size of k_p is governed by the nature of the monomer and the reactivity of the propagating radical. Styrene has a relatively low k_p (thus polymerizes relatively slowly) since the styryl radical is resonance stabilized by the phenyl group.

$$R_p = \frac{-\mathrm{d}\,[M]}{\mathrm{d}t} = k_p[P^{\bullet}][M] \qquad (1.2)$$

where k_p is the rate coefficient for propagation, $[P^{\bullet}]$ is the propagating radical concentration and [M] is the monomer concentration.

Monomer	k_p (L mol^{-1} s^{-1})	Temperature (°C)
Styrene	341 [9]	60
tert-Butyl acrylate	22300 [10]	40
Methyl methacrylate	812 [11]	60
N,*N*-dimethylacrylamide	29198 [12]	30
Vinyl acetate	9500-19000 [12]	60

Table 1.1: Propagation rate constants of selected monomers

Pulsed laser polymerization (PLP) is used to measure k_p in conjunction with GPC analysis.[1]It is the most accurate method used for determining k_p independently of other kinetic coefficients, including those for termination. PLP determines the value for k_p through initiation of polymerization from a photo-initiator illuminated by a pulsed laser.

Chain transfer involves the radical chain reacting with a non-radical species to produce a dead polymer chain and a new radical ($Y^{\bullet}$), which adds onto monomer to initiate a new propagating radical chain. Chain transfer to small species such as monomer[13] and solvent[14] can lead to low molecular weight tailing in GPC traces. Chain transfer to solvent is minimized by using solvents without hydrogen atoms that can be abstracted or by carrying out polymerizations at lower temperatures.

Termination occurs when two propagating radical chains react to produce a dead polymer chain. It can either occur by combination in which two propagating radical chains combine to form a dead polymer chain, or by disproportionation, in which hydrogen is transferred from one radical chain to another, producing a saturated and unsaturated chain.

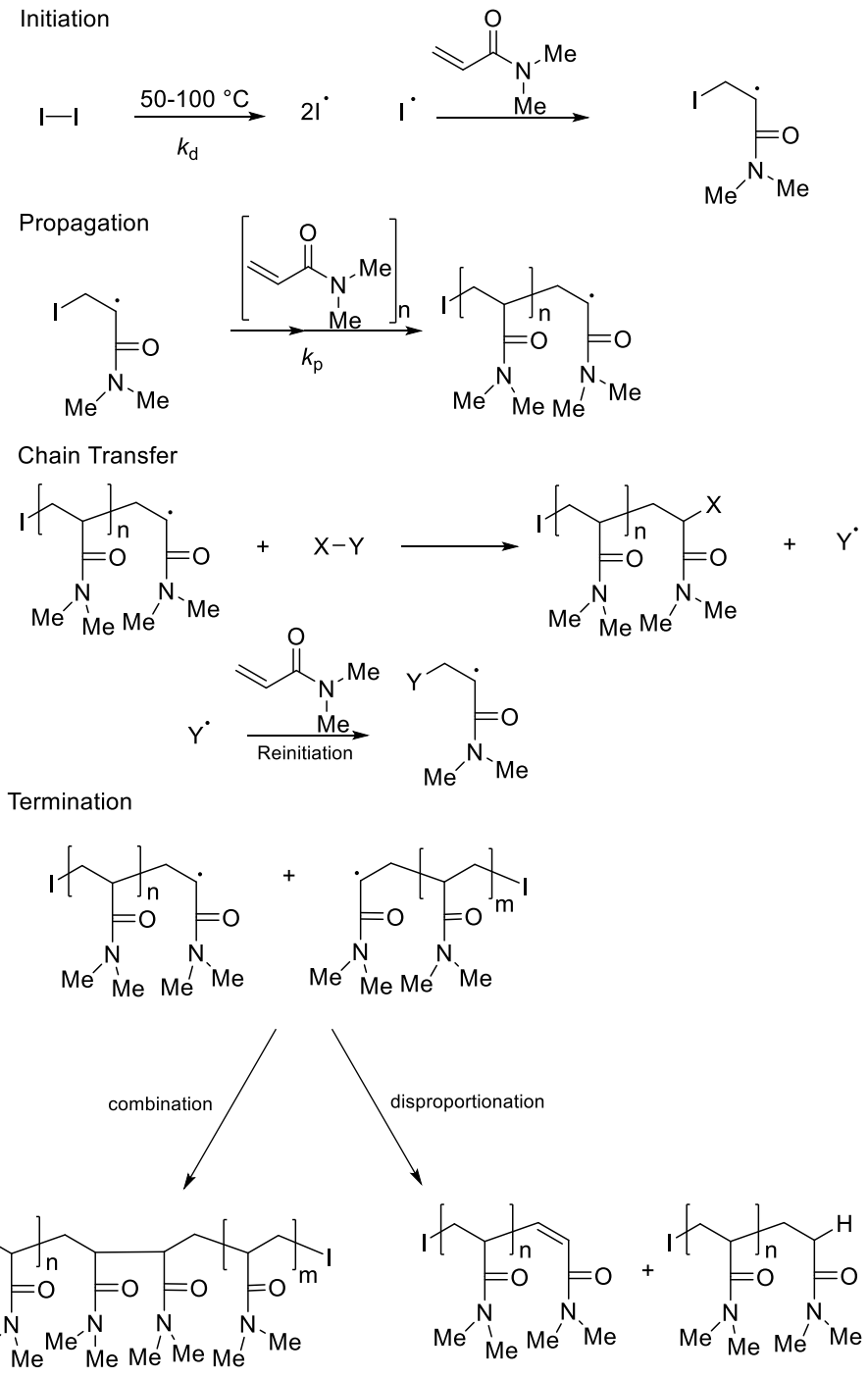

Scheme 1.1: Conventional radical polymerization of *N*,*N*-dimethylacrylamide (DMA)

1.3 Reversible Deactivation Radical Polymerization (RDRP)

1.3.1 Introduction

Nitroxide Mediated Polymerization (NMP) was the first established controlled/living radical polymerization technique with work by Solomon in 1985,[15] and then Georges in 1993.[16] In 1995 Matyjaszewski and Sawamoto used CuCl/bpy and $RuCl_2(PPh_3)_3$ complexes, respectively, to control polymerizations in the first uses of Atom Transfer Radical Polymerization (ATRP).[17-18] The CSIRO in 1998 introduced Reversible Addition-Fragmentation chain Transfer (RAFT) polymerization,[19] with similar work being carried out independently by Zard on Macromolecular Design *via* Interchange of Xanthate (MADIX), which follows the same mechanism as RAFT.[20]

The significance of reversible deactivation radical polymerization is that it allows for the creation of polymers with molecular weights which are a function of conversion, and narrow molecular weight distributions. Polymers retain end-group functionality allowing chain extension, so enabling block copolymer synthesis that is not possible with conventional radical polymerization.

NMP and ATRP are based on reversible dissociation-combination, while RAFT (MADIX) is a type of degenerative chain transfer process. Degenerative chain transfer is defined as the generation of a new chain carrier and a new chain transfer agent with the same reactivity as the original chain carrier and chain transfer agent.[21] For narrow polydispersities to be achieved the transfer of the end group (agent) has to be rapid (see section 1.3.4).

1.3.2 Nitroxide Mediated Polymerization (NMP)

NMP involves the reversible trapping reaction between the propagating radical ($P^{\bullet}$) and the mediating nitroxide radical ($T^{\bullet}$) to extend the lifetime of the propagating species by minimizing the likelihood of two $P^{\bullet}$ reacting together (terminating). (Scheme 1.2)

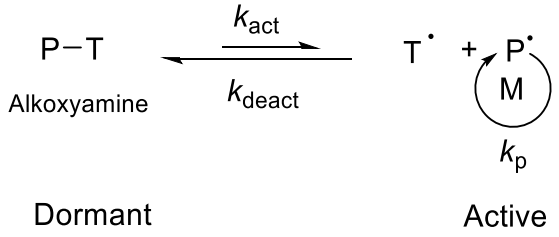

Scheme 1.2: Reversible activation/deactivation equilibrium reaction in NMP

The nitroxide is a bench-stable free radical (Figure 1.1). At suitably high temperatures the P-T bond is dissociated back into a propagating radical $P_n^{\bullet}$ and the stable nitroxide radical $T^{\bullet}$ with a rate coefficient for activation (k_{act}).

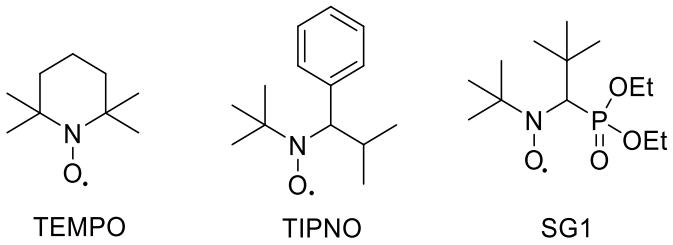

Figure 1.1: 2,2,6,6-Tetramethylpiperidine-1-oxyl (TEMPO), 2,2,5-trimethyl-4-phenyl-3-azahexane-3-aminoxyl (TIPNO) and *N*-*tert*-butyl-*N*- [1-diethylphosphono-(2,2-dimethylpropyl)] nitroxide (SG1)

In the active state the polymeric radical can propagate by addition of monomer until it is deactivated again by combining with the nitroxide radical with a rate coefficient for deactivation (k_{deact}). The equilibrium between active and dormant polymer chains favours the dormant state as the coefficient for deactivation k_{deact} is several orders greater than that of k_{act}. The equilibrium

constant *K* defines the relationship between k_{act} and k_{deact} (equation 1.3). A low population of active propagating chains is maintained throughout the polymerization.

$$K = \frac{k_{act}}{k_{deact}} = \frac{[P^{\bullet}][T^{\bullet}]}{[P{-}T]_0} \quad (1.3)$$

TEMPO was the first nitroxide used to carry out NMP on styrene by Georges in 1993.[16] High temperatures of up to 145 °C and long polymerization times of up to 72 h were needed to achieve a high conversion of over 85%. TEMPO's ability to control polymerizations is limited to styrene and styrene derivatives.[22] TEMPO is unable to control the polymerization of other vinyl monomers due to the relatively strong C-O bond in the alkoxyamine formed.

Acyclic nitroxides such as TIPNO and SG1 (Figure 1.1) have been used to control the polymerization of a wide variety of monomers such as styrene[23], acrylamides [14, 23-25], acrylates,[23] acrylic acid[26] and acrylonitrile[23]. TIPNO and SG1 are more sterically hindered than TEMPO, which leads to a weaker C-O bond, resulting in a higher activation coefficient than TEMPO. Methacrylates are difficult to control with NMP because of disproportionation between the propagating radical and the nitroxide. McHale attempted the NMP of MMA by adding a large excess of SG1, however control was not improved due to the abstraction of the α-methyl hydrogen of the propagating PMMA radical by SG1 with increased SG1 concentration.[27] MMA can be controlled in NMP by the addition of a co-monomer like styrene[28] or acrylonitrile[29]. The co-monomer has a lower activation-deactivation equilibrium constant, *K*, which reduces the average *K* of the system, leading to a higher degree of living chains capped with nitroxide in the system.

1.3.3 Atom Transfer Radical Polymerization (ATRP)

ATRP is a transition metal-catalyzed polymerization. ATRP involves a reversible dissociation mechanism (Scheme 1.3), in which an alkyl halide is employed as an initiator with a transition metal complexed with a ligand as catalyst. The alkyl halide undergoes a reversible redox process catalyzed by the transition metal complex and facilitates abstraction of the halogen from the alkyl halide, which is reduced. One-electron reduction cleaves the R-X or P-X bond forming the carbon-centered radical $R^{\bullet}$ or $P^{\bullet}$. The $R^{\bullet}$ reacts with monomer to form a propagating radical $P_n^{\bullet}$.

$P_n^{\bullet}$ will propagate further until it is reversibly deactivated by the oxidized X-Mt^{n+1}/L into P_n-X. Alternatively it can undergo a termination reaction with another $P_n^{\bullet}$.

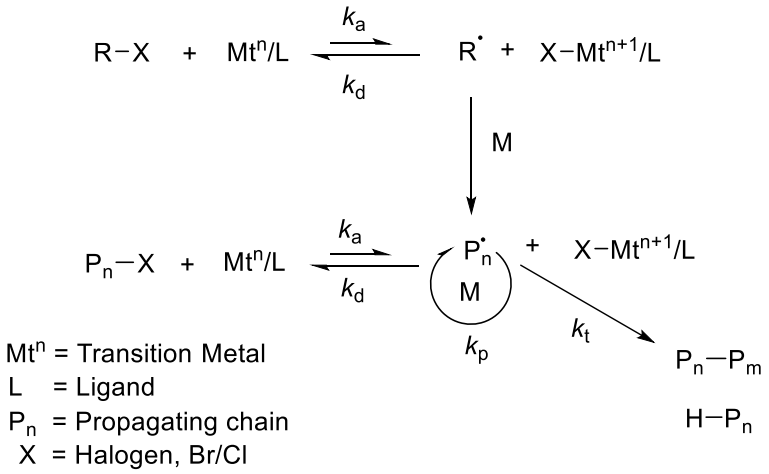

Scheme 1.3: ATRP general mechanism

The theoretical molecular weight, $M_{n,th}$, is determined by the alkyl halide initiator concentration relative to the monomer as shown in equation 1.5,

$$M_{\mathrm{n,th}} = \frac{\alpha[\mathrm{M}]_0\,\mathrm{MW_{mon}}}{[\text{Alkyl halide}]_0} + \mathrm{MW_{Alkyl\ halide}} \qquad (1.5)$$

where α is the fractional monomer conversion, $[M]_0$ is the initial monomer concentration, MW_{mon} is the molecular weight of the monomer, $[\text{Alkyl halide}]_0$ is the initial concentration of the alkyl halide initiator.

Transition metals used in ATRP include Ti(III), Mo(III)/(IV)/(V), Re(V), Fe(II), Ru(II), Os(II)/(III), Rh(I), Co(II), Ni(I)/(II), Pd(II) and Cu(I)/(II).[7] Complexes of copper (such as CuCl/dNdpy) have been found to be the most efficient catalysts for a wide range of monomers. Monomers used with ATRP include styrenes, acrylates, methacrylates, acrylamides, methacrylamides, dienes, and acrylonitrile. Controlled/living polymerization of acrylic and methacrylic acids proved difficult due to coordination of the carboxylate group with the metal and reaction with the basic ligand.[30] Recently the ATRP of vinyl acetate has been performed by

Mazzotti and co-workers using CuCl, $CuCl_2$ and the ligand Me_6CyClam as catalytic system and allyl 2-chloropropionate (ACP) as initiator (Scheme 1.4).[31] Control was achieved with M_n values being close to their theoretical values and polydispersities under 1.3 up to 90% conversion. PVAc was chain extended with butyl methacrylate (BMA), MMA and 2-hydroxyethyl methacrylate (HEMA) in order to confirm the living character of PVAc. Moderate to high conversions were achieved with polydispersities under 1.4 observed. Co-catalyst system with $CuCl_2$ was used to deactivate growing chains faster and produce polymers with narrower polydispersities.

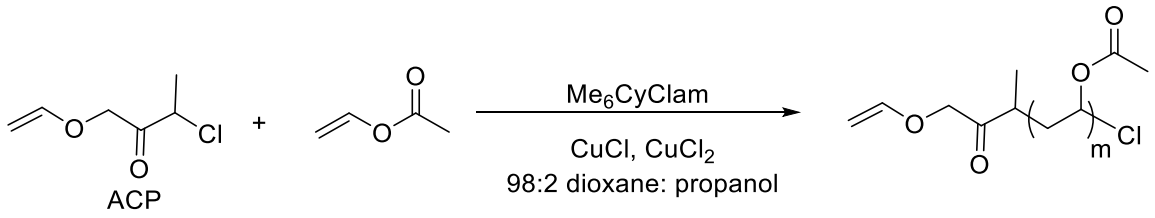

Scheme 1.4: ATRP of vinyl acetate

Radical initiators (e.g. AIBN) have also been used in ATRP alongside transition metal complexes in a high oxidation state in what has been termed reverse ATRP (Scheme 1.5).[30]

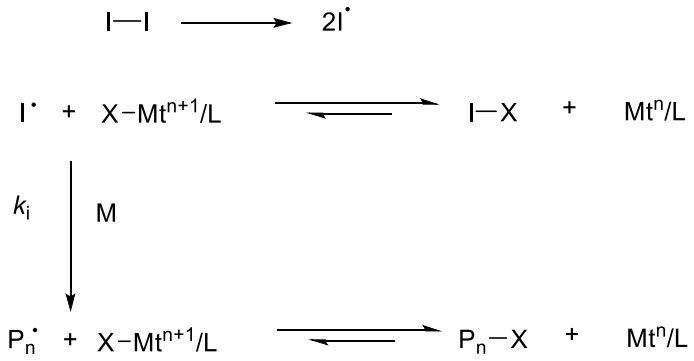

Scheme 1.5: Initiation step for reverse ATRP with a radical initiator

1.3.4 Reversible Addition-Fragmentation Chain Transfer (RAFT)

MADIX follows the same mechanism as RAFT with the only difference it uses xanthates as chain transfer agents (consequences described below). RAFT is one of the most versatile methods for controlling radical polymerization. Unlike NMP or ATRP, the RAFT process follows a degenerative transfer mechanism. Control is achieved through the addition of a suitable thiocarbonylthio compound to a conventional radical polymerization. Ideally, with the selection of a suitable chain transfer agent, the kinetics will be comparable to the equivalent conventional polymerization. Scheme 1.6 shows the mechanism for the RAFT polymerization.

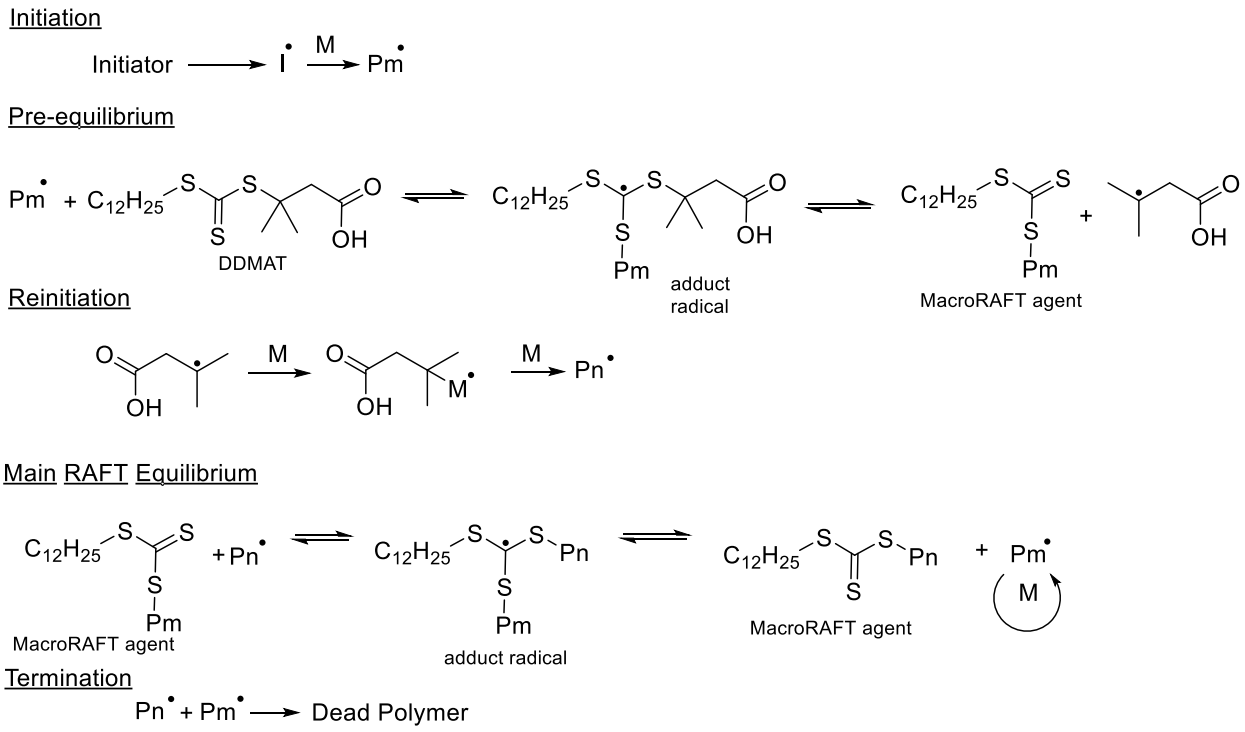

Scheme 1.6: RAFT using 2-(dodecylthiocarbonothioylthio)-2-methylpropionic acid (DDMAT)

After conventional initiation the propagating radical $P_m^{\bullet}$ reversibly adds onto the RAFT agent followed by fragmentation of the intermediate radical, forming a polymeric macroRAFT agent and a radical leaving group. For block copolymerizations, the order of polymerization is important. The monomer with the highest rate of transfer towards the RAFT agent must be

polymerized first to completion to enable fragmentation of the first block when chain extending with a monomer with a lower transfer rate e.g. when making a block copolymer of styrene and MMA, MMA must be polymerized first,[32] and when polymerizing acrylonitrile with *n*-butyl acrylate, acrylonitrile is polymerized first.[33] Re-initiation occurs when the radical leaving group adds onto monomer, initiating a new propagating radical chain ($P_n^{\bullet}$) which then adds onto the macroRAFT agent. Rapid equilibrium is achieved between the active propagating radicals and the macroRAFT agent through the RAFT intermediate radical ensuring that all the chains have an equal probability of growing. It is advantageous to use small amounts of initiator and short polymerization times, since bimolecular termination directly corresponds to the number of radicals generated from the decomposition of the initiator during the polymerization.[34] Termination leads to an unwanted broadening in MWDs, but does not lead to a loss of "living" chains, since the number of living chains (substituted by the trithiocarbonate end group) remains constant throughout the polymerization. Ideally, superior controlling character and efficient block copolymer synthesis is achieved when the vast majority of chains originate from the RAFT agent rather than the initiator.

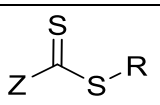	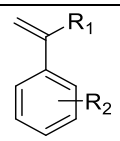 styrenes	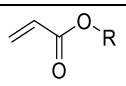 acrylates	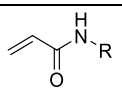 acrylamides	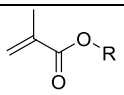 methacrylates	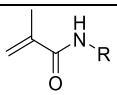 methacrylamides	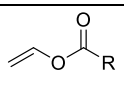 vinyl esters	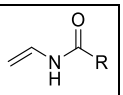 vinyl amides
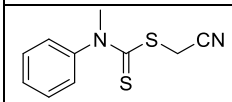	-	-	-	-	-	+++	+++
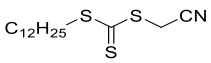	+++	+++	+++	-	-	-	-
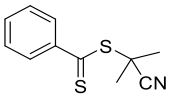	++	+	-	+++	+++	-	-
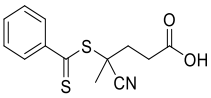	++	+	+	+++	+++	-	-
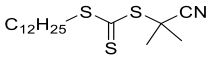	+++	++	++	+++	+++	-	-
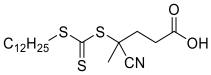	+++	++	++	+++	+++	-	-
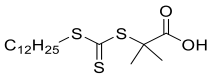	+++	+++	+++	+	+	-	-

Table 1.2: RAFT agent compatibility table[35]

Table 1.2 shows the compatibility between RAFT agents and various monomer classes. The Z and R groups are important in the compatibility of the RAFT agent with the monomer. The R group must make a better radical leaving group than the incoming propagating radical and initiate a new propagating radical chain as most chains should originate from the RAFT agent. The Z group activates or deactivates the thiocarbonyl double bond and affects the stability of the intermediate radical.[36] The rate of addition of the propagating radical onto the RAFT agent is increased when Z = Ph or S(R') allowing stabilization of the adduct radical (Scheme 1.6). A more stable adduct radical makes the RAFT agent more suitable for monomers such as styrenes, acrylates, methacrylates, acrylamides and methacrylamides, which are more activated monomers (MAMs). The rate of addition of the propagating radical onto the RAFT agent is decreased when Z = OR', or NR' making the RAFT agent suitable for RAFT polymerizations of more reactive monomers such as vinyl esters and vinyl amides, which are less activated monomers (LAMs). Resonance structures of xanthates and dicarbamates explain the lowered activity of the

thiocarbonyl double bond through delocalization of the lone pairs on O and N (Scheme 1.7). This lowers the rate of addition onto the sulfur atom, which forms an unstabilized tertiary radical intermediate leading to rates of fragmentation, which compete with higher monomer k_p. Xanthates have been used with vinyl acetate, achieving excellent control with low polydispersities and high conversions,[37] as well as other monomers such as *N*-vinylcaprolactam,[38] *N*-vinyl pyrrolidone and *N*-vinyl carbazole.[39]

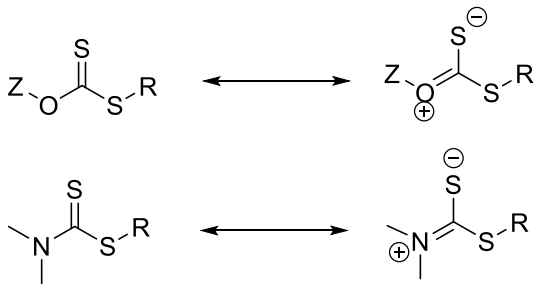

Scheme 1.7: Resonance structures of xanthate and dicarbamate

1.4 Supercritical Carbon Dioxide ($scCO_2$)

A supercritical fluid is defined as a substance at a temperature and pressure above its critical point where distinct liquid and gas phases do not exist. It has a gas-like diffusivity and liquid-like density and can dissolve materials like a liquid. Carbon dioxide has a critical point of 31.1 °C and 7.38 MPa (Figure 1.2),[40] which is less extreme than other supercritical fluids such as water (374.2 °C and 22.05 MPa).[41] Applications for $scCO_2$ include the decaffeination of coffee and its use in the dry-cleaning industry. CO_2 is an inert linear molecule with zero dipole-moment. Under supercritical conditions it becomes slightly non-linear with a weak dipole. This allows $scCO_2$ to dissolve a large number of organic molecules. The density and dissolving power of $scCO_2$ can be tuned by small changes in temperature and pressure.[42] CO_2 is an inert, non-toxic, non-flammable, inexpensive, commercially available and recyclable gas. It also cannot undergo chain transfer reactions and is inert to radical reactions, making it suitable for radical initiated polymerizations.

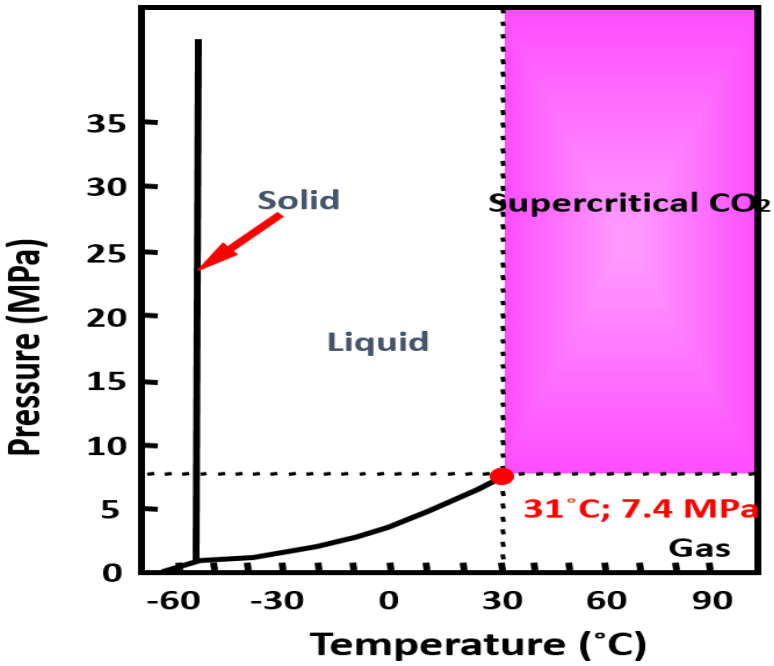

Figure 1.2: Phase diagram for carbon dioxide[43]

Many types of heterogeneous polymerization can be carried out in $scCO_2$ such as precipitation, solution, (mini)emulsion and suspension. The only solution (homogeneous) polymerizations possible are involve fluoropolymers and siloxanes, which are completely soluble in $scCO_2$ throughout the polymerization. DeSimone and co-workers carried out the first homogenous radical polymerizations in $scCO_2$, with polytetrafluoroethylene (PTFE), also known as Teflon™, being commercially produced in $scCO_2$.[44-45]

1.5 Overall Aims & Objectives

Upon starting this PhD, the focus was controlled/living heterogeneous polymerizations in $scCO_2$ with NMP being the most commonly used.[43] Aldabbagh *et al.* had reported NMP precipitation and dispersion polymerizations,[42, 46-52] as well as controlled/living inverse suspension polymerization of *N*-isopropylacrylamide (NIPAM).[53] Thus, the PhD set out to invent new controlled/living heterogeneous polymerizations in $scCO_2$, which would be environmentally friendly and industrially applicable. This led to the discovery of new heterogeneous systems using RAFT with all previous work with this degenerative chain transfer process being precipitation/dispersion polymerizations.[54-58] The work with $scCO_2$ was extended to Polymerization Induced Self Assembly (PISA), which led to the preparation of high-order morphologies in $scCO_2$ for the first time.

The Aldabbagh group has had a long interest in stimuli-responsive polyacrylamides, in particular well-defined thermoresponsive poly(NIPAM)s.[24, 52, 59] The aim of this work was to discover alternative stimuli-responsive polyacrylamides to allow the synthesis of new heterocycle-containing monomers. These acrylamides were incorporated into pH-responsive amphiphilic block copolymers using RAFT polymerizations.

CHAPTER 2

RAFT POLYMERIZATION IN SUPERCRITICAL CARBON DIOXIDE BASED ON AN INDUCED PRECIPITATION APPROACH: SYNTHESIS OF 2-ETHOXYETHYL METHACRYLATE/ACRYLAMIDE BLOCK COPOLYMERS

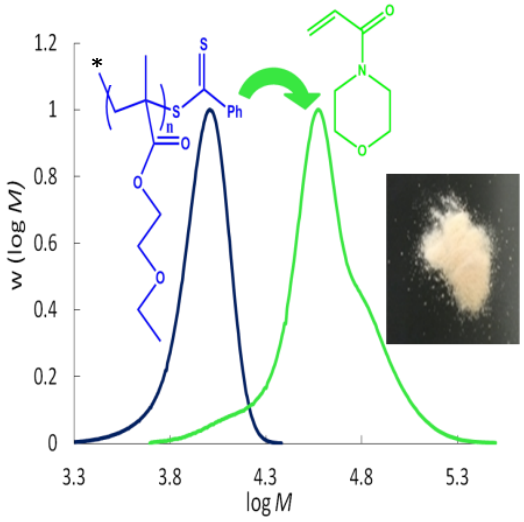

2.1 Introduction

Over the past decade, heterogeneous controlled/living radical polymerizations in benign supercritical carbon dioxide ($scCO_2$) have become commonplace, and have been the subject of recent reviews.[43, 60-61] Nitroxide-mediated polymerization (NMP),[42-43, 52-53, 60, 62] atom transfer radical polymerization (ATRP), [43, 60, 63-64] reversible addition-fragmentation chain transfer (RAFT),[43, 60, 65-67] and iodine transfer polymerization (ITP)[68-69] have all been reported in $scCO_2$. Most of these systems are classified as precipitation or dispersion polymerizations, where the monomer was initially soluble in the reaction medium, but the resultant polymer precipitates at a critical degree of polymerization (J_{crit}).[42] The polymerization then proceeded to high conversion in a controlled/living manner in the particle phase. An exception is the NMP of *N*-isopropylacrylamide (NIPAM), which proceeded in a controlled/living manner to high conversion as an inverse suspension polymerization.[52-53] Howdle and co-workers have reported many different controlled/living dispersion RAFT polymerizations giving well-defined microparticles with high blocking efficiency achieved.[43, 60, 65, 67]

In this chapter, a new controlled/living heterogeneous system based on induced precipitation of a macroRAFT agent occurring prior to polymerization on pressurization with CO_2, to form seed particles that are swollen with monomer is described.[70] The use of CO_2 to induce particle formation in heterogeneous polymerization systems has previously been reported for conventional (non-living) radical polymerization under non-supercritical conditions. Zetterlund and co-workers have shown that polymer nanoparticles can be made by exploiting the anti-solvent effect of gaseous CO_2 to induce an emulsion in a polymer solution at a point known as the homogenous expansion limit (HEL).[71]A polymeric macroazoinitiator was dissolved in a solvent and monomer. CO_2 was added to create a two-phase system with a dispersed phase with droplets containing polymer and monomer, and a CO_2-rich continuous phase containing monomer and solvent. The droplets in the dispersed phase acted as mini-reactors for polymerization and the formation of nanoparticles that are generally better defined and smaller than the particles formed in the corresponding CO_2-free dispersion polymerizations. As such the mechanism is similar to a miniemulsion polymerization.[72]

The present RAFT seeded precipitation polymerization in $scCO_2$ used poly(2-ethoxyethyl methacrylate) as the macroRAFT agent, which is precipitated prior to polymerization with *N*,*N*-dimethylacrylamide (DMA) and 4-acryloylmorpholine (4AM) to give block copolymers.

Potential applications for these poly(2-ethoxyethyl methacrylate) containing block copolymers are numerous due to the presence of both ether and ester groups imparting flexibility and hydrogen bonding, while also offering the possibility for biomedical applications due to their thermoresponsiveness.[73] Controlled/living character for the heterogeneous polymerizations in $scCO_2$ is compared with the equivalent solution polymerizations in toluene.

2.2 Experimental

2.2.1 Materials

2-Ethoxyethyl methacrylate (>98%, TCI), *N*,*N*-dimethylacrylamide (DMA, >99%, TCI), and 4-acryloylmorpholine (4AM, >98%, TCI) were distilled under reduced pressure before use. 2,2'-Azoisobutyronitrile (AIBN, DuPont Chemical Solution Enterprise) was recrystallized twice from methanol before use. 2-Cyano-2-propyl benzodithioate (>97%, Aldrich), petroleum ether (Aldrich), *N*,*N*-dimethylformamide (DMF, 99.9%, Aldrich), tetrahydrofuran (THF, 99.9%, Aldrich), diethyl ether (>98%, Aldrich), toluene (99%, Aldrich), $CDCl_3$ (99.8 atom %, Aldrich) and LiBr (99%, Aldrich) were used as received.

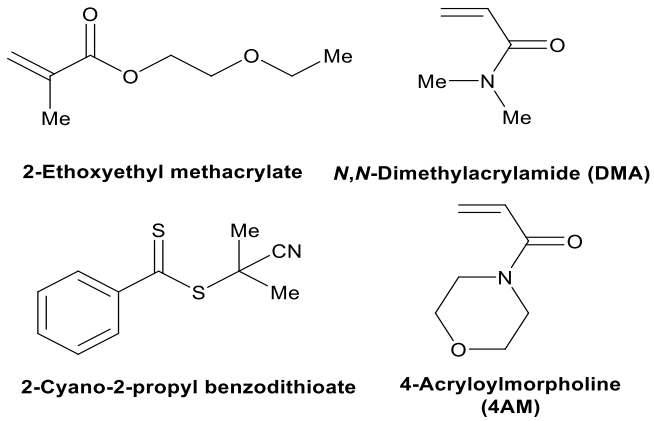

Scheme 2.1: Reagents used

2.2.2 Preparation of macroRAFT agent

Poly(2-ethoxyethyl methacrylate) (macroRAFT agent, M_n = 9000, M_w/M_n = 1.10) was prepared by bulk polymerization of 2-ethoxyethyl methacrylate (10.4 mL, 63.2 mmol) at 60 °C for 10 h using AIBN (41.5 mg, 0.253 mmol) and 2-cyano-2-propyl benzodithioate (0.28 g, 1.26 mmol) as initiator and RAFT agent respectively. The polymer was isolated by solubilizing the resultant mixture using a minimum of THF with precipitation into an excess of petroleum ether. The polymer was dried under vacuum to give the macroRAFT agent (8.98 g, 87%).

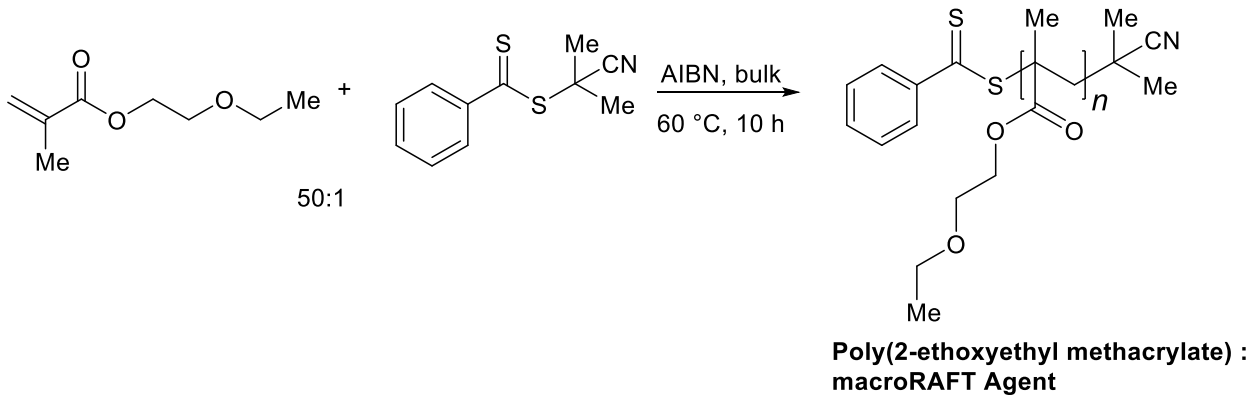

Scheme 2.2: Synthesis of the macroRAFT agent

2.2.3 Measurements for polymerizations

M_n and polydispersity (M_w/M_n) were measured using a gel permeation chromatography (GPC) system consisting of a Viscotek DM 400 data manager, a Viscotek VE 3580 refractive index detector, and two Viscotek Viscogel GMH_{HR}-M columns. Measurements were carried out at 60 °C at a flow rate of 1.0 mL min^{-1} using HPLC-grade DMF containing 0.01 M LiBr as the eluent. The columns were calibrated using twelve poly(styrene) standards (M_n = 580-6035000 g mol^{-1}). M_n is given in g mol^{-1} throughout. All GPC measurements corresponds to polymer before purification, unless otherwise stated. The use of poly(styrene) standards inevitably leads to error, however control/living character can be assessed based on the shapes of molecular weight distributions (MWDs) and trends in M_n and M_w/M_n versus conversion.

The GPC measures detector response (mV) versus elution time (min). The instrument converts using a calibration curve produced from a set of narrow MWD polymer standards (see above) of known molecular weight, allowing the molecular weight distribution to be plotted as a function of molar mass ($dw/d\log M$ versus $\log M$). The signal height from the GPC is manipulated using excel by normalizing to 1 in order to obtain w(log *M*) versus log *M*.

^{1}H NMR spectra were recorded using a Joel GXFT 400 MHz instrument equipped with a DEC AXP 300 computer workstation. ^{1}H NMR spectra were obtained in $CDCl_3$ and used for conversion measurements from polymerization mixtures prior to precipitation. Conversions for

the polymerizations of DMA were obtained by comparing the integrals of the copolymer peak at 2.7-3.2 ppm (CH_3, 6H) with the monomer vinyl peak at ~5.65 ppm with deduction of the monomer contribution from the copolymer peak. Conversions for the polymerizations of 4AM were obtained by comparing the integrals of the copolymer peak at 3.1-3.9 ppm (CH_2, 8H) with the monomer vinyl peak at ~5.69 ppm with deduction of the monomer and macroRAFT contributions from the copolymer peak. For polymerization of 4AM to ≥70% conversion in $scCO_2$, conversion was also measured by gravimetry with measurements found to be in close agreement (within 1%) to that obtained from ^{1}H NMR.

The theoretical number-average molecular weights ($M_{n,th}$) were calculated according to:

$$M_{n,th} = \frac{\alpha[M]_0 \, MW_{mon}}{[macroRAFT]_0} + MW_{macroRAFT} \qquad (2.1)$$

where α is the fractional monomer conversion, $[M]_0$ is the initial monomer concentration, $[macroRAFT]_0$ is the initial macroRAFT concentration, MW_{mon} is the molecular weight of the monomer, and $MW_{macroRAFT}$ is the molecular weight of the macroRAFT determined by GPC.

SEM images were obtained using a FEI Phenom SEM with light optical magnification fixed at 20 times, electron optical magnification 120-20,000 times, and digital zoom of 12 times. The sample was mounted on a stub and then coated in gold before being placed in the SEM.

2.2.4 Equipment

Polymerizations in $scCO_2$ were conducted in a 25 mL stainless steel Parr reactor with maximum operating pressure and temperature of 40 MPa and 130 °C, respectively, or a 100 mL stainless steel Thar reactor (Fig. 2.1) with a maximum operating pressure and temperature of 41.4 MPa and 125 °C, respectively. The pressure was produced by a Thar P-50 series high pressure pump to within ±0.2 MPa and the temperature was monitored by a Thar CN6 controller to within ±0.1 °C. The reactors are connected to a Thar automated back pressure regulator (ABPR, a computer-controlled needle valve) for controlled venting. For the 25 mL reactor stirring was achieved using a magnetic stirring bar, the 100 mL reactor is equipped with a Magdrive which maintained stirring at ~1200 rpm and 180° sapphire viewing windows.

(a)

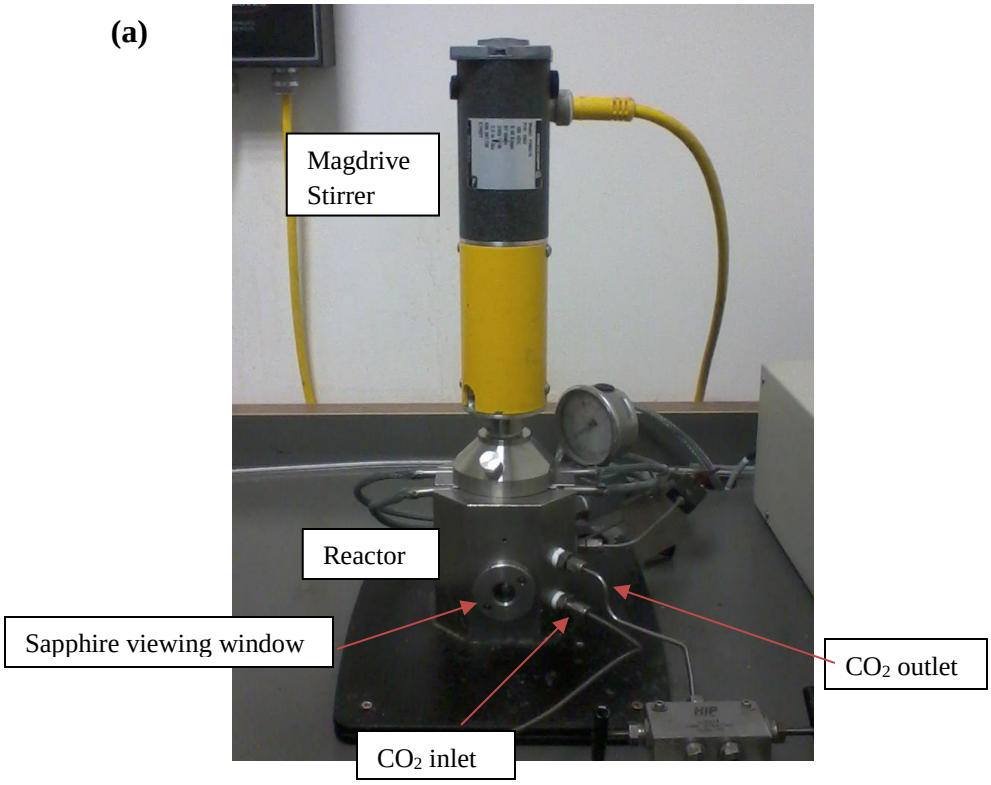

(b)

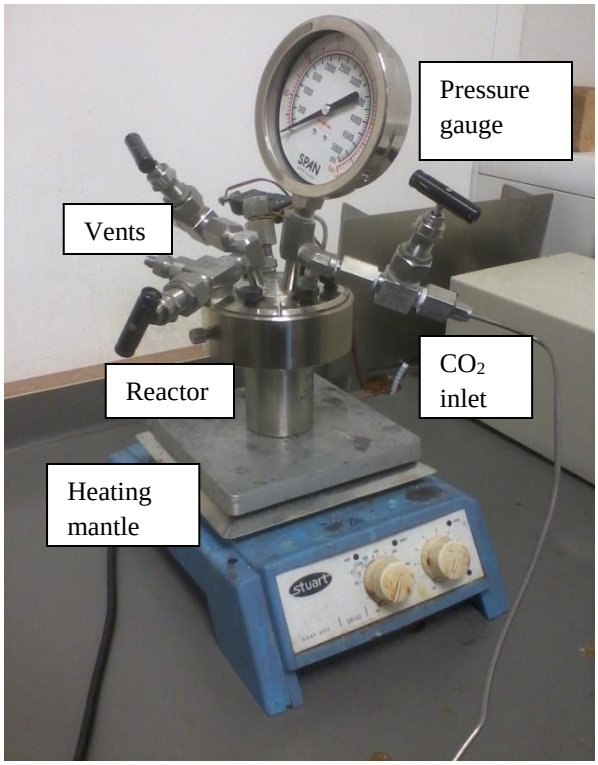

Figure 2.1: Images of **(a)** 100 mL and **(b)** 25 mL stainless steel $scCO_2$ reactors

2.2.5 Polymerizations in $scCO_2$

The macroRAFT agent (5.67 g, 0.63 mmol) and AIBN (20.7 mg, 0.126 mmol) were dissolved in DMA (12.5 g, 0.126 mol) in the 25 mL stainless steel reactor. Alternatively, the above macroRAFT agent (4.70 g, 0.52 mmol) and AIBN (17.2 mg, 0.104 mmol) were dissolved in 4AM (15.25 g, 0.108 mol) in the 25 mL stainless steel reactor. The reaction mixture was purged for 20 minutes by passing gaseous CO_2 through the mixture to remove oxygen. Liquid CO_2 (~5 MPa) was added and the reactor immersed in an oil bath. The temperature was raised to the reaction temperature of 65 °C and then the pressure to 30 MPa by further addition of CO_2. The reaction was quenched at various times by submersion of the reactor into an ice-water bath. When at approximately room temperature, the CO_2 was vented slowly from the reactor into a conical flask to prevent loss of the polymer. The polymers were isolated by dissolving the reaction mixture in THF and precipitation by dropwise addition into cold petroleum ether (DMA) or diethyl ether (4AM). The polymerizations of 4AM taken to ≥70% conversion were purified using $scCO_2$. The light pink powder obtained after venting of CO_2 (was not precipitated using organic solvent), was purified by washing three times with $scCO_2$ at 50 °C and 30 MPa. The polymer was filtered and dried under vacuum for 24 h at room temperature.

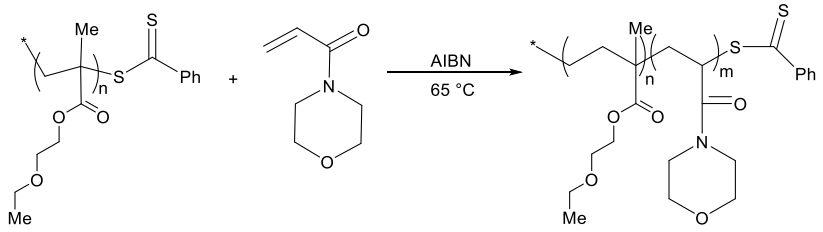

Scheme 2.3: Preparation of block copolymer from 4AM

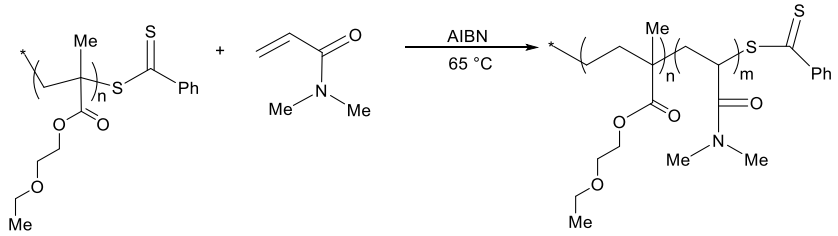

Scheme 2.4: Preparation of block copolymer from DMA

2.2.6 Solution polymerizations

The macroRAFT agent (0.450 g, 0.050 mmol) and AIBN (1.65 mg, 0.01 mmol) were dissolved in DMA (1.00 g, 10 mmol) and toluene (1 mL) was added. For 4AM, the macroRAFT agent (0.302 g, 0.0335 mmol) and AIBN (1.16 mg, 0.007 mmol) were dissolved in 4AM (1.00 g, 7.08 mmol) and toluene (0.63 mL) was added. Polymerization reaction mixtures were added to Pyrex ampoules and subjected to several freeze-degas-thaw cycles to remove oxygen before sealing under vacuum. The ampoules were heated at 65 °C in an aluminum heating block for various times. Polymerizations were stopped by placing ampoules in an ice-water bath.

2.3 Results and Discussion

2.3.1 Induced Precipitation polymerization in $scCO_2$

Polymerizations were conducted in a 100 mL stainless steel reactor equipped with two 180° sapphire windows,[42] which allowed for the observation of the solubility of the poly(2-ethoxyethyl methacrylate) macroRAFT agent in $scCO_2$ at 65 °C and 30 MPa. Under these conditions, the macroRAFT agent (~19 g; M_n = 9000 g/mol, M_w/M_n = 1.10) was found to be insoluble in $scCO_2$, forming a whitish emulsion. For polymerizations, a similar quantity of macroRAFT agent was first dissolved in the acrylamide monomer, which is miscible with $scCO_2$.[52] Upon introduction of CO_2 at 5 MPa and 24 °C, a phase separation was induced, which was observed as a whitish emulsion indicating the presence of particles (a dispersed phase) prior to polymerization. The dispersion persisted under $scCO_2$ conditions (30 MPa/ 65 °C) used for polymerization of the monomers DMA and 4AM with 2,2'-azoisobutyronitrile (AIBN) as initiator.

2.3.2 RAFT polymerizations in $scCO_2$

Reasonably narrow MWDs (M_w/M_n < 1.38) shifting to higher MWs with conversion for the RAFT polymerizations of DMA (Fig. 2.2) and 4AM (Fig. 2.3) at $[monomer]_0/[macroRAFT]_0$ = 200 and 400 are indicative of good controlled/living character. MWs increased approximately linearly with conversion and were mostly close to the theoretical number average molecular weight ($M_{n,th}$) lines, although some discrepancy is expected because the M_n values are based on polystyrene standards (Figs. 2.4 and 2.5). It is noted that for DMA, M_n values tended to deviate to lower M_n than $M_{n,th}$ to a greater extent than for the RAFT of 4AM in $scCO_2$ reflecting a greater loss in control in comparison to 4AM. Overall, the fact that reasonable controlled/living character was observed indicates minimal macroRAFT agent partitioning into the continuous phase. Generally, decreasing the $[macroRAFT]_0$ concentration by a factor of two (from $[monomer]_0/[macroRAFT]_0$ = 200 to 400) resulted in almost doubling of M_n.

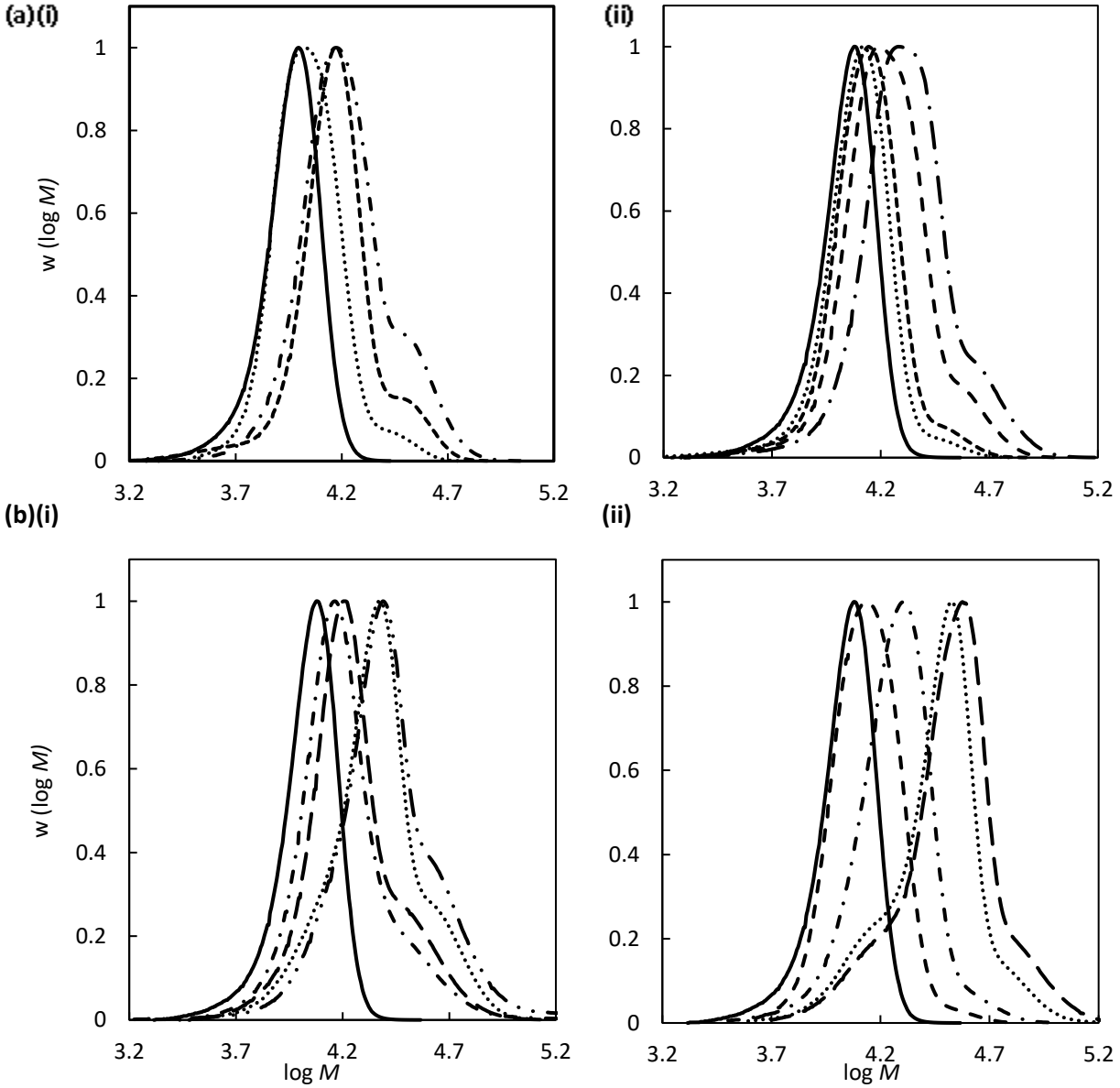

Figure 2.2 MWDs for polymerization mixtures of the RAFT of DMA at 65 °C using poly(2-ethoxyethyl methacrylate) macroRAFT agent (continuous line), where $[macroRAFT]_0/[AIBN]_0$ = 5; **(a)** $[DMA]_0/[macroRAFT]_0$ = 200 **(i)** in $scCO_2$ at 8, 26 and 41% conversion and **(ii)** in solution (toluene) at 15, 28, 34 and 47% conversion, and **(b)** $[DMA]_0/[macroRAFT]_0$ = 400 **(i)** in $scCO_2$ at 14, 21, 41 and 54% conversion and **(ii)** in solution (toluene) at 15, 26, 37 and 48% conversion

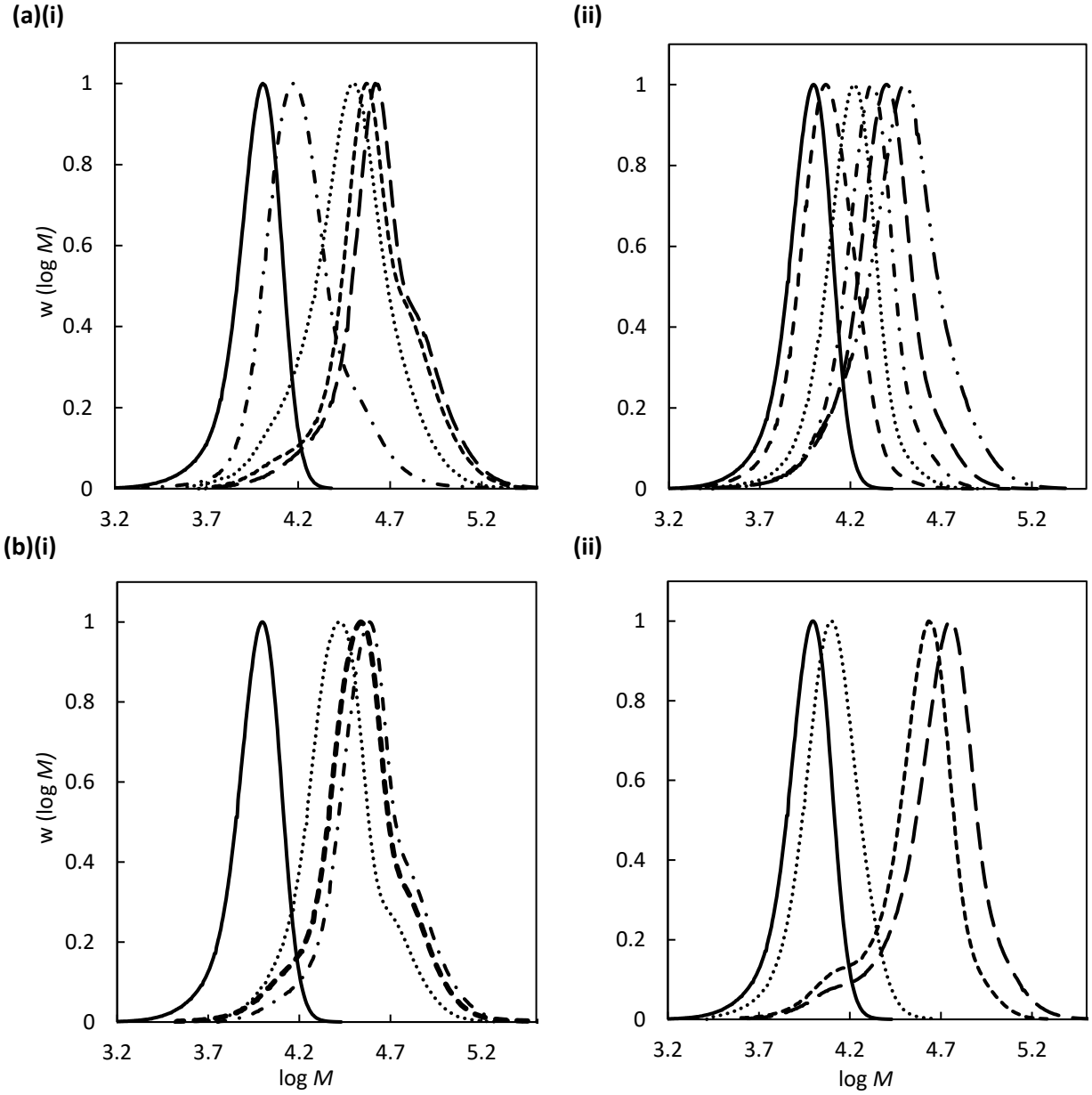

Figure 2.3 MWDs for polymerization mixtures of 4AM at 65 °C using poly(2-ethoxyethyl methacrylate) macroRAFT agent (continuous line), where $[macroRAFT]_0/[AIBN]_0$ = 5; **(a)** $[4AM]_0/[macroRAFT]_0$ = 200 **(i)** in $scCO_2$ at 21, 45, 70 and 87% conversion and **(ii)** in solution (toluene) at 11, 26, 31, 49 and 62% conversion, and **(b)** $[4AM]_0/[macroRAFT]_0$ = 400 **(i)** in $scCO_2$ at 27, 35 and 64% conversion and **(ii)** in solution (toluene) at 10, 36 and 43% conversion

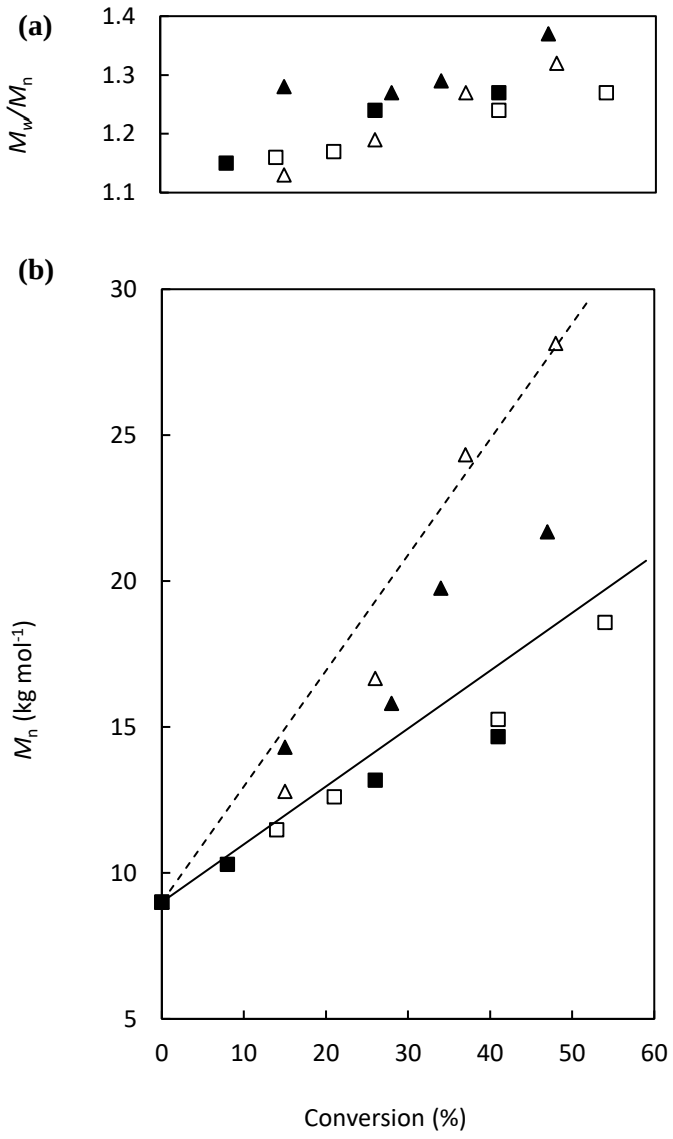

Figure 2.4 (a) M_w/M_n and **(b)** M_n versus conversion for polymerizations of DMA at 65 °C using poly(2-ethoxyethyl methacrylate) macroRAFT agent, where $[\text{macroRAFT}]_0/[\text{AIBN}]_0 = 5$. Closed symbols are in $scCO_2$ and open symbols are in solution (toluene). Squares and triangles are $[\text{DMA}]_0/[\text{macroRAFT}]_0 = 200$ and 400 with $M_{n,th}$ line full and dashed respectively

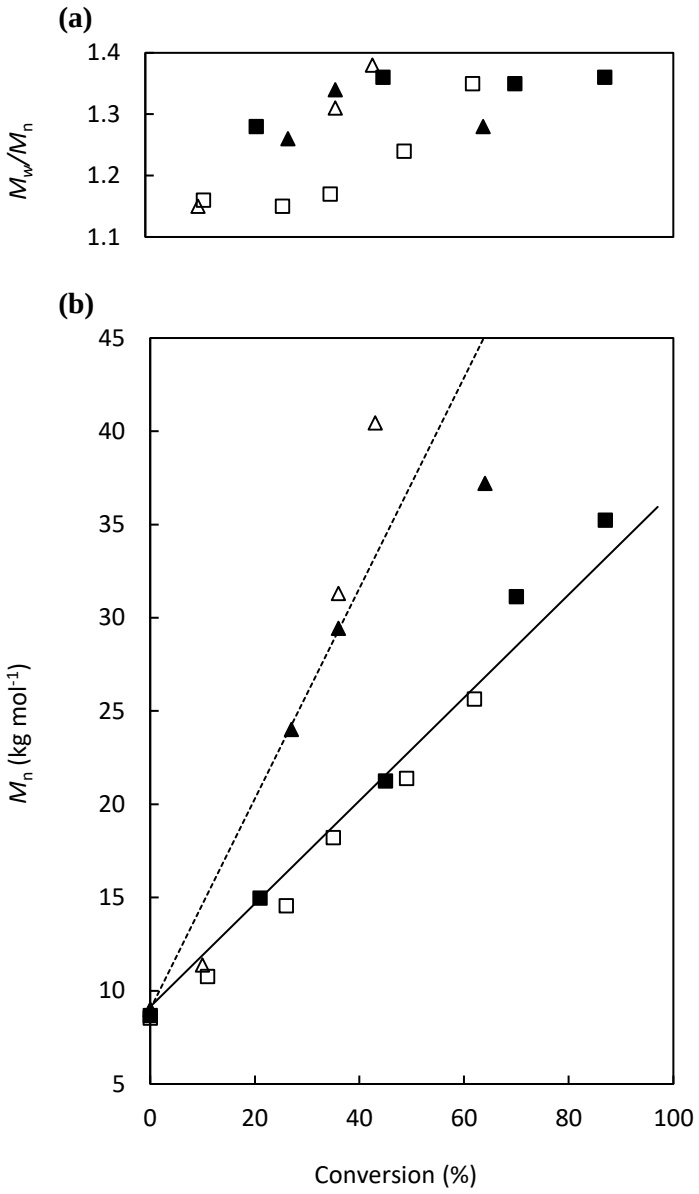

Figure 2.5 (a) M_w/M_n and **(b)** M_n versus conversion for polymerizations of 4AM at 65 °C using poly(2-ethoxyethyl methacrylate) macroRAFT agent, where $[\text{macroRAFT}]_0/[\text{AIBN}]_0 = 5$. Closed symbols are in $scCO_2$ and open symbols are in solution (toluene). Squares and triangles are $[4\text{AM}]_0/[\text{macroRAFT}]_0 = 200$ and 400 with $M_{n,th}$ line full and dashed respectively

2.3.3 Comparisons with solution RAFT polymerizations

The heterogeneous polymerizations described above were compared with homogeneous systems in toluene carried out at the same temperature, where the concentrations of AIBN, macroRAFT and monomer were the same as in the $scCO_2$-reactor (based on the entire reactor volume) (Figs. 2.4 and 2.5). Toluene was chosen as all the reaction constituents and products remained soluble to high conversion. The polymerizations were significantly faster in solution than in $scCO_2$ (Fig. 2.6) - polymerizations were about 4.5 and 1.5-2 times faster in solution for DMA and 4AM, respectively. Work done by Suzuki and co-workers showed that the RAFT polymerization of hydrophobic monomers such as styrene in aqueous miniemulsions (i.e. another type of dispersed system) is typically markedly faster than the corresponding homogeneous system as a result of compartmentalization effects (segregation) on bimolecular termination.[74] The rate retardation is caused by bimolecular termination between the intermediate and propagating radicals. This is suppressed in a miniemulsion polymerization by separating the radicals into different loci of polymerization.[75] However in the present system, the particle size is significantly larger than in miniemulsions (~100 nm), and moreover, the monomer solubility in $scCO_2$ is much higher than that of hydrophobic monomers in water. As a consequence of the latter, significant monomer partitioning to the continuous phase would occur in the $scCO_2$ system, resulting in less monomer being available at the main locus of polymerization (the particles) and hence a reduction in polymerization rate. Overall, the influence of system heterogeneity on polymerization rate is complex, including also possible effects of initiator partitioning and the termination rate coefficient (k_t) being different in the two systems. A decrease in polymerization rate at the onset of heterogeneity has previously been observed in RAFT dispersion polymerization in non-CO_2 systems (although the opposite may also occur depending on the particular system). Armes and co-workers found that for the block copolymerization of poly(glycerol monomethacrylate) (PGMA) with 2-hydroxypropyl methacrylate (HMPA) at 46% conversion micelles began to self-assemble trapping monomer inside at high concentration, which led to a five-fold increase in the rate of polymerization.[76] Pan and co-workers found that for the block copolymerization of poly(vinylpyridine) with divinylbenzene however, the polymerization rate slowed down after the formation of micelles, which is attributed to the restriction of diffusion and high concentration of RAFT end groups in the core of the micelles.[77]

The longer polymerization times in $scCO_2$ led to higher dispersities in comparison to the solution polymerizations due to the cumulative number of radicals generated from AIBN decomposition increasing with time (assuming no other radical side reactions, the number of termination events corresponds to half the number of radicals generated by AIBN). This is manifested as an increasing low MW tail with conversion as well as prominent high MW shoulders at the highest conversions due to termination by coupling.[78] In addition, it is possible that the heterogeneity of the system results in some broadening of the MWD due to different particles having different [monomer]/[macroRAFT] ratios.

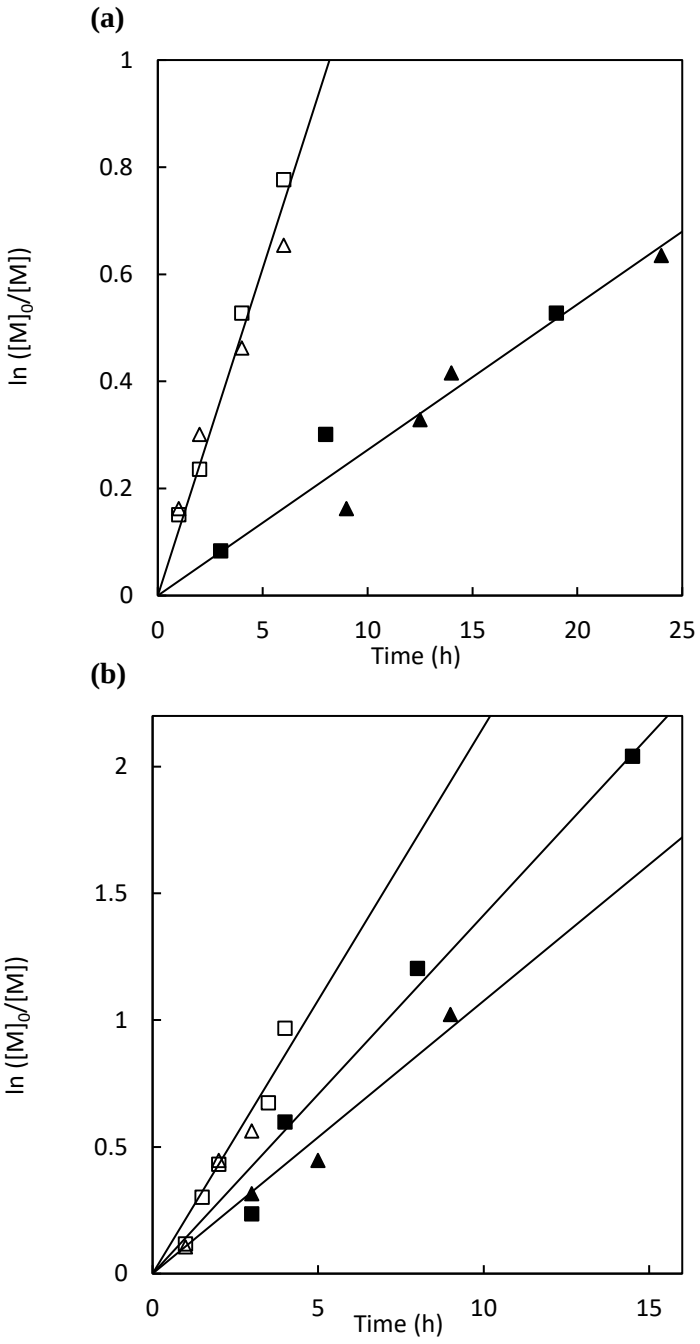

Figure 2.6 First order plots for polymerizations at 65 °C using poly(2-ethoxyethyl methacrylate) macroRAFT agent, where $[\text{macroRAFT}]_0/[\text{AIBN}]_0 = 5$ in $scCO_2$ are closed symbols and in solution (toluene) are open symbols with squares and triangles are $[\text{monomer}]_0/[\text{macroRAFT}]_0 =$ 200 and 400, respectively; **(a)** DMA and **(b)** 4AM. Lines are of best fit.

2.3.4 High conversion RAFT polymerizations in $scCO_2$

Given that polymerizations in $scCO_2$ of 4AM were 4–5 times faster than DMA, and that it took ~24 h to reach intermediate conversions of around 47% with DMA, it was decided to only take polymerizations of 4AM to high conversion. The products of the RAFT polymerizations of 4AM taken to ≥70% conversion in $scCO_2$ were isolated as powders upon venting of the CO_2 (Fig. 2.7). The powders were repeatedly washed with $scCO_2$ at 50 °C and 30 MPa in order to remove all traces of monomer (see Figs. 2.8 and 2.9 for NMR of purified polymers). Thus the technique was suitable for large-scale synthesis of block copolymers without the requirement for toxic and hazardous volatile organic solvents. The SEM image of a sample of the powder revealed the formation of large irregularly shaped particles, which were similar to those obtained from precipitation NMP of styrene,[49] and inverse suspension polymerization NMP of *N*-isopropylacrylamide in $scCO_2$,[53] although there are less prominent cavities from the expulsion of CO_2 present.

The MWDs for the RAFT polymerization of 4AM in $scCO_2$ at 70 and 87% conversions were reasonably narrow (Fig. 2.3; M_w/M_n ~ 1.35), and controlled/living character is evident and M_n remains close to theoretical values (Fig. 2.5).

(a)

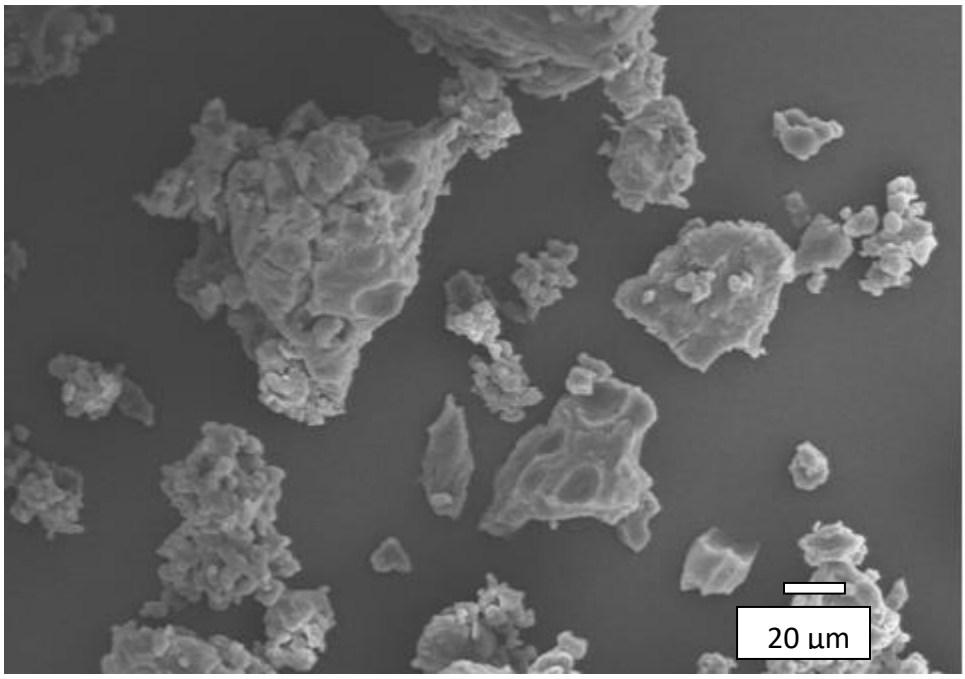

(b)

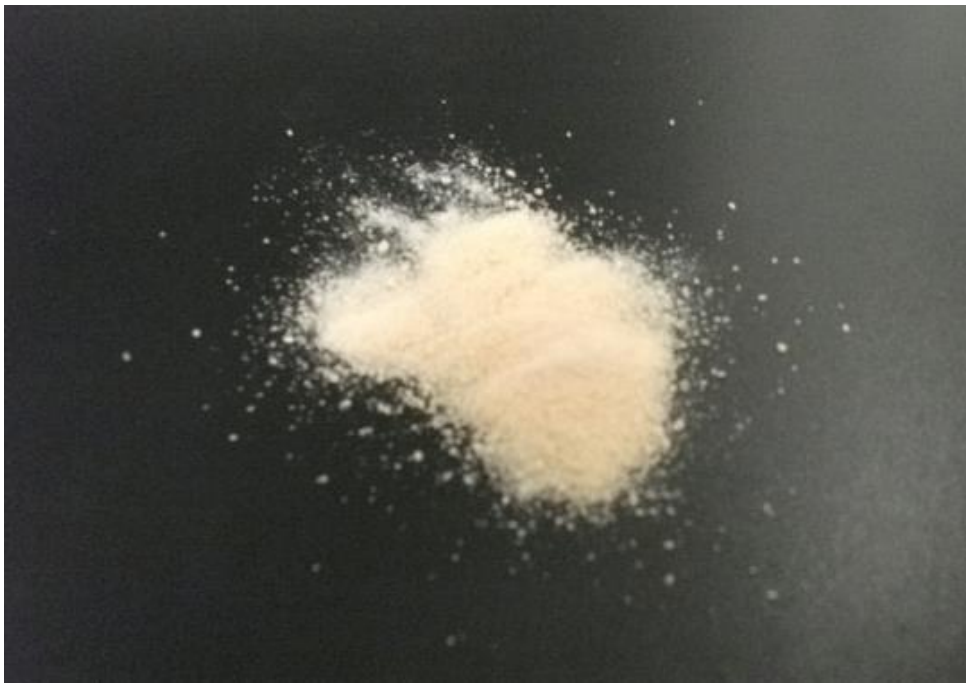

Figure 2.7 (a) SEM image and **(b)** optical image of poly(2-ethoxyethyl methacrylate)-*b*-poly(4AM) powder obtained at 70% conversion from the RAFT polymerization of 4AM in supercritical CO_2

(a)

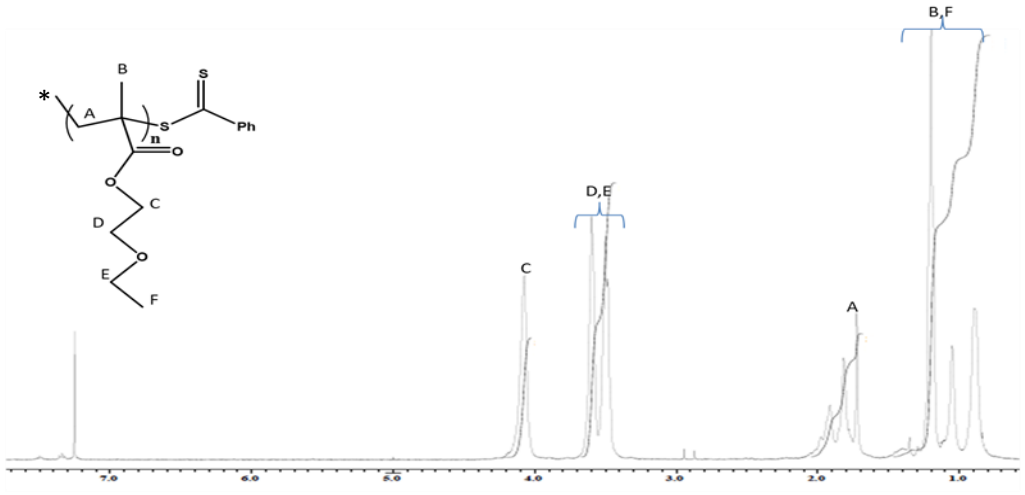

(b)

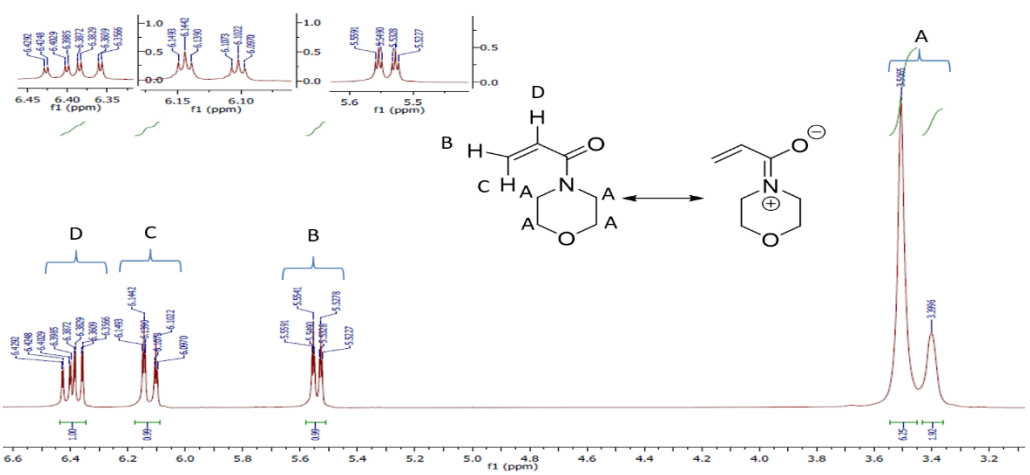

(c)

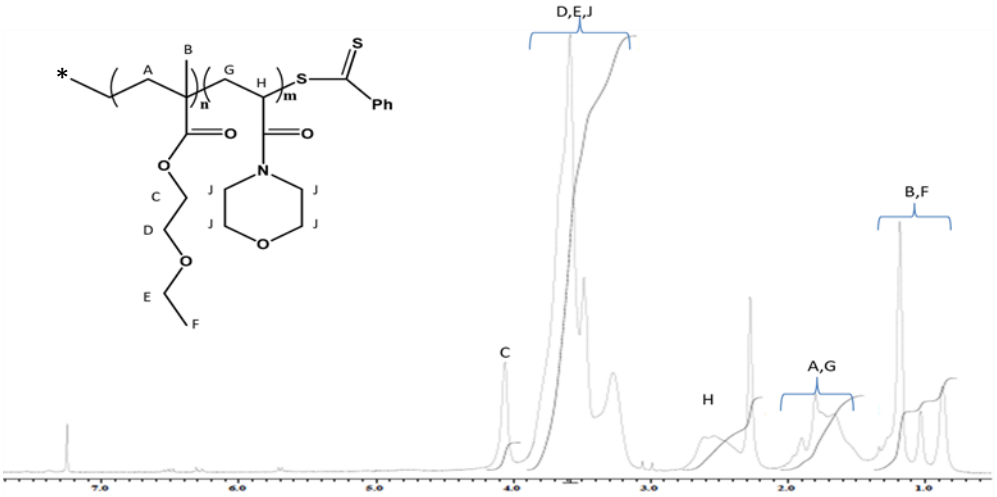

Figure 2.8: ^{1}H NMR (in $CDCl_3$) of monomer and purified polymers: **(a)** poly(2-ethoxyethyl methacrylate) (MacroRAFT) **(b)** 4-acryloylmorpholine **(c)** poly(2-ethoxyethyl methacrylate)-*b*-poly(4AM). There are several signals for methyl B due to tacticity effects.

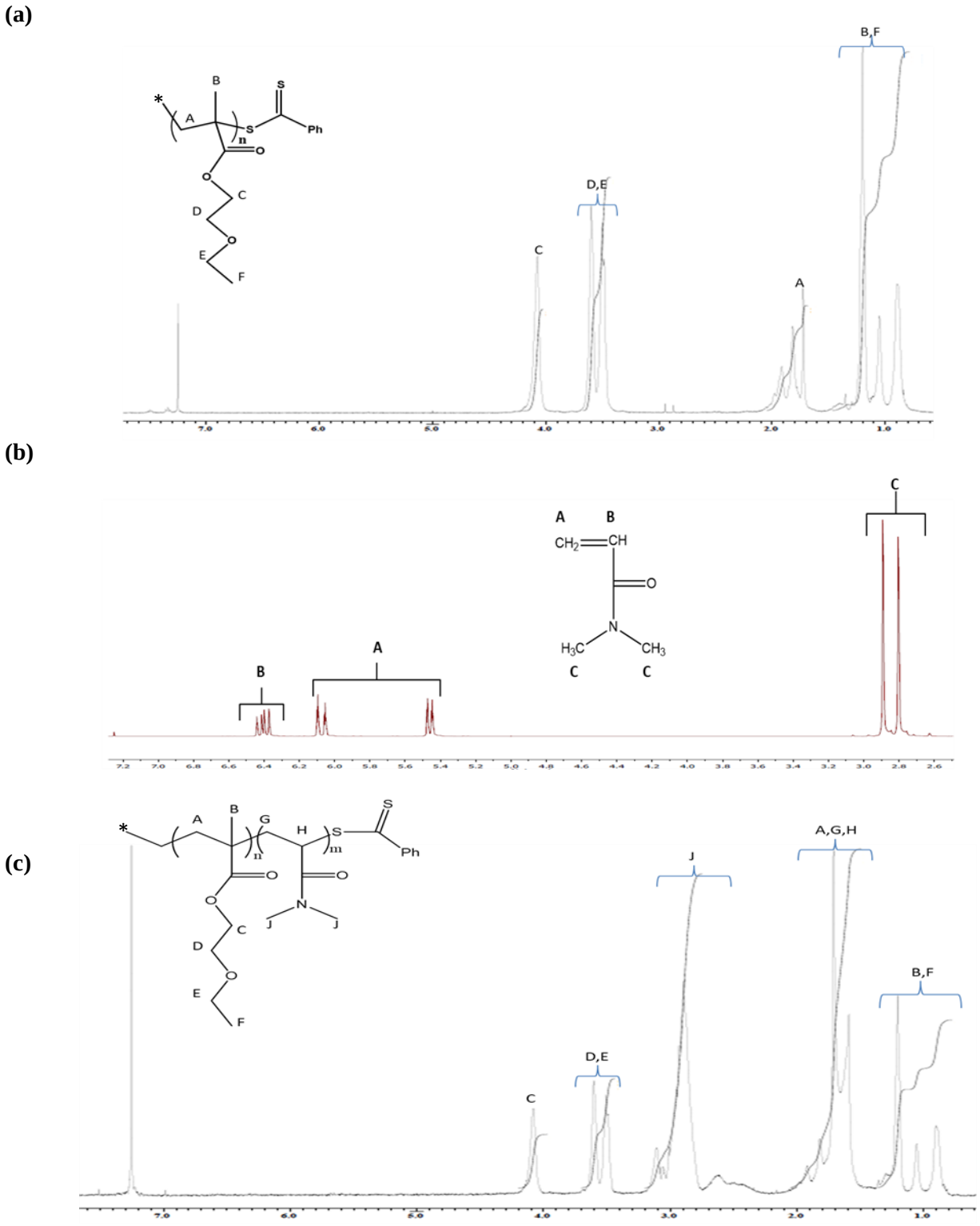

Figure 2.9: ^{1}H NMR (in $CDCl_3$) of monomer and purified polymers: **(a)** poly(2-ethoxyethyl methacrylate) (MacroRAFT) **(b)** dimethylacrylamide **(c)** poly(2-ethoxyethyl methacrylate)-*b*-poly(DMA)

2.4 Conclusions

Poly(2-ethoxyethyl methacrylate)-*b*-poly(acrylamide) polymers with important biotechnology applications were prepared using a new controlled/living heterogeneous polymerization technique in scCO_2. Applications of poly(2-ethoxyethyl methacrylate) include the preparation of hydrogels in the production of lenses and as part of drug delivery systems.[79-81] Poly(4-acryloylmorpholine) and poly(dimethylacrylamide) have both been used in the production of hydrogels and used as part of drug delivery systems.[82-84] The new heterogeneous polymerization technique involves the formation of seed particles swollen with monomer by precipitation of the macroRAFT agent by the introduction of CO_2. Despite the precipitation of the macroRAFT agent prior to polymerization, controlled/living character comparable to the equivalent solution system was achieved. The block copolymers of 4AM were isolated as powders in multi-gram scale at high conversions without the requirement for volatile organic solvents providing future potential green chemistry and commercial advantages.

CHAPTER 3

POLYMERIZATION INDUCED SELF ASSEMBLY (PISA) USING ATRP IN SUPERCRITICAL CARBON DIOXIDE

3.1 Introduction

3.1.1 Background

The self-assembly of amphiphilic block copolymers in selective solvents to produce aggregates of various morphologies has been extensively studied by various groups such as those of Eisenberg and Bates.[85-86] The two-step process involves dissolving the block copolymer post-polymerization in a common organic solvent and gradually replacing with the non-solvent water or others to induce self-assembly as the water content increases. However the block copolymer concentrations are low (<1.0% w/w) making it difficult to use on a large scale.

Polymerization Induced Self-Assembly (PISA) or the *in-situ* synthesis of the amphiphilic block copolymer involves the solvophilic polymer being chain extended with a second soluble monomer in a suitable solvent that polymerizes into a solvophobic block that becomes increasingly insoluble in the solvent. As the solvophobic block grows, the diblock will reach a certain length in which self-assembly occurs (Scheme 3.1). The solvophilic block is pre-prepared in a solution polymerization, and acts as a steric stabilizer for the solvophobic block formed in a dispersion or aqueous emulsion polymerization.[87-88] When in the solvent, the solvophobic blocks will move to the interior of the micelle to avoid contact with the solvent while the solvophilic blocks will stay on the outside to maximize contact with the solvent to self-assemble into a variety of structures. The shape of the nano-object created is dependent on the size of the solvophobic block relative to the solvophilic block. By adjusting the ratio of solvophobic block size to the solvophilic block size different structures or nano-objects can be obtained. This method has the advantage of allowing nano-objects of various morphologies to be prepared at relatively high concentrations of up to 50% w/w in comparison to the two-step post-polymerization process. The advent of more efficient Reversible Deactivation Radical Polymerizations (RDRP) techniques[21] has been crucial to the discovery of PISA, since block copolymer formation is not possible using conventional radical polymerization and other living addition polymerizations (such as anionic or cationic), which are monomer restrictive, and not compatible with aqueous/alcoholic heterogeneous polymerization techniques.

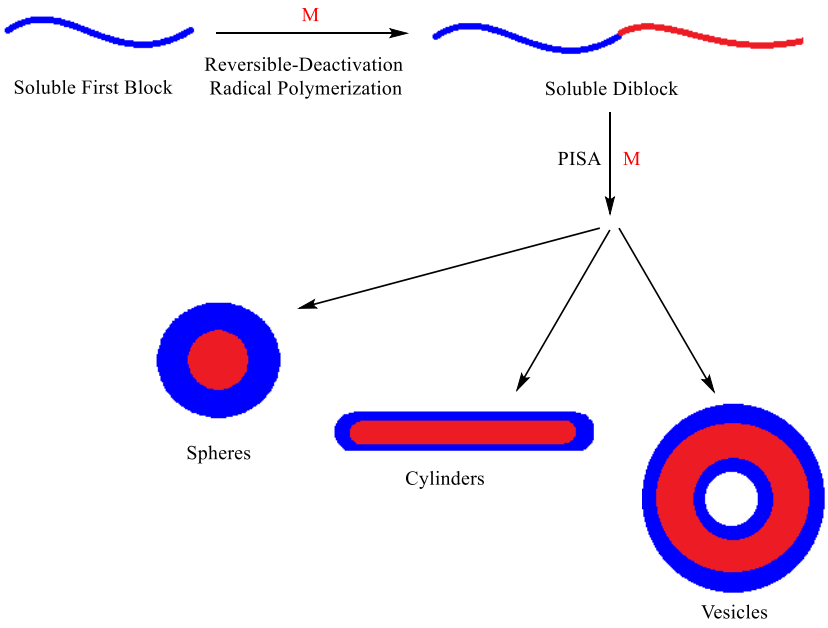

Scheme 3.1: Synthesis of nano-objects via Polymerization Induced Self-Assembly (PISA)

Charleux and co-workers have carried out PISA by using emulsion polymerizations with NMP and RAFT.[89-90] The water soluble first block is an alkoxyamine macroinitiator, or a macroRAFT agent that is chain extended with a water immiscible monomer. The emulsion polymerization proceeds within the monomer swollen micelles formed and dispersed throughout the aqueous medium. The NMP was performed using poly(sodium acrylate)-SG1 as the alkoxyamine macroinitiator and was chain extended with *n*-butyl acrylate and styrene in water.[89] In both cases the hydrophobic block is much longer than the hydrophilic one with $PNaA_{21}$-PS_{920} and $PNaA_{21}$-PBA_{400} synthesized. Control was lost at higher conversions for both polymers. Dynamic light scattering (DLS) was used to obtain measurements for the particles, including the number average diameter which for the PS particles was 65 nm and for PBA was 90 nm in an aqueous solution of pH = 7. In an aqueous acidic solution of pH = 4 average diameters decreased to 55 nm for PS and 76 nm for PBA, as the PNaA chains are converted to poly(acrylic acid) chains and contract into a compact conformation from a solvated coil conformation.[91] The RAFT polymerization used a macroRAFT agent made with water-soluble poly(ethylene oxide) (PEO) (Scheme 3.2) extended with *n*BA or *n*BA and MMA, and the polymerizations proceeded to high conversions with good control.[90] As the size of the PEO block increased, the size of the particles

decreased, from PEO = 1000 g mol^{-1} with a particle size of 340 nm to PEO = 2000 g mol^{-1} with 184 nm, and PEO = 5000 g mol^{-1} with 71 nm. Cryo-TEMs, where the samples are studied at cryogenic temperatures of polymers chain extended from the macroRAFT agent made with PEO = 2000 g mol^{-1} showed hollow spherical particles of uniform size of around 200 nm for the homopolymerization and less spherical hollow raspberry like particles around 150 nm in size for the copolymerization, which may be the result of the aggregation of smaller individual particles during the polymerization.

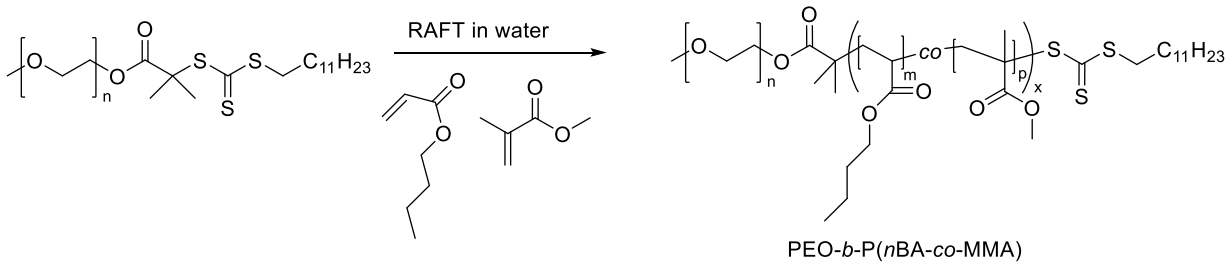

Scheme 3.2: Copolymerization of *n*BA and MMA in RAFT aqueous emulsion[90]

PISA has been performed using aqueous dispersion polymerization, in which a water-soluble polymer is chain extended with a water miscible monomer with the resultant block copolymer becoming increasingly insoluble upon polymerization. Hawker and co-workers were one of the first groups to use microwave assisted RAFT aqueous dispersion polymerizations using macroRAFT agents to synthesize thermoresponsive nanoparticles (Scheme 3.3).[92] The microwave irradiation allowed for efficient polymerization with 90-100% monomer conversion being obtained within 5 minutes. A macroRAFT agent made with *N*,*N*-dimethylacrylamide (DMA), was chain-extended with *N*-isopropylacrylamide (NIPAM) in water to produce spherical particles. In the absence of the crosslinker *N,N'*-methylenebisacrylamide (BIS), the nanoparticles dissociated into double-hydrophilic block copolymers after cooling to room temperature due to the transition of the PNIPAM block to being soluble below its lower critical solution temperature (LCST) of 32 °C. The use of a crosslinker resulted in fully hydrophilic nanoparticles at room temperature.

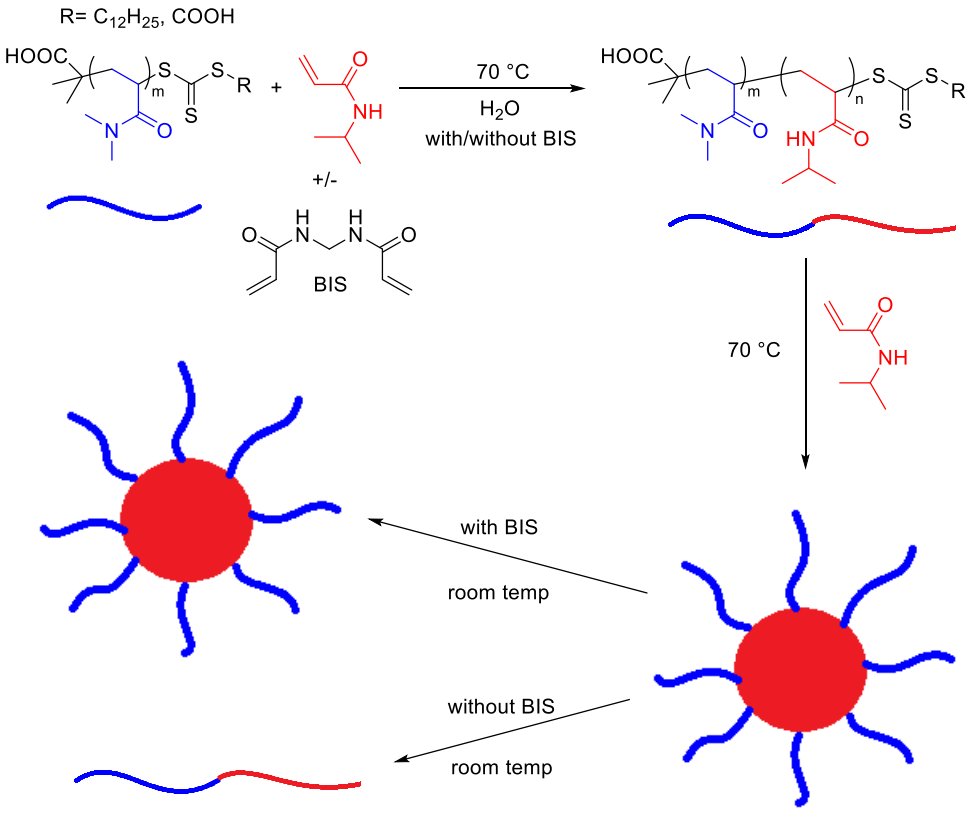

Scheme 3.3: RAFT polymerization of NIPAM with and without crosslinker BIS[92]

Armes and co-workers carried out RAFT dispersion polymerizations of benzyl methacrylate (BzMA) using four different macroRAFT agents synthesized from glycerol monomethacrylate (GMA), 2-(methacryloyloxy)ethyl phosphorylcholine (MPC), 2-(dimethylamino)ethyl methacrylate (DMAEMA) or methacrylic acid (MAA) (Scheme 3.4).[93] These macroRAFT agents were chain extended with benzyl methacrylate (BzMA) in alcohols at 60-70 °C, where self-assembly is not compromised by lateral electrostatic repulsion between highly charged chains as observed in the work of Charleux.[94] Alcohols were preferred over water because their lower surface tension can aid particle deposition into planar substrates. High conversions were achieved with good control with M_w/M_n values of under 1.3 observed. Nano-objects of various morphologies were observed depending on the steric stabilizer chains employed as macroRAFT. With the degree of polymerization of BzMA relative to the macroRAFTs dictating the formation of nano-objects with spheres being observed first, then worms, then vesicles as the BzMA block increased in size. Since the hydrophilic steric stabilizer chains were soluble in water, as well as

alcohols, these nano-objects could be transferred by dialysis without any loss in colloidal stability, which allowed their characterization by electrophoresis.

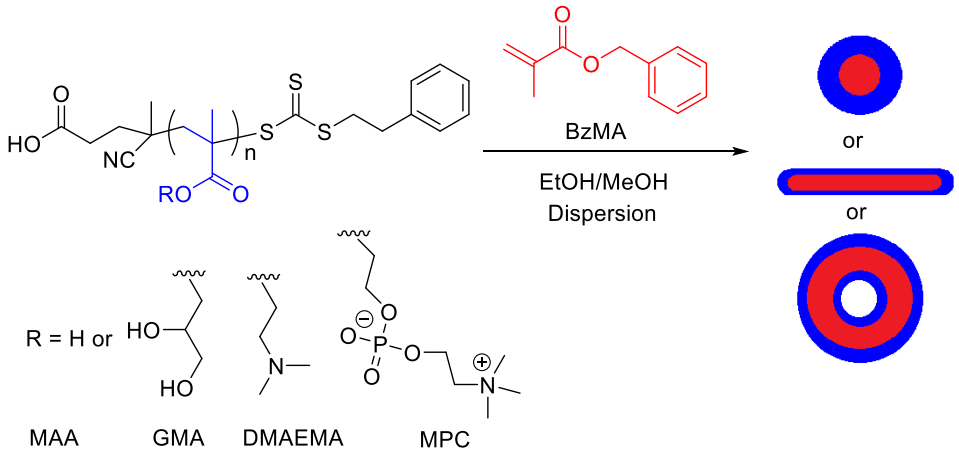

Scheme 3.4: RAFT dispersion polymerization of BzMA in alcohols[93]

Later Armes and co-workers carried out RAFT dispersion polymerizations of BzMA using a mixture of two macroRAFT agents made with different size blocks of PMAA in ethanol.[95] The polymerization of BzMA with the binary mixture of macroRAFT agents led to the formation of vesicles of relatively narrow size distribution with the PMAA block with shorter chains forming the inner layer. The PMAA-PBzMA diblock was then further extended with 2,2,2-trifluoroethyl methacrylate.[96] High conversions with good control and M_w/M_ns of under 1.45 were achieved for the ABC copolymer formation *via* dispersion polymerization in alcohols. The addition of the semi-fluorinated block produced a range of complex triblock copolymer morphologies.

Pan and co-workers synthesized spherical micelles from a macroinitiator *via* a dispersion atom transfer radical polymerization (ATRP) in 1:1 mixture of water: ethanol (Scheme 3.5).[97] A macroinitiator made from poly(ethylene oxide) (PEO) was chain extended with 4-vinylpyridine (4VP) in the presence of the crosslinker BIS to form PEO-*b*-(4VP-*co*-BIS). Polymerization proceeded with good control with M_w/M_n of under 1.1 observed. Spherical particles with a P(4VP- *co*-BIS) core and PEO corona were observed by TEM with an average size of 30 nm.

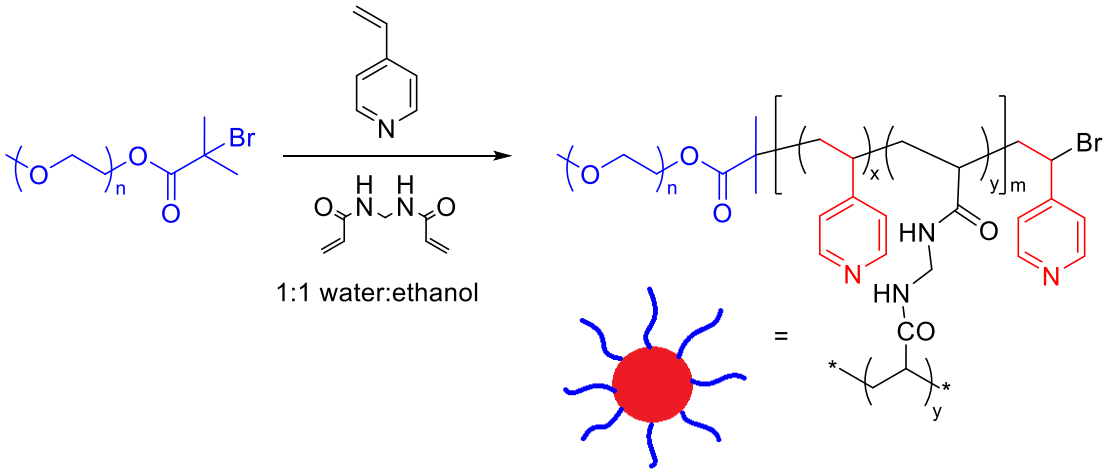

Scheme 3.5: ATRP dispersion polymerization with crosslinker BIS[97]

Matyjaszewski and co-workers performed PISA using initiator for continuous activator regeneration (ICAR) ATRP, which allowed a diminished copper catalyst concentration to be used compared to regular ATRP (Scheme 3.6).[98] The macroinitiator poly(oligo(ethylene oxide) methyl ether methacrylate) (POEOMA) block was made in an aqueous solution polymerization using ICAR using the water-soluble initiator VA-044.

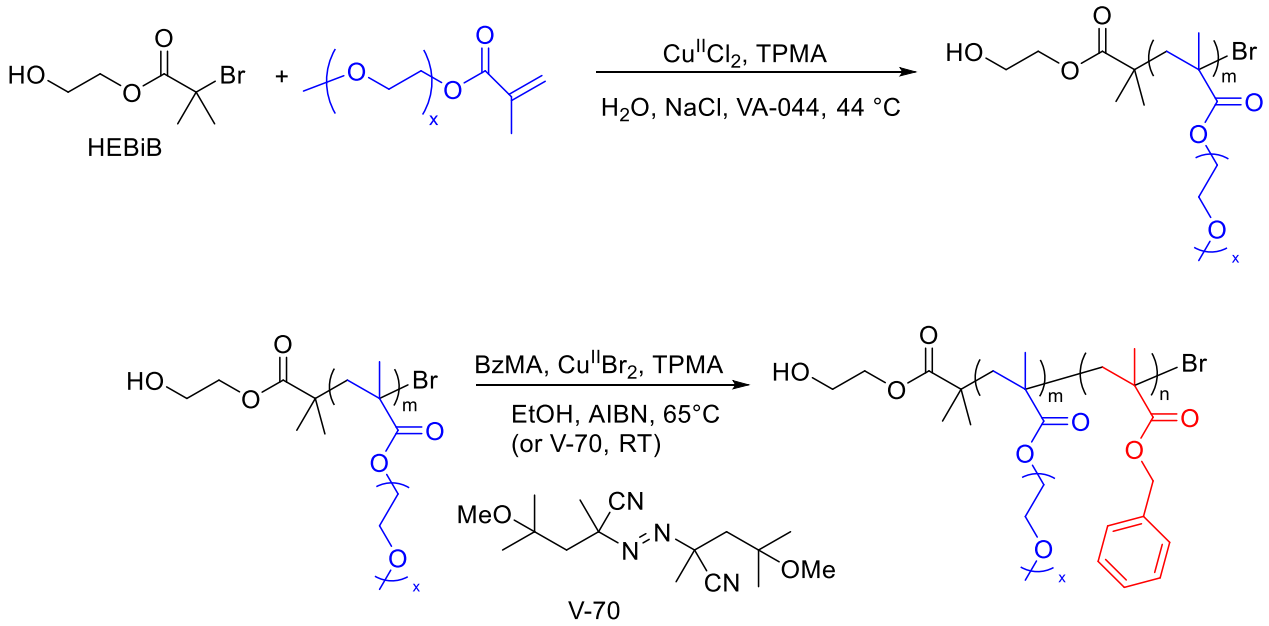

Scheme 3.6: Synthesis of POEOMA macroinitiator and ICAR dispersion ATRP of BzMA[98]

The use of ICAR overcomes problems of polymer radical termination, which exists with ATRP in water due to high ATRP equilibrium constant (k_a / k_d, Scheme 3.7), partial halide hydrolysis, and Cu(I) ligand dissociation. The initiator overcomes the requirement for high Cu loadings by continuously generating low concentrations of Cu(I) with NaCl added in order to suppress loss of deactivator by dissociation of Br-Cu(II). Other modifications that reduce catalyst loadings include regenerating the Cu(I) activator by electron transfer (Activator Regenerated Electron Transfer: ARGET) ATRP, which uses a reducing agent or an electrical current (eATRP).[99-101] AIBN was used to polymerize BzMA at 65 °C and V-70 at room temperature *via* an ICAR ATRP dispersion polymerization in ethanol.[98] The morphology of the nano-objects formed was dependent on temperature and composition of the reaction system. At room temperature, spherical or rod-like particles were observed depending on the solid content and degree of polymerization (DP). At 65 °C spheres or worm-like particles were observed depending solely on the DP of poly-BzMA. Furthermore, nano-objects formed at room temperature changed morphology when heated to 65 °C, with spheres changing into worms and short worms changing into vesicles. The difference in morphology between room temperature and 65 °C was believed to be caused by the temperature-dependent plasticization of the core-forming BzMA block below and above its glass transition temperature (T_g) of 54 °C.

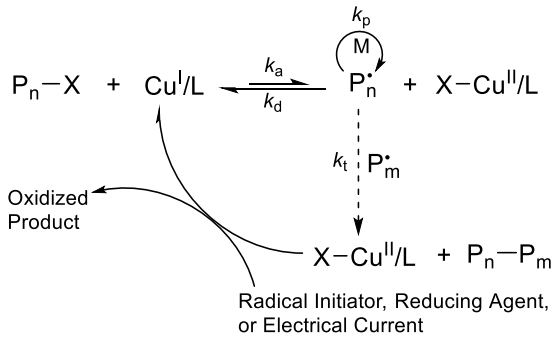

Scheme 3.7: Activator Regeneration ATRP mechanism[99]

3.1.2 Polymerization Induced Self Assembly in supercritical carbon dioxide

In 2009 Aldabbagh, Zetterlund and Okubo reviewed heterogeneous controlled/living radical polymerizations in supercritical CO_2 ($scCO_2$).[43] At the time of the review most examples of heterogeneous polymerizations in $scCO_2$ were precipitation and dispersion polymerizations. In $scCO_2$ the initiator, control agent(s) and monomer are typically soluble at the start, and the polymer becomes increasingly CO_2-phobic as it slowly grows precipitating at its critical degree of polymerization (J_{crit}).[42] There are two possibilities for preventing coagulation at J_{crit} and thus achieving a dispersion polymerization: (i) the non-initiating stabilizer approach or (ii) initiating stabilizer (initiation and stabilization "inistab" or stabilizing macroRAFT agent) approach. The second approach (ii) can now be termed PISA.

The work by Okubo and co-workers using a dispersion ATRP with MMA by chain extending a bromine-terminated poly(dimethylsiloxane) (PDMS) 'inistab' (initiator + stabilizer) macroinitiator can now be considered pioneering as far as the concept of PISA in $scCO_2$ (Scheme 3.8).[102]

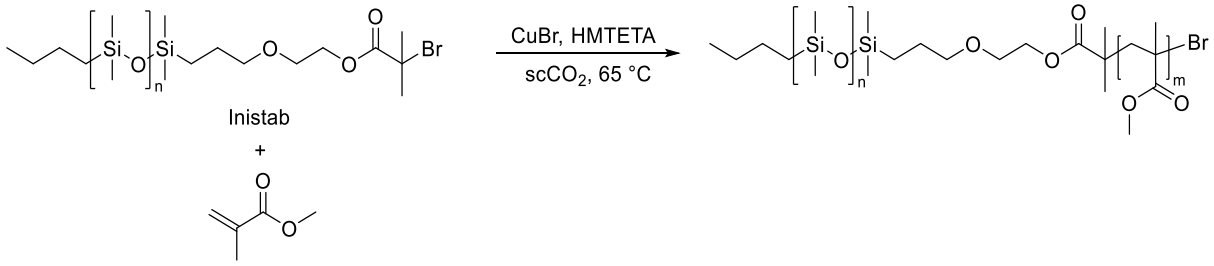

Scheme 3.8: ATRP of MMA in $scCO_2$ with a bromine terminated inistab[102]

The 'inistab' is the solvophilic block, which sterically stabilizes the growing MMA block in a dispersion ATRP. High conversion (91%) was achieved and the copolymer was obtained as a free-flowing powder. M_n of 55600 g mol^{-1} was obtained with a low M_w/M_n of 1.24 from a PDMS-Br initiator with an M_n of 6200 g mol^{-1} and M_w/M_n of 1.06. The particles were measured to be ~300 nm however were not spherical in shape indicating imperfect stabilization. TEM

showed that PDMS domains form inside the particles due to coagulation of the PDMS blocks at an early stage in the dispersion ATRP.

Aldabbagh and Okubo performed the first dispersion NMP by generating the inistab *in situ* by heating the poly(dimethylsiloxane) (PDMS)-based azo-initiator (VPS-0501) with SG1 (Scheme 3.9).[46] Control for the styrene polymerizations was limited due to the bifunctional nature of the initiator and the very large equilibrium constant for the reversible cleavage of the alkoxyamine between the initiating radicals and SG1.[27] SEM of the PS powder generated showed that stabilization was imperfect with significant coagulation presumably due to chains growing from both ends, so that the middle part extends into the $scCO_2$ medium reducing the colloidal protective layer.

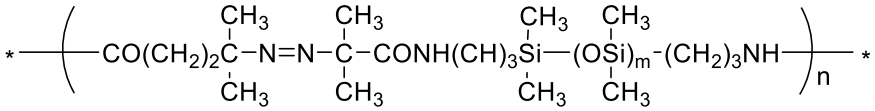

VPS-0501

Scheme 3.9: VPS-0501

A more efficient SG1-inistab was subsequently prepared from PDMS-Br and extended with styrene using ATRP with SG1 exchange of the bromine ω-end group (Scheme 3.10).[47] A more efficient dispersion NMP of styrene was achieved in terms of control/livingness, and giving uniform spherical PS particles. This inistab had anchor solubility balance of 4500/6500 g mol^{-1} (PS:PDMS), which is within the range of 1/3 to 3/1 reported to be suitable for colloidal stabilization.[103]

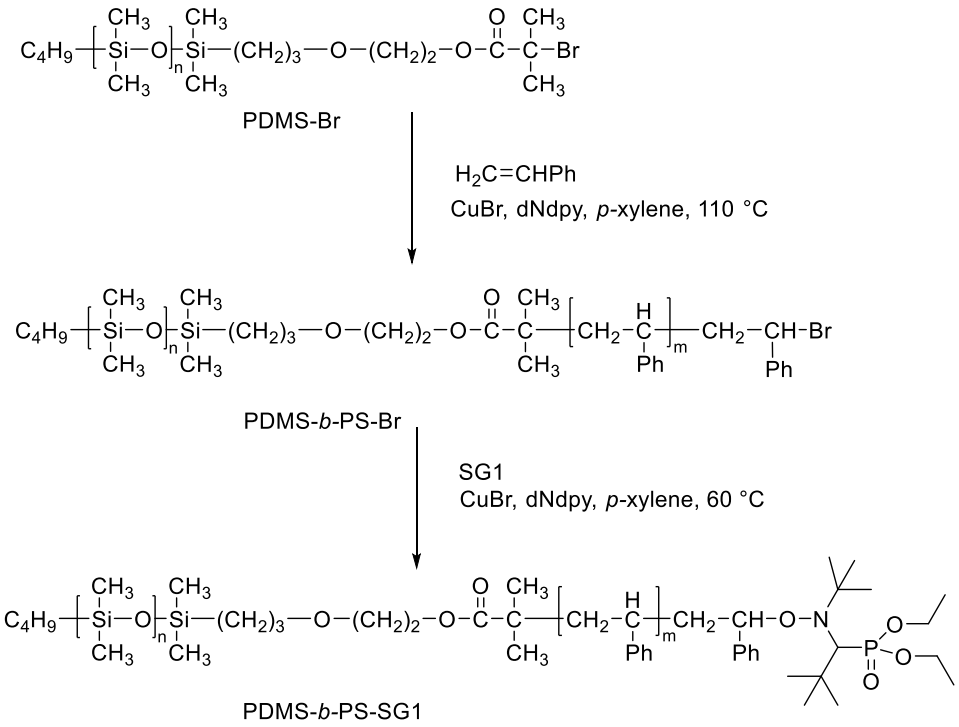

Scheme 3.10: Synthesis of PDMS-*b*-PS-SG1 (n ≈ 49, m ≈ 41)[47]

Okubo with Fukuda used VPS-0501 to perform dispersion polymerizations in $scCO_2$ of styrene using iodine transfer dispersion polymerization (dispersion ITP) with CHI_3 and reversible chain transfer catalyzed with GeI_4 (RTCP) (Scheme 3.11).[68]

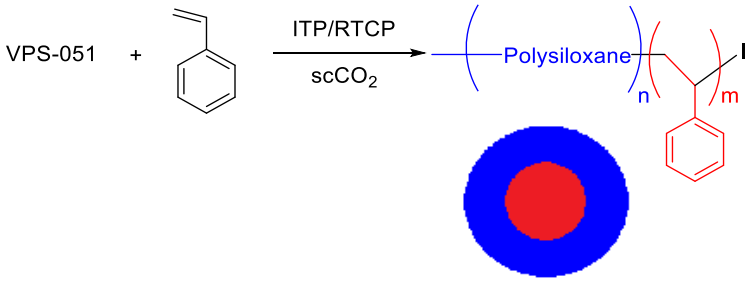

Scheme 3.11: ITP/RTCP polymerization of styrene in $scCO_2$[68]

ITP is based on a degenerative chain transfer (DT) process in which iodide compounds such as CHI_3 are used as transfer agents. ITP is limited by the difficulty in getting narrow polydispersities due to the low exchange frequencies of the iodide compounds. RTCP is a

reversible chain transfer (RT) process that uses a catalytic amount of GeI_4 to increase the exchange frequency and achieve narrow polydispersities (Scheme 3.12). GeI_4 acts as a deactivator and produces $^{\bullet}GeI_3$ and P-I *in situ*. $^{\bullet}GeI_3$ acts as an activator producing $P^{\bullet}$ and GeI_4 and the activation and deactivation allows for better control. High conversion (80%) was reached for both systems after 21 h with RTCP achieving better control than ITP with M_w/M_ns between 1.3-1.5 for RTCP and 1.5-1.7 for ITP. Spherical particles of ~670 nm were observed for both dispersions.

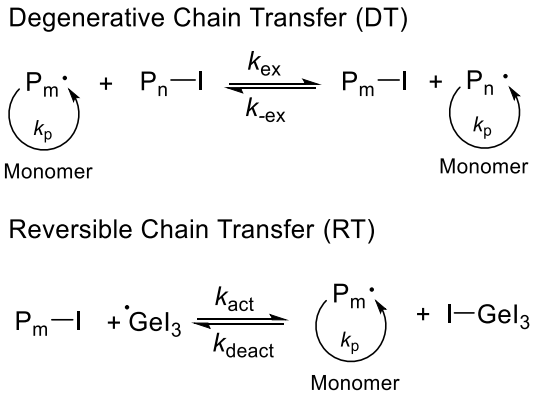

Scheme 3.12: ITP/RTCP mechanism[68]

Howdle and co-workers performed a dispersion RAFT polymerization with MMA by using the CO_2-philic macroRAFT agent made from the fluorinated monomer 1*H*,1*H*,2*H*,2*H*-perfluorooctyl methacrylate (M_n = 15000 g mol^{-1}) (Scheme 3.13). High conversion (99%) was achieved after 20 h with the M_n of 76000 g mol^{-1} in close agreement of the theoretical value of 74970 g mol^{-1}, with an 80:20 ratio of CO_2-phobic to CO_2-philic chains of the block copolymer, and a narrow polydispersity (M_w/M_n of 1.22), and well-defined spherical particles of a broad size distribution observed.[57]

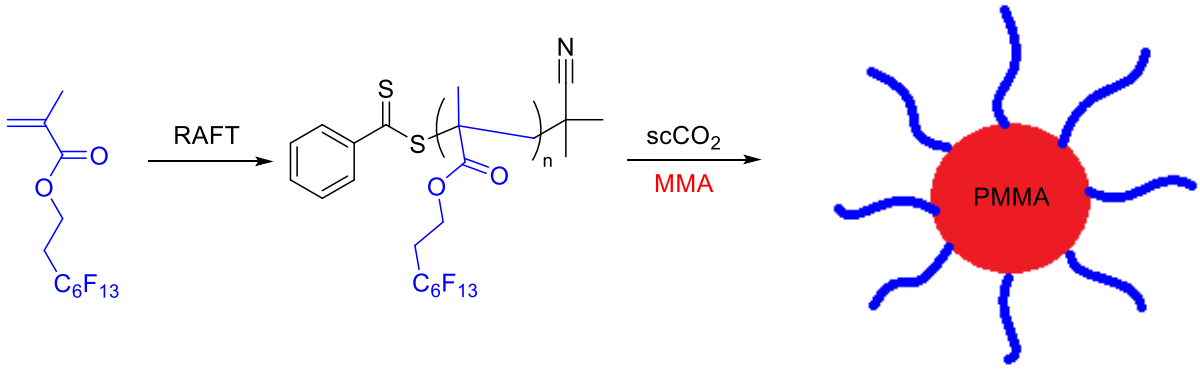

Scheme 3.13: RAFT polymerization of MMA with CO_2-philic macroRAFT agent[57]

Later Howdle used methacrylate terminated PDMS (PDMS-MA) macromonomer as stabilizer for dispersion RAFT of MMA in $scCO_2$ (Scheme 3.14). [104]

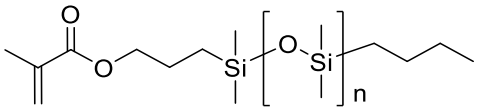

Scheme 3.14: Structure of PDMS-MA

3.2 Aims and Objectives

The aim of this chapter was to perform pioneering work on creating non-spherical nanoparticle objects *via* polymerization induced self-assembly (PISA) in $scCO_2$. ATRP has been chosen as the controlled/living technique and benzyl methacrylate as the dispersion polymerization in supercritical CO_2 using bromine terminated poly(dimethylsiloxane) as an 'inistab' macroinitiator.

For the morphology to change from spheres to rods/vesicles, the generated CO_2-phobic block needs to be sufficiently long relative to the first CO_2-philic (PDMS) block. A criterion which seems to have already been satisfied in many other inistab and macroRAFT dispersion polymerizations in $scCO_2$ (see section 3.1.2 above). However there needs to be sufficient mobility in the core, *i.e*. the effective T_g needs to be low enough. In most of the dispersion polymerizations in section 3.1.2, the second block created *in situ* was polystyrene or PMMA. Even though the temperature has been high (above 100 °C) in the NMP of styrene work in $scCO_2$, it might it be that the T_g in the core has still been too high, despite some presumably swelling with monomer and CO_2, thus giving spheres not high order nano-objects.[46, 27, 47]

In the case of PISA dispersion polymerizations in alcohols/water, it is well-known that benzyl methacrylate (BzMA) can more readily give rods/vesicles than when styrene is used as the second solvophobic block.[93, 95-96, 98] This is mainly due to the T_g of poly(BzMA) being only 54 °C, i.e. well below that of poly(styrene) and poly(MMA), 100 °C and 105 °C, respectively.[105] To get rods/vesicles with styrene, typically a vast excess of styrene is used to swell the core and increase mobility.[106-109] Thus this chapter attempted PISA polymerization in $scCO_2$ where the second block has a markedly low T_g to form poly(BzMA) in an *in situ* controlled/living dispersion polymerization with the aim to get higher order morphologies.

3.3 Experimental

3.3.1 Materials

BzMA (Sigma-Aldrich, 96%) was distilled *in vacuo* to remove radical inhibitor. Anisole (Honeywell, 99%), THF (Sigma-Aldrich, ≥99%) and diethyl ether (Sigma-Aldrich) were distilled over Na wire and benzophenone (Sigma-Aldrich, 95%). CH_2Cl_2 (Sigma-Aldrich, ≥99%), $CDCl_3$ (Sigma-Aldrich, 99.8 atom%), hydroxyl terminated poly(dimethylsiloxane) (Sigma-Aldrich, av. M_n ~4670 g mol^{-1}), 1,1,4,7,10,10-hexamethyltriethylenetetramine (HMTETA, Sigma-Aldrich, 97%), triethylamine (Sigma-Aldrich, ≥99%), 2-bromoisobutyl bromide (Sigma-Aldrich, 98%), glacial acetic acid (Sigma-Aldrich, ≥99.5%), absolute ethanol (Sigma-Aldrich, ≥99.5%) were used as received.

CuBr (Acros Organics, 98%) was purified according to the method by Keller and Wycoff:[110] CuBr was washed slowly with glacial acetic acid (4 x 25 mL) followed by absolute ethanol (3 x 30 mL) and anhydrous diethyl ether (6 x 15 mL). CuBr was placed in a vacuum oven at ~75 °C for 25 mins and stored in an airtight container.

3.3.2 Measurements for polymerizations

Gel Permeation Chromatography (GPC). M_n and polydispersity (M_w/M_n) were measured using a gel permeation chromatography (GPC) system consisting of a Viscotek DM 400 data manager, a Viscotek VE 3580 refractive index detector, a Polar Gel-M guard column (50 × 7.5 mm) and two Mixed -C columns (300 × 7.5 mm). Measurements were carried out at 50 °C at a flow rate of 1.0 mL min^{-1} using THF as the eluent. The columns were calibrated using twelve PS standards (EasiVial PS-H 2 mL, Agilent) (M_n = 580-6035000 g mol^{-1}). M_n is given in g mol^{-1} throughout. All GPC corresponds to polymer before purification, unless otherwise stated. The use of PS standards inevitably leads to error, however control/living character was assessed based on the shapes of molecular weight distributions (MWDs) and trends in M_n and M_w/M_n versus conversion.

Nuclear Magnetic Resonance (NMR) Spectroscopy & Polymer Conversion Measurements. ^{1}H NMR spectra were recorded using a Joel GXFT 400 MHz instrument equipped with a DEC AXP 300 computer workstation. Conversion for solution polymerizations was estimated from ^{1}H NMR spectra obtained in $CDCl_3$. Conversions for the polymerizations of BzMA in anisole were obtained by comparing the integrals of the copolymer peak at 4.79-5.10 ppm (CH_2, 2H) relative to the monomer peak at 5.22 ppm (CH_2, 2H). See Figure 3.1 for monomer and purified polymer spectra.

Conversions for dispersion polymerizations in $scCO_2$ were measured by gravimetry.

The theoretical number-average molecular weights ($M_{n,th}$) were calculated according to:

$$M_{\mathrm{n,th}} = \frac{\alpha[\mathrm{BzMA}]_0 \text{ x } \mathrm{MW}_{\mathrm{BzMA}}}{[\mathrm{PDMS{-}Br}]_0} + \mathrm{MW}_{\mathrm{PDMS-Br}} \qquad (3.1)$$

where α is the fractional monomer conversion, $[BzMA]_0$ is the initial BzMA monomer concentration, $[PDMS\text{-}Br]_0$ is the initial PDMS-Br concentration, MW_{BzMA} is the molecular weight of the monomer, and $MW_{PDMS\text{-}Br}$ is the molecular weight of the initiator (PDMS-Br) determined by GPC.

Scanning Electron Microscopy (SEM). SEM images were obtained using a FEI Phenom SEM with light optical magnification fixed at 20 times, electron optical magnification 120-20,000 times, and digital zoom of 12 times.

Transmission Electron Microscopy (TEM). TEM images were obtained using a Hitachi H7000 using formvar/carbon 200 mesh Cu grids. A small amount of sample (~5 mg/mL) was suspended in pentane and sonicated for 10 min. One drop (~ 0.1 ml) of the colloidal solution was placed on the copper grid and allowed to settle. After 2 min excess solution was carefully removed with filter paper and allowed to dry prior to TEM analysis.

(a)

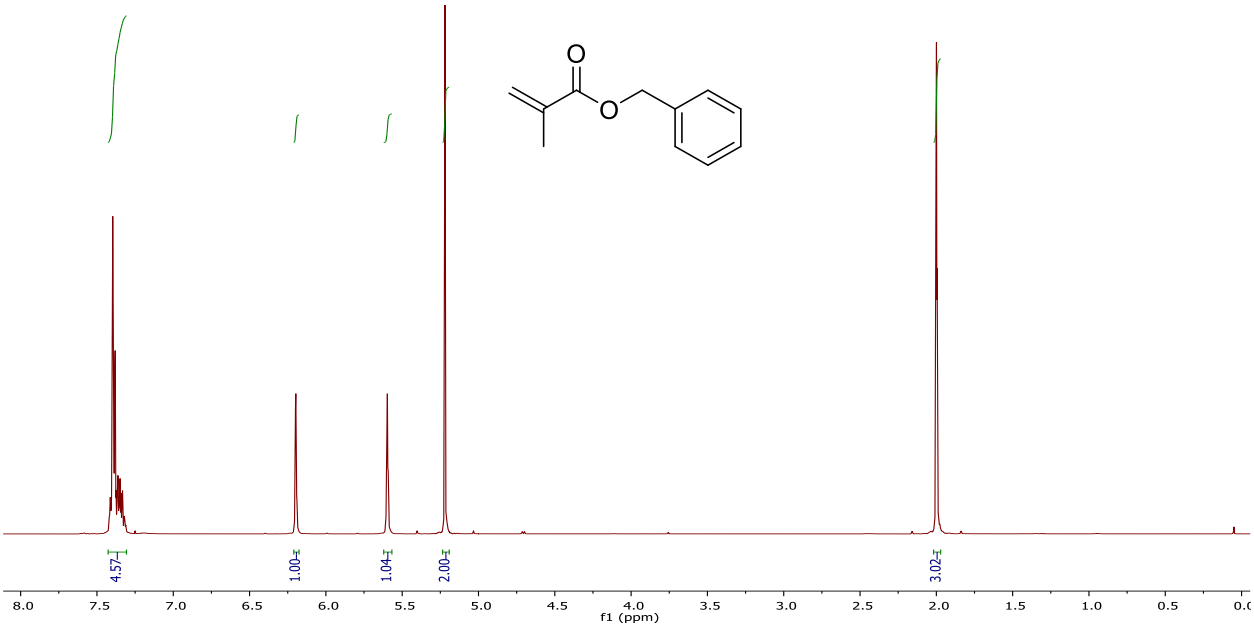

(b)

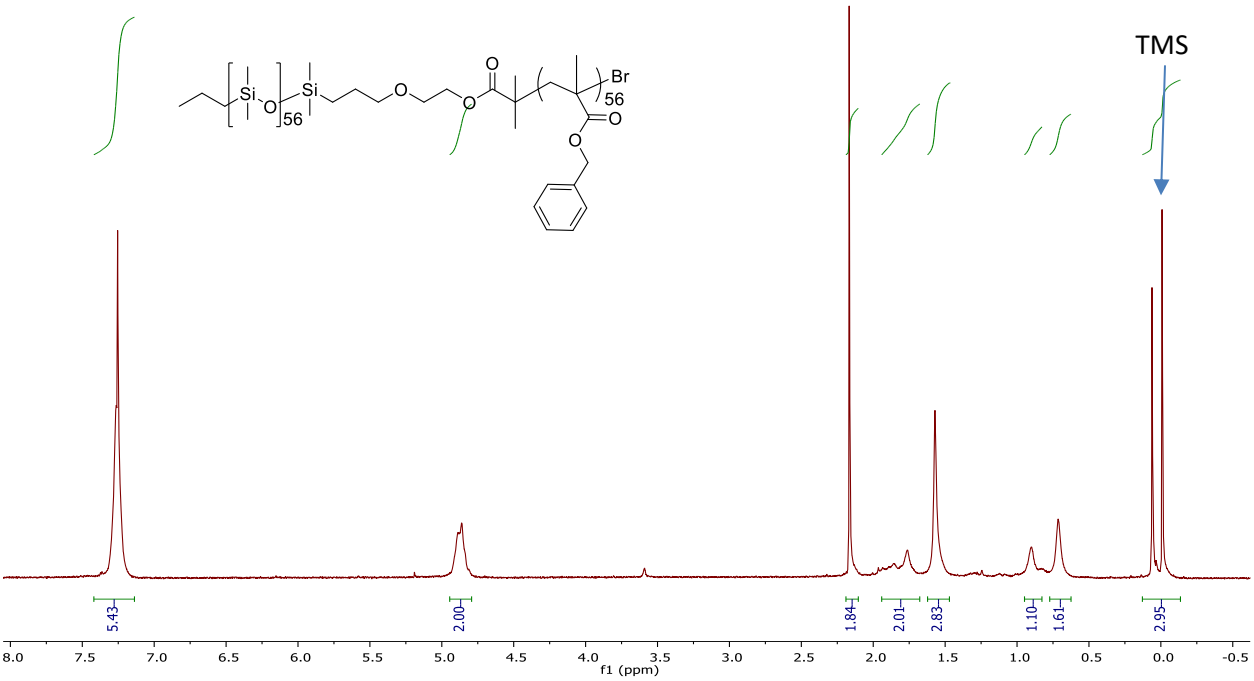

Figure 3.1: ^{1}H NMR spectra ($CDCl_3$) of **(a)** BzMA monomer and **(b)** purified PDMS-*b*-BzMA

3.3.3 Equipment

Polymerizations in $scCO_2$ were conducted in a 25 mL stainless steel Parr reactor with maximum operating pressure and temperature of 40 MPa and 130 °C, respectively. The pressure was produced by a Thar P-50 series high pressure pump to within ±0.2 MPa and the temperature was monitored by a Thar CN6 controller to within ±0.1 °C. Heating was achieved with an oil bath and stirring was achieved using a magnetic stirring bar.

3.3.4 Preparation of bromo-terminated PDMS macroinitiator

PDMS-Br was synthesized according to the procedure by Haddleton and co-workers (Scheme 3.15).[111] PDMS-OH (10.00 g, 2.20 mmol) and triethylamine (1.54 mL, 11.10 mmol) were dissolved in anhydrous THF (300 mL). 2-Bromoisobutyl bromide (0.69 mL, 5.55 mmol) was added dropwise to the mixture whilst stirring. The solution was left overnight to stir at ambient temperature. The solution was filtered and evaporated to dryness. CH_2Cl_2 (300 mL) was added to the yellow residue and washed with saturated $NaHCO_3$ solution (3 x 200 mL). The organic layer was separated, dried with $MgSO_4$, filtered and solvent evaporated to give the product as yellow oil (9.08 g, 88% yield).

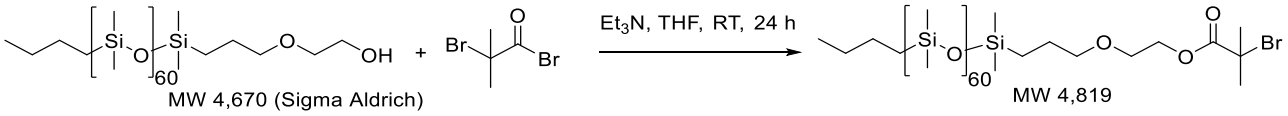

Scheme 3.15: Synthesis of PDMS-Br

3.3.5 Polymerizations of BzMA in anisole

CuBr (5.26 mg, 0.037 mmol), BzMA (0.73 g, 4.13 mmol), PDMS-Br (0.192 g, 0.042 mmol) and anisole (1.00 mL) were added to a test tube containing a stirrer. The tube was sealed with a septum and flushed with N_2 for 30 min. The mixture was heated to 80 °C for 10 min before the addition of HMTETA (8.40 mg, 0.037 mmol) dissolved in anisole (0.30 mL).[111] Polymerizations

were stopped by placing test tubes in an ice-water bath. Conversion (^{1}H NMR), M_n, and M_w/M_n were measured as described above.

3.3.6 Dispersion ATRP of BzMA in $scCO_2$

ATRP of BzMA in $scCO_2$ was conducted in a 25 mL stainless steel reactor. BzMA (9.10 g, 0.052 mol), PDMS-Br (2.40 g, 0.53 mmol), CuBr (66.4 mg, 0.46 mmol) and HMTETA (106.7 mg, 0.46 mmol) were added to the reactor. The reaction mixture was purged for 20 min by passing gaseous CO_2 through the mixture to remove oxygen. Liquid CO_2 (~5 MPa) was added and the reactor immersed in an oil bath. The temperature was raised to the reaction temperature of 80 °C followed by the pressure to the reaction pressure of 30 MPa by addition of CO_2. The reaction was quenched by submersion of the reactor into an ice-water bath. When at approximately room temperature, the CO_2 was vented slowly from the reactor into a conical flask to prevent loss of the polymer. The light blue crystalline solid (9.09 g), was obtained after venting of CO_2, and conversion was measured by gravimetry taking into account remaining monomer using ^{1}H NMR: (79% conversion).

3.3.7 Purification using $scCO_2$

The polymer contained unreacted monomer soluble in $scCO_2$. The polymer was not precipitated using organic solvent, but purified by washing three times using $scCO_2$ at 50 °C and 30 MPa to remove unreacted monomer.[53, 70] ^{1}H NMR was used to confirm that the blue polymer powder was free of BzMA monomer.

3.4 Results and Discussion

3.4.1 Preparation of PDMS-Br

The condensation of PDMS-OH with 2-bromoisobutyryl bromide gave PDMS-Br macroinitiator in high yield of 88%. PDMS-OH was completely converted to PDMS-Br as indicated by the ^{1}H NMR spectrum in Figure 3.2 with the less than quantitative yield presumably due to losses upon extraction. NMR assignments were in agreement with Okubo et al, and Haddleton et al.[102, 111]

PDMS-Br ^{1}H NMR δ: 4.31 (t, J = 4.9 Hz, 2H, CH_2OCO), 3.66 (t, J = 4.9 Hz, 2H), 3.44 (t, J = 7.0 Hz, 2H), 1.96 (s, 6H) with the remaining spectrum presumably the PDMS block by comparison to the ^{1}H NMR spectrum of PDMS-OH.

3.4.2 Polymerizations of BzMA in anisole

These were carried out in order to help optimize ATRP of BzMA in $scCO_2$. The solution polymerizations were based on the method of Matyjaszewski and co-workers, in which BzMA underwent ATRP in anisole at 90 °C with a ratio of BzMA / EBriB / CuBr / HMTETA = 113 / 1 / 0.5 / 0.5 (Scheme 3.16).[112]

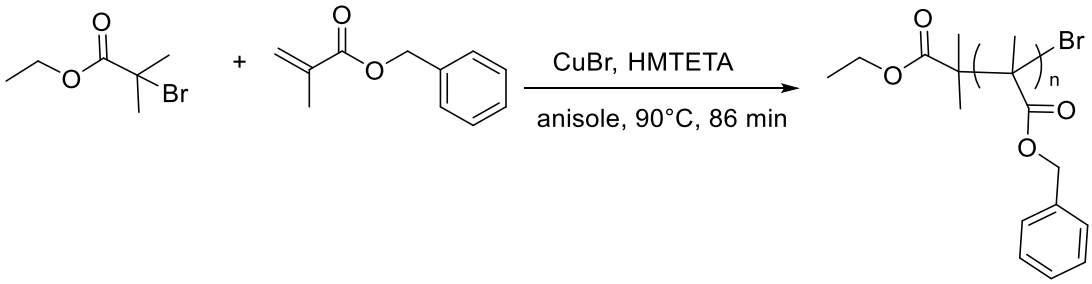

Scheme 3.16: ATRP of BzMA in anisole

After 86 min, 80% conversion was achieved with M_n = 18230 g mol^{-1} and M_w/M_n of 1.26, which was close to the $M_{n,th}$ = 15980 g mol^{-1}. On using these reaction conditions, BzMA/PDMS-Br/CuBr/HMTETA = 113/1/0.5/0.5, after 90 min, 89% conversion was achieved with M_n = 14450 g mol^{-1} and M_w/M_n = 1.20 compared to the $M_{n,th}$ = 22980 g mol^{-1} (Figure 3.3). The

disparity between the experimental and theoretical M_n may be attributed to heterogeneity since the PDMS polymerization solution appeared cloudy.

(a)

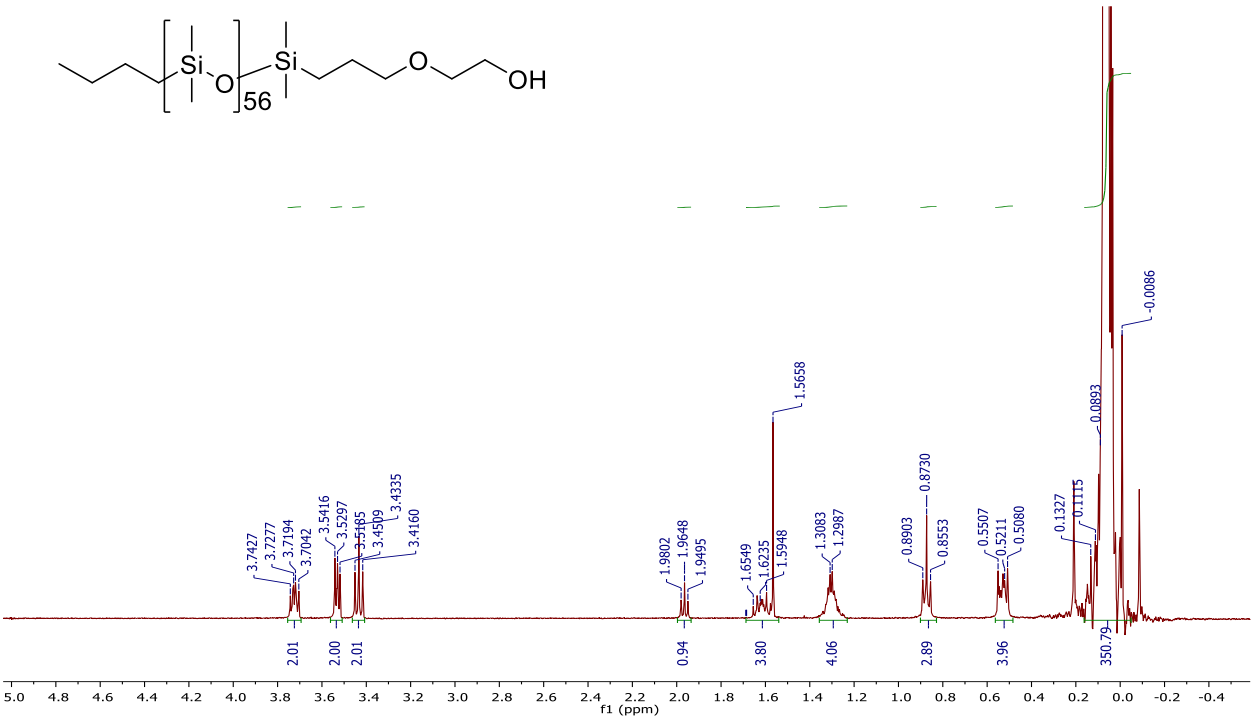

(b)

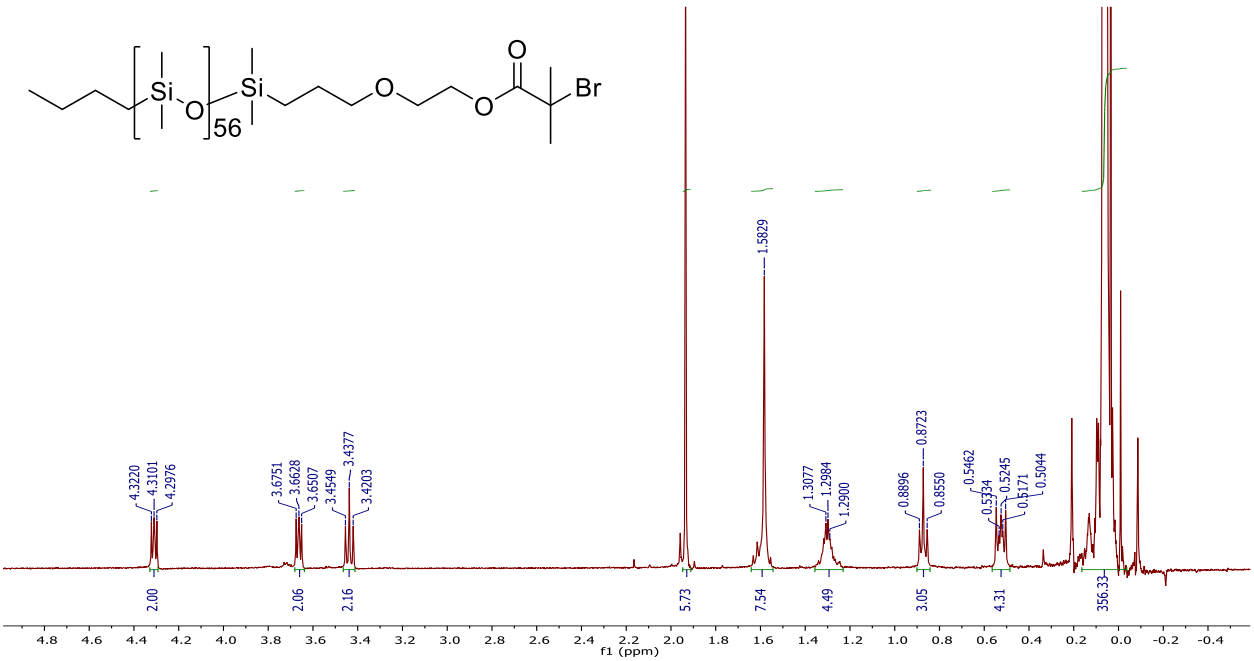

Figure 3.2: ^{1}H NMR spectra ($CDCl_3$, 400 MHz) of **(a)** PDMS-OH (bottom) and **(b)** PDMS-Br

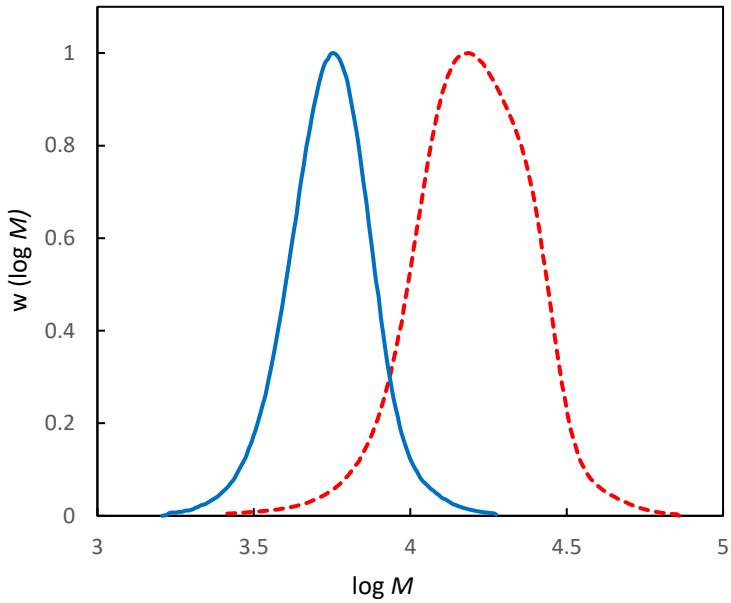

Figure 3.3 MWDs of ATRP polymerization of BzMA in anisole from PDMS-Br (blue solid line) at 89% after 90 min (red dashed line) using the same conditions as Matyjaszewski and co-workers

In order to slow down the polymerization and improve control, the temperature was lowered from 90 to 80 °C with BzMA / PDMS-Br / CuBr / HMTETA = 98 / 1 / 0.88 / 0.88 in anisole used. Figure 3.4 shows that controlled/living character was achieved after 5 and 18 h with narrow MWDs with M_n = 6700 g mol^{-1} and M_w/M_n = 1.19, compared to the $M_{n,th}$ = 11550 at 41% conversion and M_n = 9000 g mol^{-1} and M_w/M_n = 1.32, compared to the $M_{n,th}$ = 18400 at 81% conversion. For polymerizations in anisole, it seems that heterogeneity may have led to MWs about half those expected based upon conversion.

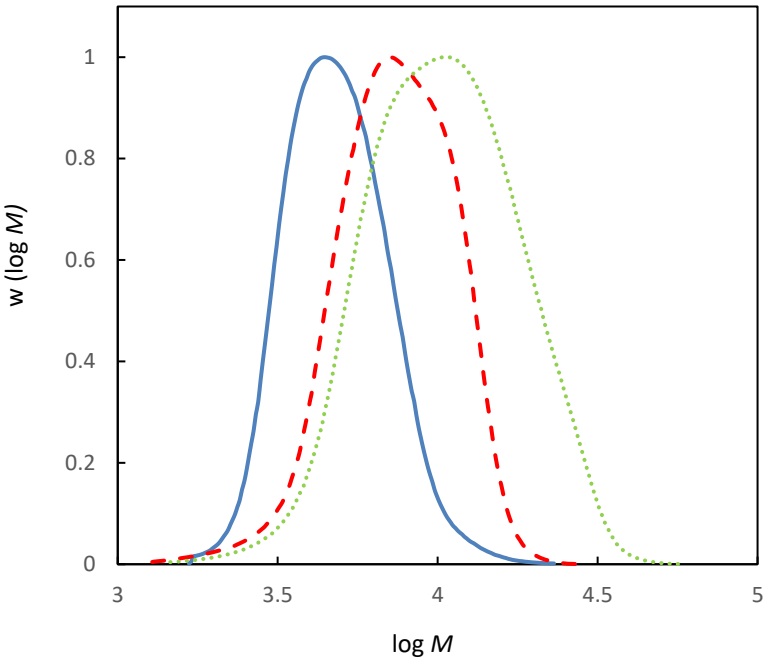

Figure 3.4: MWDs of ATRP polymerizations of BzMA at 80 °C in anisole from PDMS-Br (blue solid line) after 5 h (red dashed line, 41%) and (green dotted, 81% conversion)

3.4.3 Dispersion ATRP of BzMA in $scCO_2$

The dispersion ATRP was performed at 80 °C with BzMA / PDMS-Br / CuBr / HMTETA = 98 / 1 / 0.88 / 0.88. Polymerization using the PDMS-Br macroinitiator (M_n = 4500 g mol^{-1}, M_w/M_n = 1.14) with BzMA yielded a diblock copolymer at 79% conversion with M_n = 14300 g mol^{-1} ($M_{n,th}$ = 18000 g mol^{-1}) and M_w/M_n = 1.27 after 18 h at 80 °C in $scCO_2$ (Figure 3.5). Polymerizations in anisole and $scCO_2$ were similar in rate however monomer concentration was greater in anisole. Narrower MWD was obtained compared to the equivalent polymerization in anisole, although M_n was less than theoretically expected, M_n was however closer to the $M_{n,th}$ than that of the ATRP of BzMA in anisole. The GPC trace shows a low molecular weight tail, possibly due to the generation of short chains by thermal means given the long polymerization time of 18 h.

A light blue powder was obtained which contained up to 10% unreacted monomer, which was separated from the polymer by washing several times with $scCO_2$. ^1H NMR spectroscopy showed the polymer powder to be free of monomer (Figure 3.1b). SEM of the polymer powder showed cavities attributed to the venting process (Figure 3.6a). TEM analysis was carried out by suspending the PDMS-*b*-BzMA sample in pentane followed by sonication. The sample was re-dispersed in pentane to remove any residual stabilizer without affecting the polymer morphologies.[48] A mixture of morphologies was apparent with spherical micelles, as well as higher order objects such as vesicles and rods of a large size range from about 100 nm to 4.5 µm (Figure 3.7).

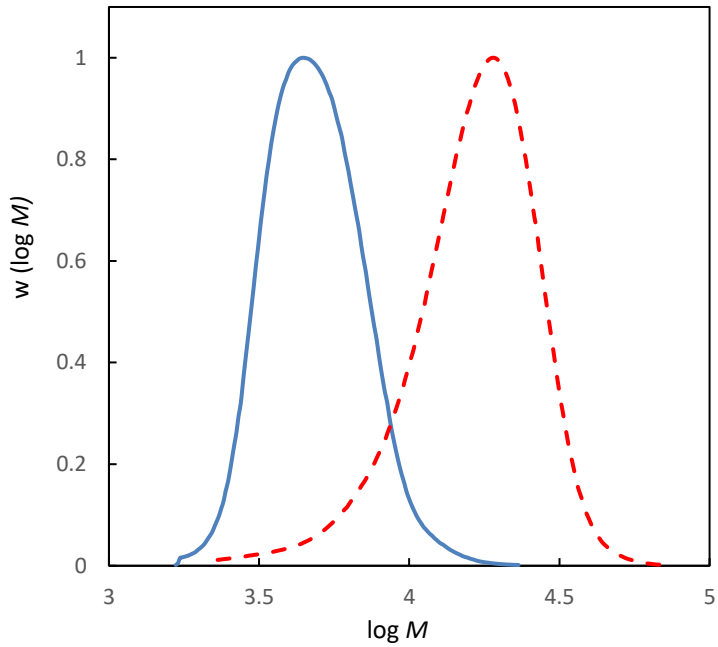

Figure 3.5 MWDs of ATRP dispersion polymerization of PDMS-Br (blue solid line) with BzMA at 79% conversion after 18 h (red dashed line) at 80 °C in $scCO_2$.

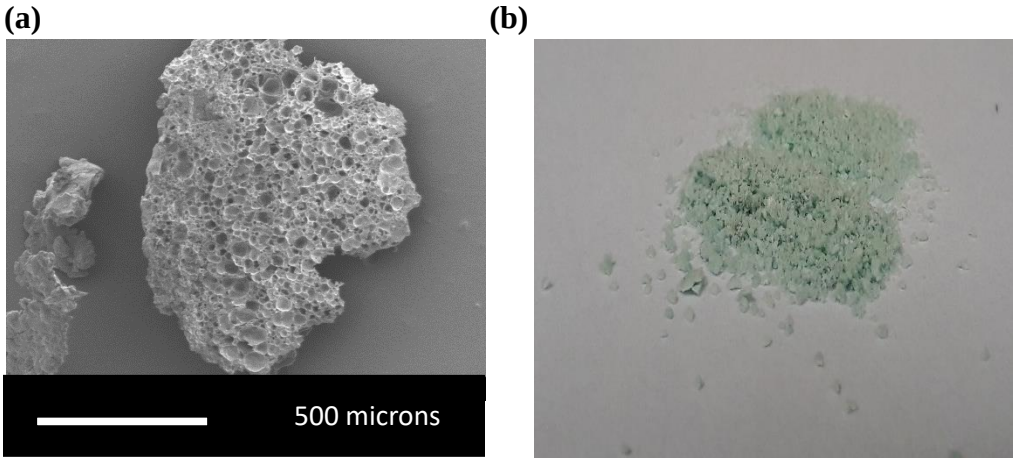

Figure 3.6 (a) SEM and **(b)** optical image of the dry PDMS-*b*-BzMA powder after purification using $scCO_2$

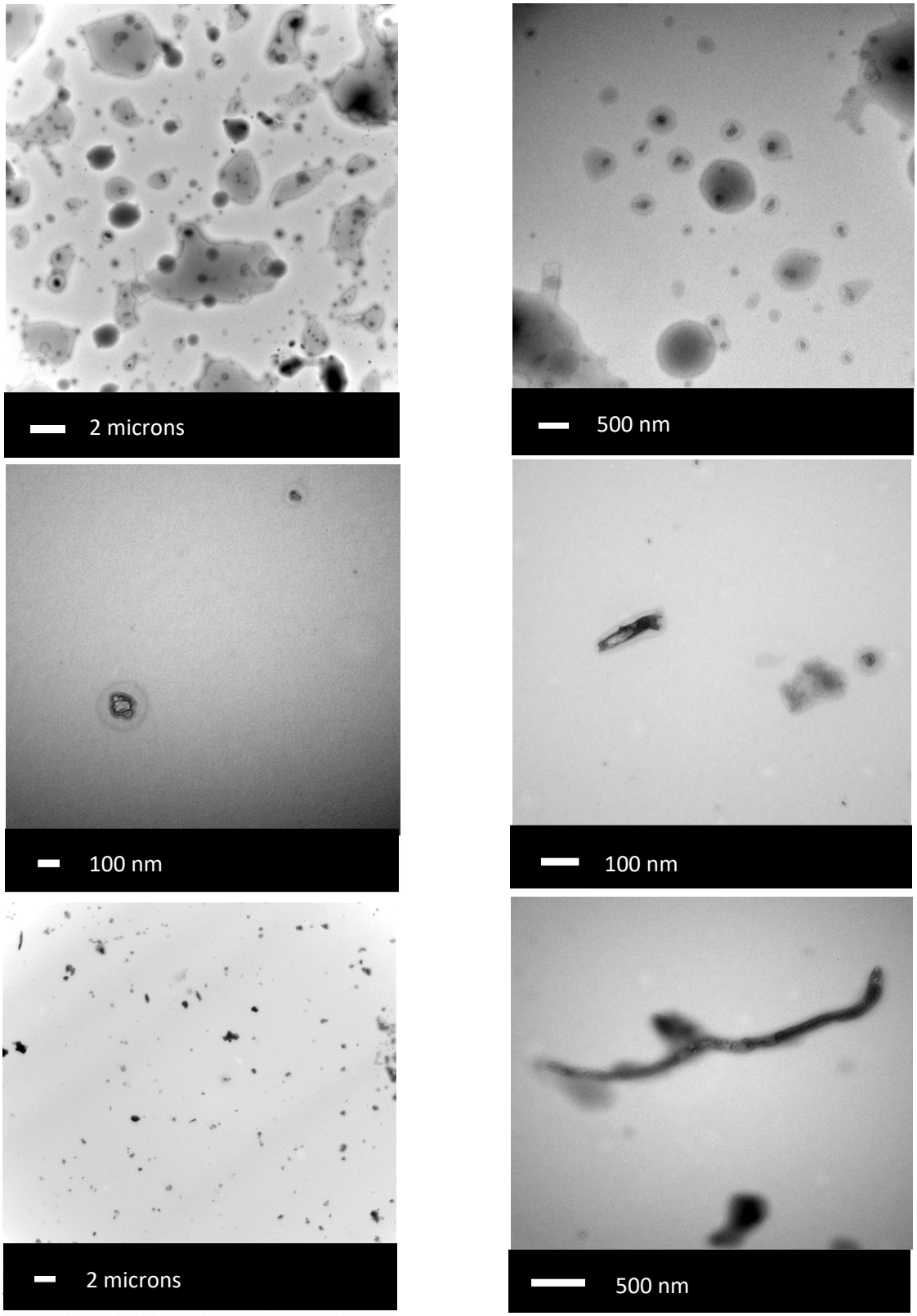

Figure 3.7 TEMs of PDMS-*b*-BzMA after purification using $scCO_2$ and re-dispersed in pentane.

3.5 Conclusions

This chapter has shown that the dispersion polymerization of BzMA in $scCO_2$ using PDMS-Br as a CO_2-philic macroinitiator, where BzMA forms a solvophobic block, can result in PISA leading to non-spherical higher order morphologies than previously observed by using a monomer with a lower T_g than styrene. Reasonable control/living character for the dispersion ATRP in $scCO_2$ of BzMA was achieved up to ~80% conversion with M_n = 14300 g mol^{-1} ($M_{n,th}$ = 18000 g mol^{-1}) and M_w/M_n = 1.27. The polymer was obtained as a free-flowing powder, without the requirement of volatile organic solvents. TEM was carried out by re-dispersing the polymer powder in pentane in order to observe vesicular structures.

Future ATRP will involve adjustments to the size of the solvophobic BzMA block relative to the solvophilic PDMS block in order to improve steric stabilization and self-assembly. Abdullah Alzahrani is the PhD student continuing this work.

Chapter 4

FACILE SYNTHESIS OF THE *N*-[(CYCLOALKYLAMINO)METHYL] ACRYLAMIDE MONOMER CLASS AND RAFT POLYMERIZATIONS GIVING pH-RESPONSIVE POLYACRYLAMIDE BLOCK COPOLYMER VESICLES

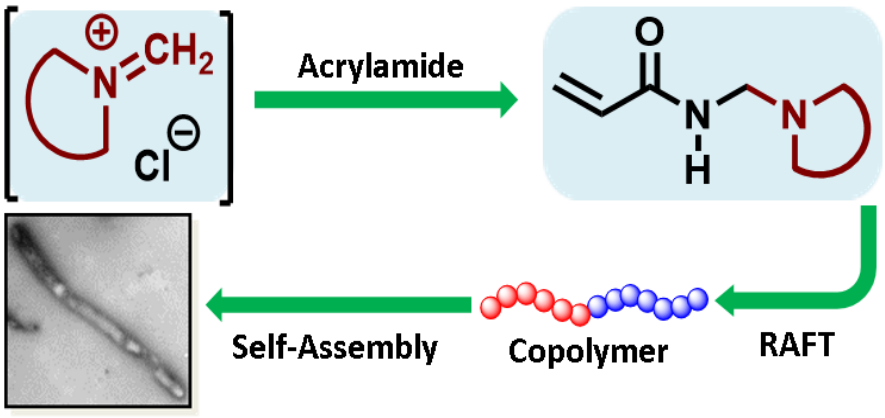

4.1 Introduction

Amphiphilic block copolymers containing saturated nitrogen heterocycles (SNH) have recently been used as the tertiary amino groups can be ionized allowing rapid and reversible changes between a hydrophobic and hydrophilic state. Gao and co-workers have synthesized block copolymers containing PEO and monomers containing SNH substituents, which self-assembled into pH responsive micelles.[113] The pH insensitive dye tetramethyl rhodamine (TMR) was added to the blocks containing the SNH substituents in order to investigate the pH responsive properties of the polymer (Scheme 4.1). At higher pH values the SNH blocks would self-assemble into the hydrophobic cores of the micelles and quench the fluorescence of the TMR moieties. At lower pH values, the SNH blocks became protonated and the micelles disassembled causing an increase of fluorescence from the TMR moieties.

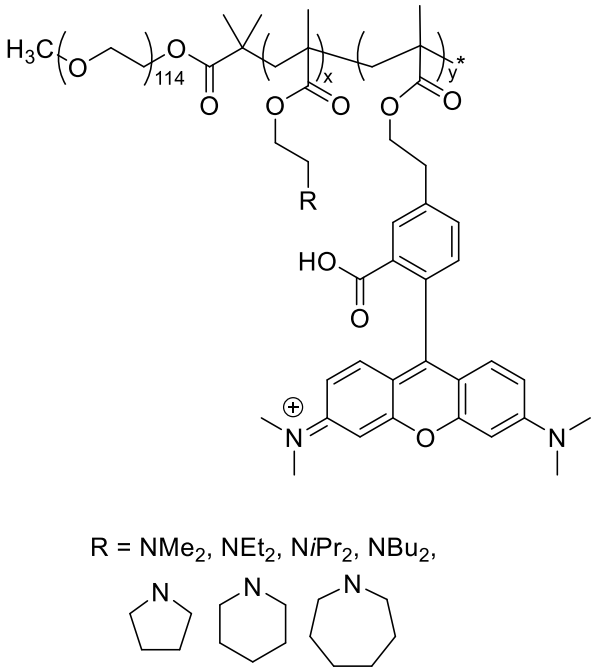

Scheme 4.1: Structures of the PEO-*b*-SNH copolymers

Li and co-workers reported the synthesis of pH-responsive nanoparticles made from platinum prodrug incorporated dendrimers containing pH-sensitive azepane substituents enabling nanoparticle collapse in the acidic environments of tumour cells.[114] The polymerizations of 2-(cycloalkylamino)ethyl (meth)acrylates or 2-(cycloalkylamino)ethyl (meth)acrylamides using

RDRP[21] with NMP,[14] ATRP,[113, 115] and RAFT[114, 116-118] (Scheme 4.2a) containing pH-responsive SNHs have been reported. However, there are few reports of polymerizations of *N*-[(cycloalkylamino)methyl] (meth)acrylamides containing a methylene amine rather than an ethyl amine pendent probably due to difficulties in the synthesis of these monomers (Figure 4.2b).[119-122]

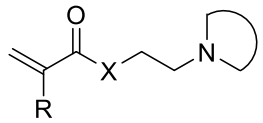

R = H, Me
X = O, NH

a) Well Established Monomer Class

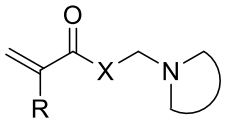

b) Not Utilized in Block Copolymers

Scheme 4.2: Saturated nitrogen heterocycle (SNH) containing monomers

The NMR data for *N*-[(morpholino-4-yl)methyl]prop-2-enamide **1a** (Scheme 4.3) that was published in literature was inaccurate.[121] Monomer preparations have been reported by Müller and co-workers based on a one-pot Mannich reaction approach using formaldehyde and acrylamide to give *N*-(hydroxymethyl)acrylamide followed by addition of the secondary amine to yield the monomer.[119-120] Repeating the procedure resulted in low yields due to inadvertent thermal polymerization or degradation of the monomer or intermediates at the elevated reaction temperatures (~80 °C) with monomer isolation requiring difficult distillations from the aqueous reaction mix.

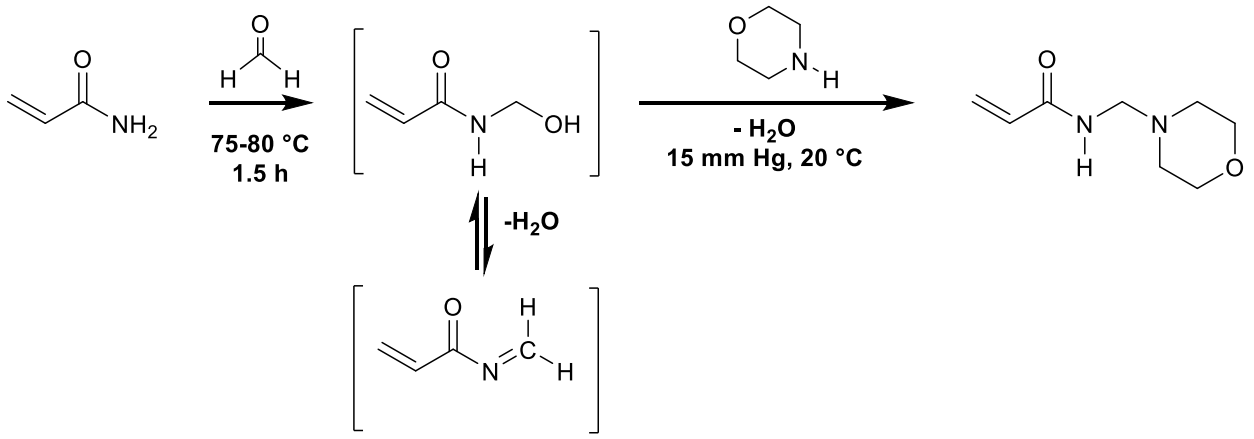

Scheme 4.3: Synthesis of monomer by the one-pot Mannich reaction approach

A new method for the synthesis of *N*-[(cycloalkylamino)methyl] acrylamides was invented (Scheme 4.4), involving the quaternization of an aminal to generate a methylene Schiff base salt, [123-124] followed by the nucleophilic addition of acrylamide onto the Schiff base salt to give the monomer as a hydrochloride salt. The new method has allowed the efficient preparation of acrylamide monomer **1a-1c** on a multi-gram scale *via* basification of the respective hydrochloride salts **1a.HCl-1c.HCl**. The new method allowed for the first controlled/living polymerizations of these monomers,[125] as well as their respective hydrochloride salts, with amphiphilic polyacrylamide block copolymers shown to form vesicles, and pH-responsive nanoparticles.

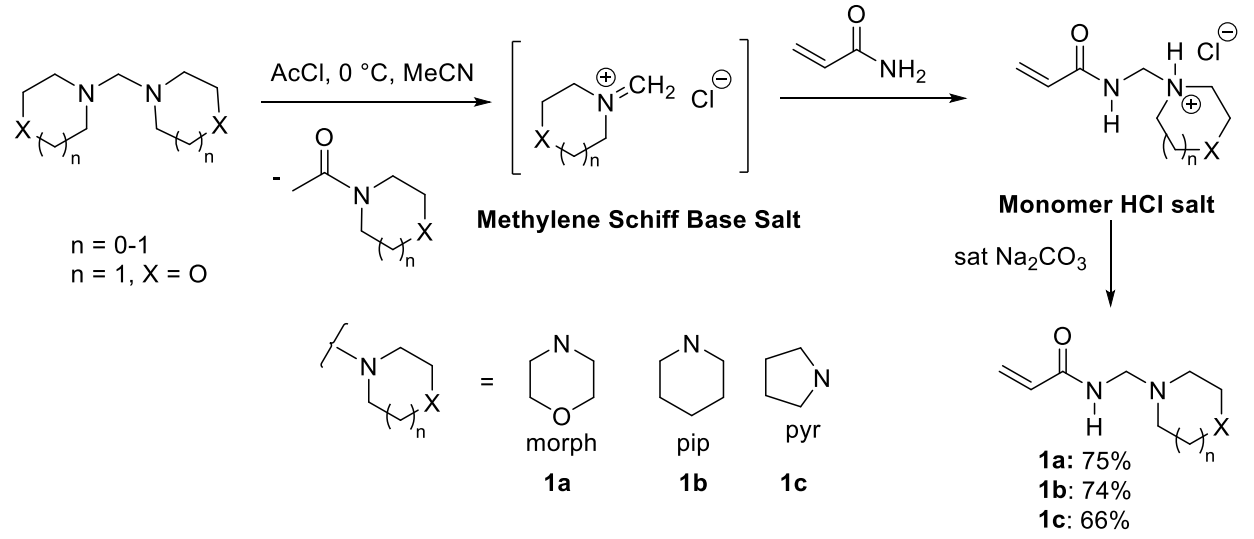

Scheme 4.4: New approach to synthesis of *N*-[(cycloalkylamino)methyl] acrylamides

4.2 Experimental

4.2.1 Materials

Aminal 4,4ˈ-methylenebis(morpholine) bp 66-67 °C (0.25 mmHg), 1,1ˈ-methylene dipiperidine bp 62-64 °C (0.25 mmHg) and 1,1ˈ-methylene dipyrrolidine bp 50-52 °C (0.25 mmHg)] were readily prepared in high yields (78-98%) from formalin (Sigma-Aldrich, 37%) and cycloamine [morpholine (Sigma-Aldrich, ≥99%), piperidine (Sigma-Aldrich, ≥99%), and pyrrolidine (Across Organics, 99%) respectively] using a literature procedure (Scheme 4.5).[126-127]

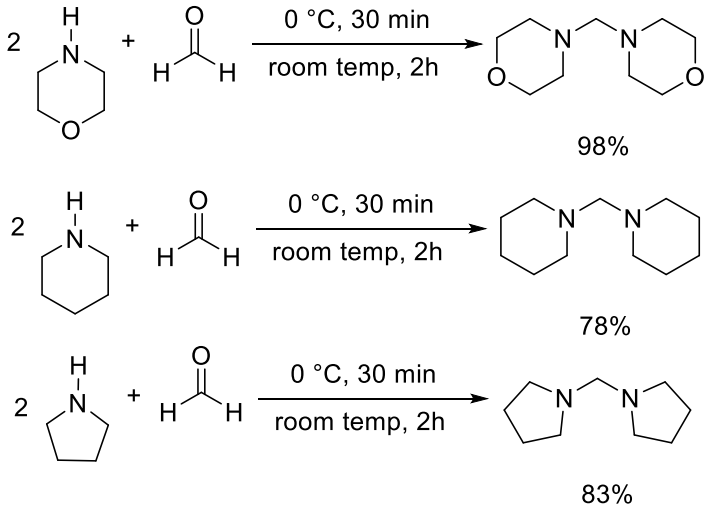

Scheme 4.5: Synthesis of Aminals

Distilled aminals were stored under vacuum in dry desiccators at room temperature. Acetyl chloride (AcCl, Sigma-Aldrich, 98%) and acrylamide (Aldrich, 97%) were used as received. 2,2′-Azobisisobutyronitrile (AIBN, DuPont Chemical Solution Enterprise) was recrystallized twice from MeOH before use. 2,2′-Azobis[2-(2-imidazolin-2-yl)propane]dihydrochloride (VA-044, Wako) and 2-(dodecylthiocarbonothioylthio)-2-methylpropionic acid (DDMAT, Sigma-Aldrich, 98%) were used as received. 1,4-Dioxane (Sigma-Aldrich, ≥99.0%) and Milli-Q water were used directly as solvents for polymerization. *N*-*tert*-Butylacrylamide (TBAM, TCI Chemicals) was recrystallized from hexanes and *N*,*N*-dimethylacrylamide (DMA, TCI, 98%) was distilled *in vacuo* to remove radical inhibitor. Acetonitrile (MeCN, Sigma-Aldrich, ≥99.9%), CH_2Cl_2 (Sigma-Aldrich, ≥99%), *N*,*N*-dimethylformamide (DMF, Sigma-Aldrich, HPLC-grade,

≥99.9%), diethyl ether (Et_2O, Sigma-Aldrich, ≥99.5%) hydrochloric acid (Sigma-Aldrich, 36.5-38%), $CDCl_3$ (Sigma-Aldrich, 99.8 atom%), D_2O (99.9 atom%, Sigma-Aldrich), and LiBr (Sigma-Aldrich, 99%) were used as received. For monomer synthesis MeCN was distilled over 3 Å molecular sieves then CaH_2 (Sigma-Aldrich, 95%), and Et_2O was distilled over Na wire and benzophenone (Sigma-Aldrich, 95%).

4.2.2 Equipment and measurements

Polymerizations. All were carried out in borosilicate glass tubes sealed with septa and flushed with N_2 for 30 min.

Nuclear Magnetic Resonance (NMR) Spectroscopy. ^{1}H NMR spectra were recorded using a Joel GXFT 400 MHz instrument equipped with a DEC AXP 300 computer workstation. For water soluble polymers D_2O was used as the NMR solvent, and for amphiphilic polymers $CDCl_3$ was used as the NMR solvent, and conversion was estimated by sampling directly from the reaction (without purification). Conversions were estimated using the integral for a polymer peak (where appropriate deducting the monomeric contribution of peaks containing both polymer and monomer contributions) relative to a monomer vinyl peak.

Theoretical number average molecular weight ($M_{n,th}$) was calculated according to equation 4.1:

$$M_{\mathrm{n,th}} = \left(\frac{[Monomer]_0}{[RAFT]_0} \times MW_{Monomer} \times Conversion\right) + MW_{RAFT} \qquad (4.1)$$

RAFT represents DDMAT or polymeric macroRAFT agent. MW_{monomer} and MW_{RAFT} are the molecular weights of the monomer and (macro)RAFT agent respectively. Conversion was measured by ^{1}H NMR (as above).

Gel Permeation Chromatography (GPC). Molar mass distributions were measured using Agilent Technologies 1260 Infinity liquid chromatography system using a Polar Gel-M guard column (50 × 7.5 mm) and two Polar Gel-M columns (300 × 7.5 mm). DMF containing LiBr (0.01 M) was used as eluent at 1.0 mL·min^{-1} at 60 °C. Twelve narrow polydispersity poly(methyl methacrylate, MMA) standards (EasiVial PM 2 mL, Agilent) were used to calibrate the GPC system. Samples were dissolved in the eluent and filtered through a PTFE membrane with 0.2 μm pore size before injection (100 μL). Experimental molar mass (M_n) and polydispersity

(M_w/M_n) values were determined by conventional calibration using Agilent GPC/SEC Software for Windows (version 1.2; Build 3182.29519). (M_n = 550 – 2,136,000 g.mol^{-1}). Number average molecular weight (M_n) values are not absolute, but relative to linear poly(MMA) standards (as above).

Transmission Electron Microscopy (TEM). TEM images were obtained using a Hitachi H7000 using formvar/carbon 200 mesh Cu grids. One drop (~ 0.1 ml) of the colloidal solution was placed on the copper grid and allowed to settle. After 10 min excess solution was carefully removed with filter paper and allowed to dry for a further 5 min prior to TEM analysis.

4.2.3 Monomer synthesis: *N*-[(cycloamino)methyl]acrylamides (*N*-[(cycloalkylamino)methylene]prop-2-enamides) (**1a-1c**)

AcCl (14.3 mL, 0.2 mol) was added over 30 min to the aminal (0.2 mol) in MeCN (40 mL) at 0 °C. Acrylamide (14.2 g, 0.2 mol) in MeCN (40 mL) was added, and stirred at room temperature for 2 h. Et_2O (50 mL) was added and the hydrochloride salt of the monomer precipitated, filtered, and dried under vacuum. The hydrochloride salt was recrystallized, dried, and characterized.

Saturated Na_2CO_3 solution (50 mL) was added to the hydrochloride salt suspended in CH_2Cl_2 (50 mL) and the solution stirred for 20 min. The organic layer was separated and the aqueous layer was washed with CH_2Cl_2 (4 x 30 mL). The combined organic extracts were dried ($MgSO_4$), filtered, and evaporated to dryness to give the monomer, which was recrystallized.

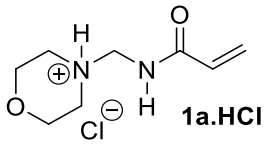

1a.HCl

***N*-[(morpholin-4-yl)methyl]prop-2-enamide hydrochloride (1a.HCl):** white solid; mp 146-148 °C (recryst. from MeCN); δ_H (400 MHz, $(CD_3)_2SO$) 2.84-3.36 (m, 4H), 3.66-4.05 (m, 4H), 4.54 (d, *J* 6.8 Hz, 2H, 1-CH_2), 5.79 (dd, *J* 10.2, 1.9 Hz, 1H, *cis*-H), 6.26 (dd, *J* 17.2, 1.9 Hz, 1H, *trans*-H), 6.43 (dd, *J* 17.2, 10.2 Hz, 1H), 9.60 (t, *J* 6.8 Hz, 1H, NH), 11.22-11.42 (brs, 1H, NH); δ_C (100 MHz, $(CD_3)_2SO$) 48.6 (CH_2), 58.6 (1-CH_2), 63.0, 128.3 (both CH_2), 130.3 (CH), 166.2 (C=O).

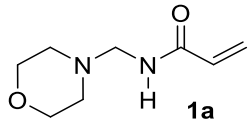

1a

***N*-[(morpholin-4-yl)methyl]prop-2-enamide (1a):** 25.5 g, 75%, white solid; mp 93-95 °C (recryst. from MeCN); ν_{max} (neat, cm^{-1}) 3254, 2860, 2825, 1669, 1648 (C=O), 1608, 1535, 1228, 1155, 1109; δ_H (400 MHz, $CDCl_3$) 2.57 (t, *J* 4.7 Hz, 4H), 3.69 (t, *J* 4.7 Hz, 4H), 4.17 (d, *J* 6.5 Hz, 2H, 1-CH_2), 5.70 (dd, *J* 10.3, 1.4 Hz, 1H, *cis*-H), 5.91-6.05 (brs, 1H, NH), 6.10 (dd, *J* 17.0, 10.3 Hz, 1H), 6.32 (dd, *J* 17.0, 1.4 Hz, 1H, *trans*-H); δ_C (100 MHz, $CDCl_3$), 50.5 (CH_2), 61.6 (1-CH_2), 66.4, 127.5 (both CH_2), 130.6 (CH), 166.2 (C=O); HRMS (ESI) *m/z* $(M+H)^+$, $C_8H_{15}N_2O_2$, calcd. 171.1134, observed 171.1136.

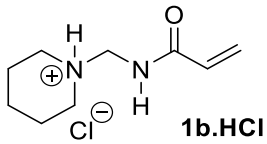

1b.HCl

***N*-[(piperidin-1-yl)methyl]prop-2-enamide hydrochloride (1b.HCl):** white solid, mp 143-145 °C (recryst. from MeCN); δ_H (400 MHz, $(CD_3)_2SO$) 1.27-1.42 (m, 1H), 1.60-1.84 (m, 5H), 2.82 (d, *J* 11.2 Hz, 2H), 3.30 (d, *J* 11.2 Hz, 2H), 4.47 (d, *J* 6.5 Hz, 2H, 1-CH_2), 5.81 (dd , *J* 10.0, 1.9 Hz, *cis*-H), 6.27 (dd *J* 17.1, 1.9 Hz, 1H, *trans*-H), 6.38 (dd, *J* 17.1, 10.0 Hz, 1H), 9.32-9.43 (brs, 1H, NH), 9.91-10.12 (brs, 1H, NH); δ_C (100MHz, $(CD_3)_2SO$) 21.4, 22.3, 49.8 (all CH_2), 58.7 (1-CH_2), 128.3 (CH_2), 130.6 (CH), 166.4 (C=O).

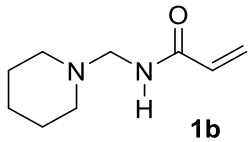

1b

***N*-[(piperidin-1-yl)methyl]prop-2-enamide (1b):** 24.9 g, 74%, white solid, mp 55-57 °C (recryst. from Et_2O); ν_{max} (neat, cm^{-1}) 3276, 2936, 2807, 1669, 1650 (C=O), 1611, 1528, 1372, 1227, 1216, 1175, 1027; δ_H (400 MHz, $CDCl_3$) 1.35-1.44 (m, 2H), 1.55 (p, *J* 5.5 Hz, 4H), 2.49 (t, *J* 5.5 Hz, 4H), 4.13 (d, *J* 6.4 Hz, 2H, 1-CH_2), 5.65 (dd, *J* 10.2, 1.4 Hz, 1H, *cis*-H), 6.10 (dd, *J* 17.0, 10.2 Hz, 2H, CH, NH), 6.29 (dd, *J* 17.0, 1.4 Hz, 1H, *trans*-H); δ_C (100 MHz, $CDCl_3$) 24.2,

26.0, 51.5 (all CH_2), 62.2 (1-CH_2) 126.8 (CH_2), 131.2 (CH), 166.6 (C=O); HRMS (ESI) *m/z* $(M+H)^+$, $C_9H_{17}N_2O$, calcd. 169.1341, observed 169.1335.

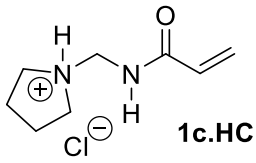

1c.HCl

***N*-[(pyrrolidin-1-yl)methyl]prop-2-enamide hydrochloride (1c.HCl):** white solid, mp 64-66 °C, (recryst. from EtOAc); δ_H (400 MHz, $(CD_3)_2SO$) 1.78-1.97 (m, 4H), 2.91-3.54 (m, 4H), 4.53 (d, *J* 6.8 Hz, 2H, 1-CH_2), 5.78 (dd, *J* 10.2, 1.9 Hz, 1H, *cis*-H), 6.24 (dd, *J* 17.2, 1.9 Hz, 1H, *trans*-H), 6.41 (dd, *J* 17.2, 10.2 Hz, 1H), 9.72 (t, *J* 6.8 Hz, 1H, NH), 10.96-11.10 (brs, 1H, NH); δ_C (100 MHz, $(CD_3)_2SO$) 23.1, 50.6 (both CH_2), 56.0 (1-CH_2), 128.3 (CH_2), 130.6 (CH), 166.4 (C=O). **1c.HCl** should be stored under vacuum in a desiccator at room temperature.

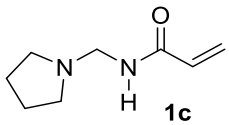

1c

***N*-[(pyrrolidin-1-yl)methyl]prop-2-enamide (1c):** 20.3 g, 66%, white solid, mp 29-30 °C, (recryst. from EtOAc), ν_{max} (neat, cm^{-1}) 3268, 2964, 1656 (C=O), 1627, 1537, 1232, 1135, 1031; δ_H (400 MHz, $CDCl_3$) 1.69-1.81 (m, 4H), 2.57-2.65 (m, 4H), 4.25 (d, *J* 6.3 Hz, 1H, 2H, 1-CH_2), 5.65 (dd, *J* 10.2, 1.4 Hz, 1H, *cis*-H), 6.10 (dd, *J* 17.0, 10.2 Hz, 1H), 6.28 (dd, *J* 17.0, 1.4 Hz, 1H, *trans*-H), 6.31-6.37 (brs, 1H, NH); δ_C (100 MHz, $CDCl_3$), 23.7, 50.9 (both CH_2), 58.3 (1-CH_2), 127.0 (CH_2), 130.9 (CH), 165.9 (C=O); HRMS (ESI) *m/z* $(M+H)^+$, $C_8H_{15}N_2O$, calcd 155.1184, observed 155.1176. Monomer **1c** should be stored under vacuum in a desiccator at room temperature.

4.2.4 General polymerization procedure to give amphiphilic copolymers

Solutions were heated in an aluminum heating block for the specified times. Polymerizations were stopped by placing test tubes in an ice-water bath. Conversion, $M_{n,}$ and M_w/M_n were measured as described above. Polymers were isolated by dissolving the polymerization mixture in a minimum amount of DMF and precipitating using an excess of Et_2O, except for TBAM containing amphiphilic block copolymers, which were precipitated using excess Et_2O/petroleum ether (1/1). The polymer was filtered and dried at room temperature under vacuum for 24 h.

4.2.4.1 Preparation of poly(**1a**)$_{60}$

Monomer **1a** (0.425 g, 2.50 mmol) was added to 1 mL solution of dioxane/water (80/20) containing DDMAT (0.03 mmol) and AIBN (0.3 x 10^{-4} mmol) from a stock solution, and heated at 65 °C for 4.5 h to give poly(**1a**) macroRAFT, M_n = 10550 g.mol^{-1}, M_w/M_n = 1.21, 76% conv., isolated = 0.29 g.

4.2.4.2 Preparation of poly(**1a**)$_{60}$-*b*-poly(**1a**)$_{70}$

Poly(**1a**)$_{60}$ macroRAFT (0.03 mmol) and **1a** (0.425 g, 2.50 mmol) were added to a 1 mL solution of dioxane/water (80/20) containing AIBN (7.5 x 10^{-5} mmol from a stock solution), and heated at 70 °C for 15 h. The polymer was isolated as described above.

4.2.4.3 Preparation of poly(**1a**)$_{60}$-*b*-poly(**1b**)$_{20}$

Poly(**1a**)$_{60}$ macroRAFT (0.06 mmol) and monomer **1b** (0.504 g, 3.00 mmol) were added to a 1 mL solution of dioxane/water (80/20) containing VA-044 (0.97 mg, 3.00 x 10^{-3} mmol) and heated at 70 °C for 2 h. The polymer was isolated as described above.

4.2.4.4 Representative preparation of amphiphilic block copolymers using TBAM

TBAM (0.127 g, 1.00 mmol) was added to a 1 mL solution of dioxane/water (85/15) containing poly(**1a**) macroRAFT agent (M_n = 22950, M_w/M_n = 1.36; 94 mg, 4.1 x 10^{-3} mmol) and VA-044

(0.1 x 10^{-3} mmol from a stock solution) and heated at 70 °C for 2 h. Poly(**1a**)$_{130}$-*b*-(TBAM)$_{171}$ was isolated as described above.

4.2.4.5 Self-assembly and TEM analysis

Self-assembly of polymer samples were carried out using the method of Zhang and Eisenberg.[85] For example, precipitated poly(**1a**)$_{60}$-*b*-(**1b**)$_{20}$-*b*-(TBAM)$_{47}$ (41.3 mg, 0.0024 mmol) was dissolved in DMF (4 mL), and distilled water (1 mL) added slowly with vigorous stirring at a rate of ~1 drop every 10 s. The resulting solution was placed in a dialysis bag (molecular weight cut-off, MWCO = 3500) and exchanged with water (500 ml) for 12 h to exclude the organic solvent. The distilled water was replaced twice and dialyzed for a further 6 h each time. A direct sample and a sample which was treated with concentrated hydrochloric acid until it had a pH of ~2 were analyzed *via* TEM (see above).

4.3 Results and Discussion

4.3.1 Monomer synthesis

As opposed to the condensation of formaldehyde with acrylamide as prescribed in the Mannich approach (Scheme 4.3),[119-122] the first step involved the preparation of aminals by the condensation of formaldehyde (37% formalin) with a secondary cyclic amine in high yields (80-99%) according to literature procedures (Scheme 4.5).[126-127] Acetyl chloride was used to quarternize the aminals (4,4ˈ-methylenebis(morpholine), 1,1ˈ-methylene dipiperidine and 1,1ˈ-methylene dipyrrolidine) in dry acetonitrile, which formed the methylene Schiff base salts *in situ*, along with the *N*-acetyl cycloamine as a side-product. Acrylamide was added to the methylene Schiff Base salt, and the hydrochloride monomer salts (**1a.HCl**, **1b.HCl**, **1c.HCl**) were isolated after precipitation from diethyl ether, which separated the *N*-acetyl cycloamine since the latter remained in solution. The HCl salts were suspended in CH_2Cl_2 and basified to give monomers **1a-1c**. The synthesis was performed at 0 °C to room temperature in order to prevent any potential thermal side-reactions giving 20-25 g of the three monomers **1a-1c**. Monomer yields for **1a** and **1b** were ~75% while **1c** had a lower yield of 66% due to its inherent hygroscopic nature and low melting point.

4.3.2 Preparation of amphiphilic block copolymers

Narrow MWD (M_w/M_n = 1.21) poly(**1a**)$_{60}$ with M_n close to $M_{n,th}$ was prepared in 80/20 dioxane/water at 76% conversion over 4.5 h at 65 °C using [DDMAT]/[AIBN] = 100 (Scheme 4.6 & Table 4.1), which was used as the macroRAFT agent in amphiphilic block copolymer synthesis. Given that it was difficult to obtain full conversion with simultaneous good control/living character for this first block, it was decided to stop polymerizations and isolate intermediate hydrophilic blocks prior to chain extensions with the hydrophobic monomer, TBAM. The low concentrations of initiator used throughout theoretically led to very low fractions of initiator-derived dead chains (according to eq. 4.2).[78, 128-129]

$$L = \frac{[RAFT]_0}{[RAFT]_0 + 2f[I]_0(1 - e^{-k_d t})\left(1 - \frac{f_c}{2}\right)} \quad (4.2)$$

Eq. 4.2 estimates the theoretical fraction of living chains (L). The factor "2" accounts for one molecule of azo-initiator yielding two primary radicals with the efficiency f (assumed to be equal to 0.5). The decomposition rate constant is k_d is taken as 4.30 x 10^{-4} s^{-1} for VA-044 at 70 °C in water/dioxane (80:20).[128] The quantity $1 - \frac{f_c}{2}$ represents the number of chains produced in a radical−radical termination event with the coupling factor f_c assumed to be zero. The chain extension of poly(**1a**)$_{60}$ with morpholine **1a** used ~0.2% AIBN relative to macroRAFT agent at 70 °C giving a more well-defined large hydrophilic first block of poly(**1a**)$_{130}$ (Figure 4.1a(i)) than from attempts to make a similar sized block directly from DDMAT, as is expected since for all reversible deactivation radical polymerizations livingness decreases as targeted $M_{n,th}$ increases. The large resultant poly(**1a**)$_{130}$ made in 15 h had a narrow MWD of $M_n \approx 23000$ ($M_W/M_n = 1.36$) at 84% conversion with M_n remarkably close to $M_{n,th}$ despite the inherent error due to GPC calibration. When extending with the hydrophobic monomer it was important to consider the influence of the RAFT agent α- and ω-end groups on self-assembly behavior, in particular the large dodecyl group of the trithiocarbonate (derived from DDMAT).[130-131] VA-044 was used as the initiator for the 2 h poly(**1a**)$_{60}$ and poly(**1a**)$_{130}$ chain extensions with TBAM at 70 °C to respectively give narrow MWD amphiphilic diblock copolymers (M_w/M_n = 1.19 and 1.27) poly(**1a**)$_{60}$-*b*-(TBAM)$_{38}$, and poly(**1a**)$_{130}$-*b*-(TBAM)$_{171}$ in 80% and 70% conversion (Figures 4.1a(i) & 4.1b(ii)). The well-defined triblock [poly(**1a**)$_{60}$-*b*-(**1b**)$_{20}$-*b*-(TBAM)$_{47}$] incorporating morpholine and piperidine SNH units were prepared over 2 h by sequential chain extensions of poly(**1a**)$_{60}$ with **1b** in 85/15 dioxane/water and TBAM in 90/10 DMF/water using VA-044 at 70 °C (Scheme 4.6). Polymerizations were taken to low conversions in order to maximize control/living character (Figure 4.2 & Table 4.1), since difficulties existed with the polymerization of **1b** due to aminolysis of the RAFT end-group under non-acidic conditions. Figure 4.3 shows the ^{1}H NMR spectra of the purified polymers after each stage of the polymerization.

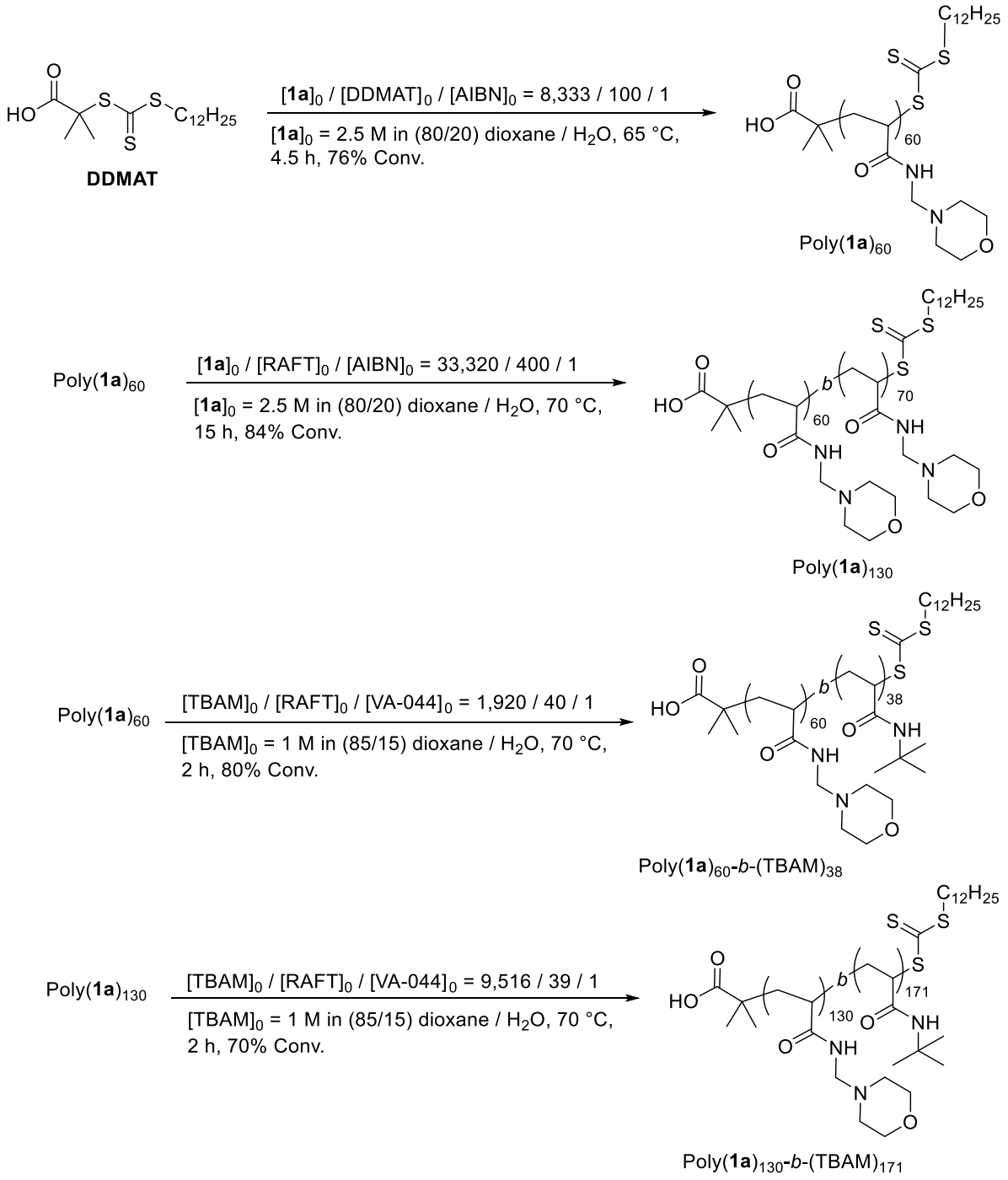

Scheme 4.6: RAFT to give Amphiphilic Diblock Polyacrylamide Copolymers

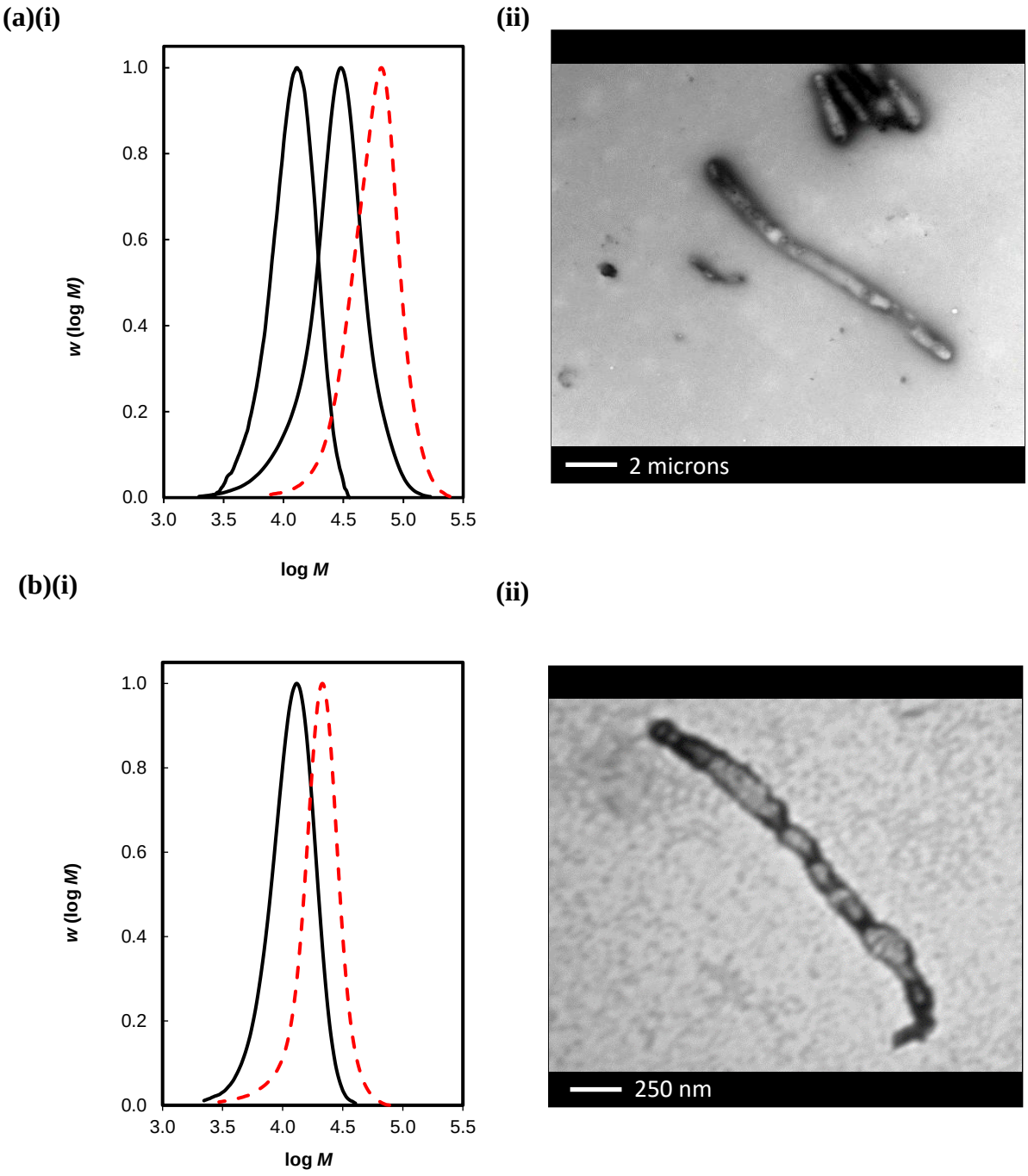

Figure 4.1: Diblock copolymers (dotted red lines) prepared starting from poly(**1a**)$_{60}$ macroRAFT (solid lines). **(a)** Poly(**1a**)$_{60}$-*b*-(**1a**)$_{70}$-*b*-(TBAM)$_{171}$, and **(b)** poly(**1a**)$_{60}$-*b*-(TBAM)$_{38}$ with **(i)** MWDs of polymer prior to precipitation and **(ii)** TEM of corresponding precipitated and dialysed block copolymer.

Polymer [a]	$M_{n,th}$ [b]	% Conv. [c]	M_n [d]	M_w/M_n [d]
Poly(**1a**)$_{60}$	11150	76	10550	1.21
Poly(**1a**)$_{60}$-*b*-(**1a**)$_{70}$	22450	84	22950	1.36
Poly(**1a**)$_{130}$-*b*-(TBAM)$_{171}$	44700	70	49600	1.27
Poly(**1a**)$_{60}$-*b*-(TBAM)$_{38}$	15400	80	18250	1.19
Poly(**1a**)$_{60}$-*b*-(**1b**)$_{20}$	13900	39	13300	1.24
Poly(**1a**)$_{60}$-*b*-(**1b**)$_{20}$-*b*-(TBAM)$_{47}$	19300	20	17200	1.37

Table 4.1. Characterization of Amphiphilic Polyacrylamides

[a]The degree of polymerization for poly(**1a**)$_{60}$ is calculated using M_n from GPC (deducting the MW of the RAFT end groups), and for all other polymers degree of polymerization is calculated from conversion by ^{1}H NMR (deducting the M_n(GPC) of the extended macroRAFT).[b]$M_{n,th}$ is calculated according to equation 1. [c]Conversion calculated by ^{1}H NMR.[d]Determined by GPC/RI in DMF (0.01 M LiBr) using commercial linear poly(MMA) as molecular weight standards.

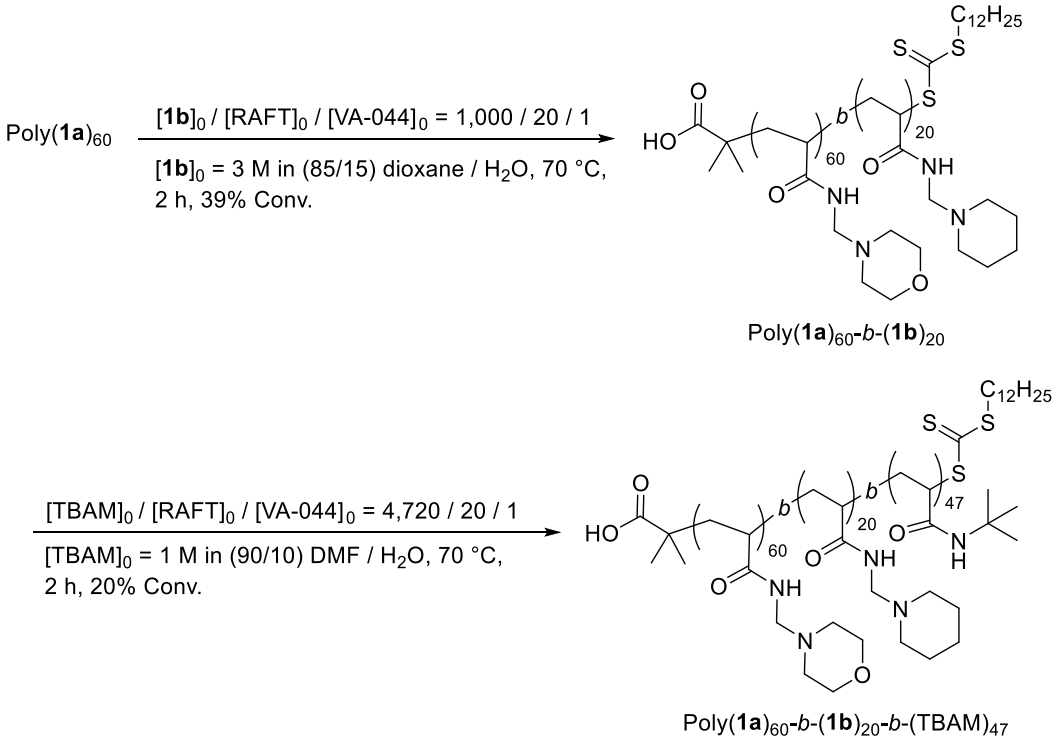

Scheme 4.7: RAFT to give Amphiphilic Triblock Polyacrylamide Copolymers

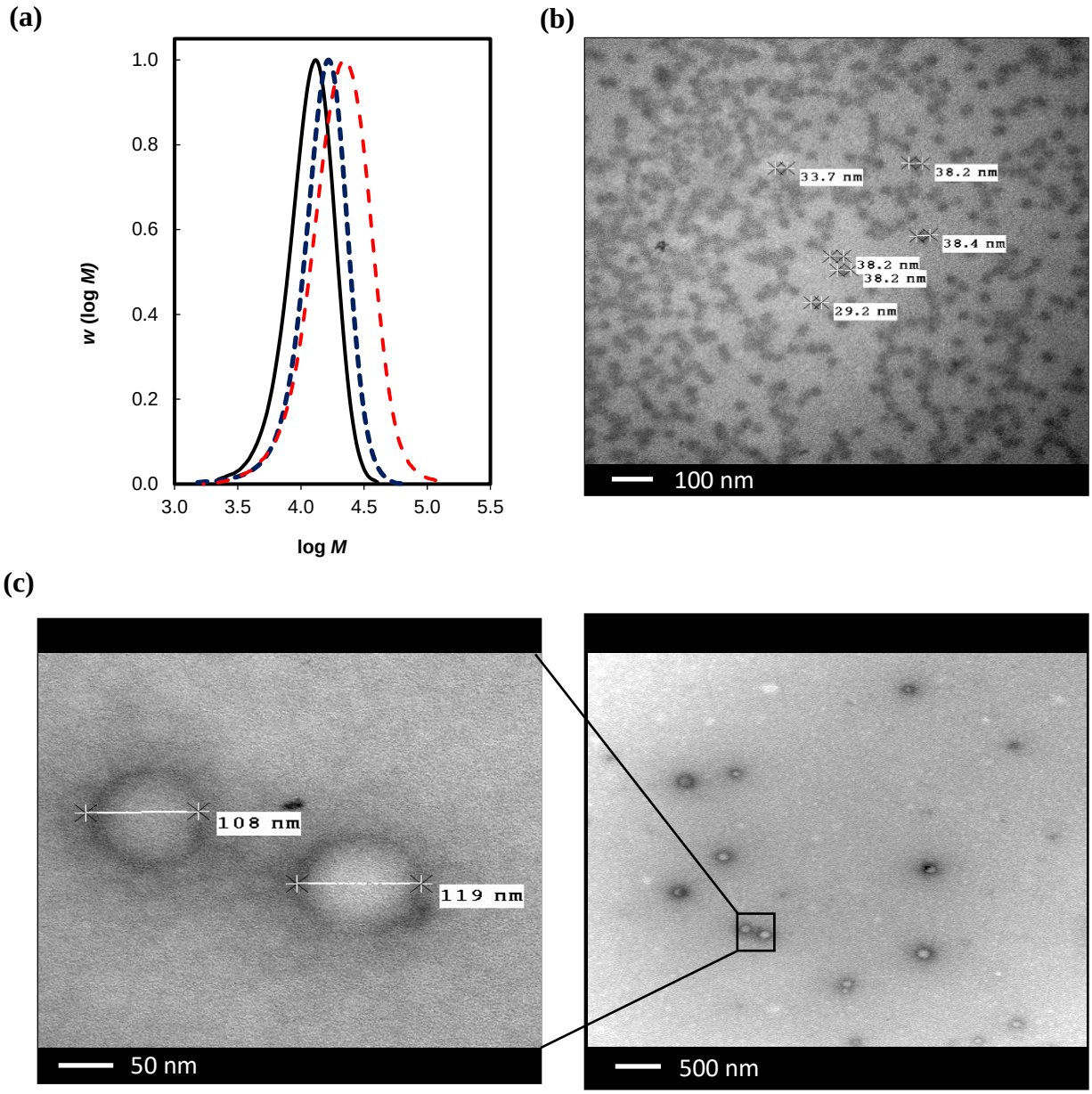

Figure 4.2: Triblock copolymer prepared starting from poly(**1a**)$_{60}$ macroRAFT (solid line) to give poly(**1a**)$_{60}$-*b*-(**1b**)$_{20}$-*b*-(TBAM)$_{47}$ (red dashed line), **(b)** TEM of corresponding precipitated and dialysed block copolymer and **(c)** following acidification with HCl solution.

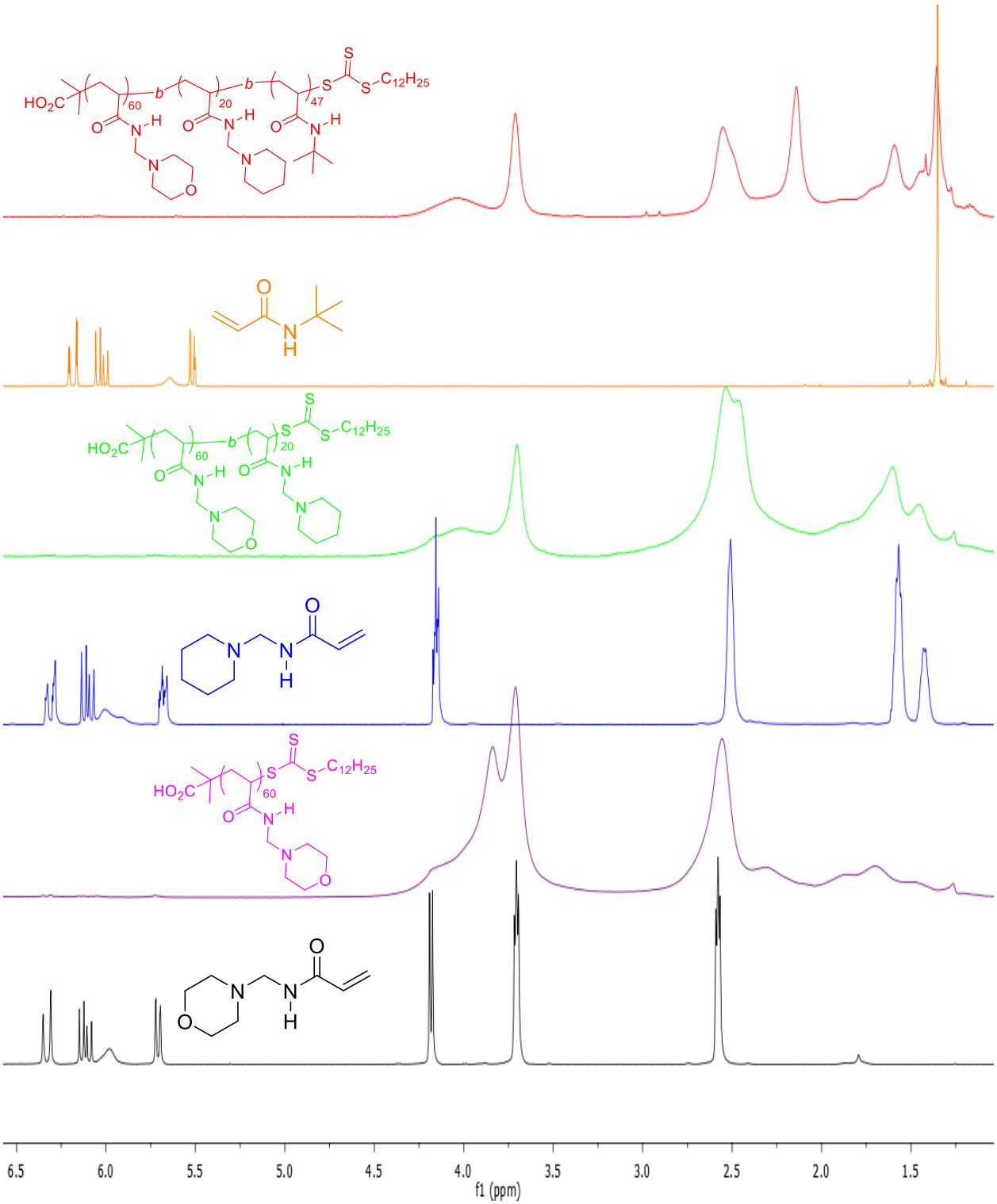

Figure 4.3: ^{1}H NMR spectra ($CDCl_3$, 400 MHz) of purified monomers and polymers: *N*-[(morpholino-4-yl)methyl]prop-2-enamide (**1a**), poly(**1a**)$_{60}$(purple), *N*-[(piperidin-1-yl)methyl]prop-2-enamide (**1b**, blue), poly(**1a**)$_{60}$-*b*-(**1b**)$_{20}$ (green), *tert*-butyl acrylamide (TBAM) (orange) and poly(**1a**)$_{60}$-*b*-(**1b**)$_{20}$-*b*-(TBAM)$_{47}$ (red).

4.3.3 Optimizing the efficiency of polyacrylamide block copolymer synthesis

For the preparation of the amphiphilic triblock copolymers, there were difficulties in getting controlled/living character at high conversion for the chain extensions with monomers **1a** and **1b**. The polymerization of the piperidine acrylamide was stopped at 39% conversion since at higher conversions there was loss of control/living character. This was due to suspected aminolysis side-reaction that cleave the trithiocarbonate end-group, preventing efficient chain extension at high conversion (Scheme 4.8). Recent work by Abel and McCormick on the RAFT polymerization of methacrylamides has shown that the aminolysis can happen as a 5-membered ring cyclization of the trithiocarbonate end-group with the elimination of the alkylthiol group. However, in the case of the piperidine **1b** it may happen as a 7-membered ring cyclization onto the trithiocarbonate end-group with elimination of the thiolate group due to the piperidine ring being more nucleophilic than the amide. Abel and McCormick also showed that trithiocarbonate end-group can be preserved by performing the polymerizations under acidic solutions, which protonate nucleophilic sites (including the N atom of the amide).[132-133] In our recent publication, the chain extension of poly(DMA) with acrylamide **1b** under acidic conditions was utilized. This led to the addition of 1.15 equivalents of HCl to the chain extension of poly(DMA)$_{41}$, which gave poly(DMA)$_{41}$-*b*-(**1b**)$_{97}$ in 97% conversion with excellent control/living character as demonstrated by narrow MWD (M_w/M_n = 1.22) with M_n (of 20800) close to $M_{n,th}$ (of 20750). The protonation of the piperidine ring of poly(**1b**) block prevented aminolysis side-reactions that degrade the living end-group, and this phenomenon is decreased or is absent for morpholine **1a** due to the electronegative oxygen atom of the heterocycle.[125]

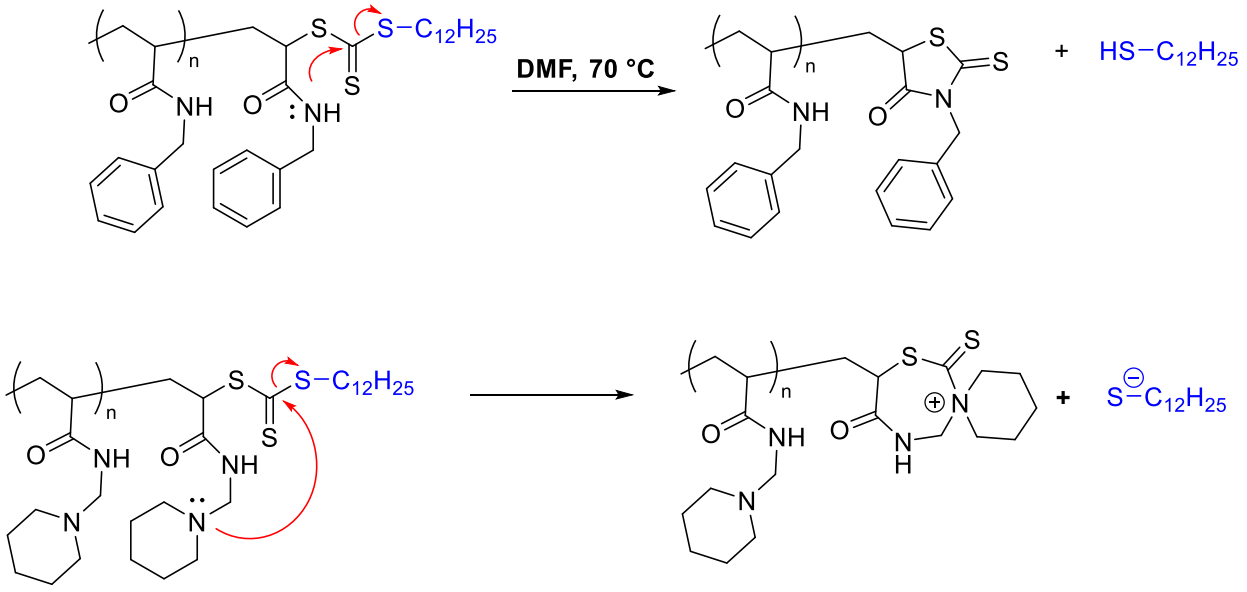

Scheme 4.8: Suspected aminolysis of the RAFT end-group

Using the knowledge acquired from the synthesis of water soluble heterocycle containing polymers,[125] it should be possible to now make amphiphilic polyacrylamide triblocks without isolation of intermediate blocks by taking each monomer preparation to high conversion using acidic conditions. This will be the subject of future work by fellow group member, Abdullah Alzahrani.

4.3.4 Self-assembly and pH-response

The traditional block copolymer self-assembly procedure of Zhang and Eisenberg was employed,[85] where the polymer is dissolved in DMF with water dialysis reducing the solvency of the hydrophobic block to give a translucent colloidal suspension at low polymer concentrations (~1 wt%). The block copolymers consisted of poly(styrene)-*b*-poly(acrylic acid) with the size of the poly(acrylic acid) (PAA) block varied to give particles with polystyrene (PS) cores and PAA coronas. Decreasing the size of the hydrophilic PAA block would change the morphology from spherical micelles of narrow size range, to rod-like, to vesicular, to spherical micelles of a much wider size range. An examination of the one of the more widely sized micelles revealed it to be a micelle filled with reverse micelles with PAA cores and PS chains (Figure 4.4).

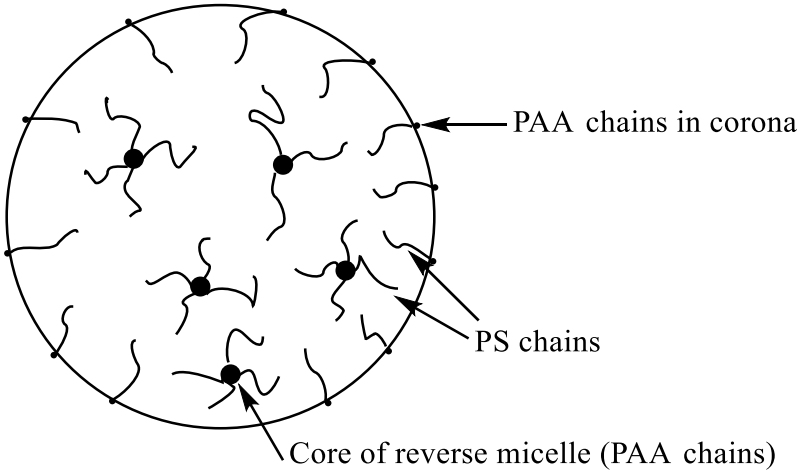

Figure 4.4: Structure of the large micelle filled with reverse micelles[85]

The shape of the nanoparticle is due to how amphiphilic block copolymers undergo self-assembly to minimize interactions between the hydrophobic block and water. The preferred shape of the nanoparticle is determined by the spontaneous curvature or packing parameter of the amphiphilic molecules. The packing of the copolymer chains affect the molecular curvature of the nanoparticle and can be predicted with the following equation (4.3),

$$p = \frac{v}{a_o l_c} \tag{4.3}$$

where p is the packing parameter, v is the volume of the hydrophobic chains, a_o is the optimal area of the head group and l_c is the length of the hydrophobic tail. In general spherical particles are favoured when $p \leq 1/3$, cylindrical particles when $1/3 \leq p \leq 1/2$, and enclosed membrane structures when $1/2 \leq p \leq 1$.[134]

The polymer aggregates were observable by TEM with their sizes directly measurable from the micrographs (Figures 4.1a(ii), 4.1b(ii) & 4.2(b)(c)). The vesicular nature is evidenced from a higher transmission through the aggregates than around the periphery. Self-assembly gave large rod-like vesicles for the AB diblock copolymers consisting of poly(**1a**) and poly(TBAM) blocks (which also contain a contribution from the hydrophobic RAFT end-group). Differences in morphology are primarily dictated by the relative volume fractions of the two blocks.[134-135] Poly(**1a**)$_{130}$-*b*-(TBAM)$_{171}$ consisted of more than double the hydrophilic block, but a greater

fraction hydrophobic block than poly(**1a**)$_{60}$-*b*-poly(TBAM)$_{38}$ (56% as opposed to 38% TBAM fraction). Poly(**1a**)$_{130}$-*b*-(TBAM)$_{171}$ gave rod-like vesicles with Figure 4.1a(ii) showing one of the large rods of ~13 μm in length with a diameter of ~0.7 μm. Less stable aggregates were observed for poly(**1a**)$_{60}$-*b*-poly(TBAM)$_{38}$ with smaller rod-like vesicles with Figure 4.1b(ii) showing a representative example ~2.5 μm in length, and a diameter of ~130 nm. The formation of large rod-like vesicles was determined by the spontaneous curvature, or packing parameter of the amphiphilic copolymer. A high curvature indicated a high level of asymmetry between the hydrophobic and hydrophilic blocks, and a preference towards high-curvature structures such as spherical micelles. Relatively symmetrical copolymers have a low spontaneous curvature and will form flat structures such as bilayers. Rod-like structures were formed by amphiphilic copolymers with a moderate spontaneous curvature, caused by a moderate level of asymmetry between the hydrophilic poly(**1a**) block and the hydrophobic poly(TBAM) block.[136]

In contrast to diblock copolymers, the TEM micrograph of the morpholine and piperidine containing triblock showed spherical aggregates of narrow size distribution of average diameter ~33 nm (Figure 4.2b). Upon acidification with hydrochloric acid to pH 2 (Figure 4.2c), less aggregation was observed as vesicles expanded upon ionization of the SNHs leading to an increase in size of spheres to 100-120 nm in diameter. The ionization of the SNHs in the corona of the spheres leads to an increase in electrostatic repulsion between the hydrophilic chains, causing the spheres to expand (Scheme 4.9).

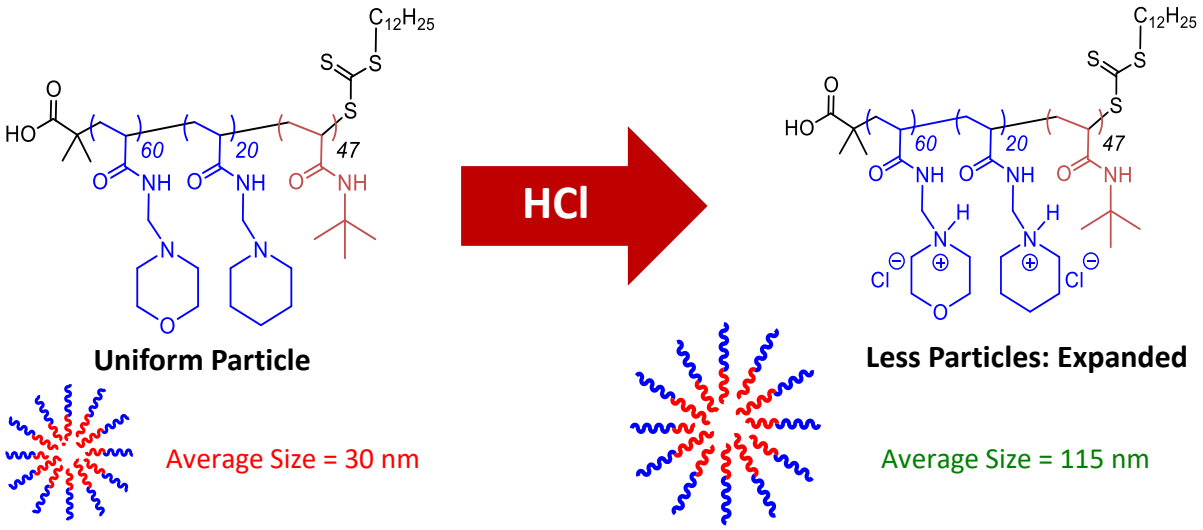

Scheme 4.9: pH-response of triblock copolymer

4.4 Conclusions

The nucleophilic addition of acrylamide onto *in situ* generated methylene Schiff base salts has allowed the multi-gram preparation of previously elusive, *N*-[(cycloalkylamino)methyl]acrylamides.[125] This new synthetic method opens the way to the facile preparation of a plethora of related methylene amine substituted acrylamide and methacrylamide monomers. A key advantage of the monomer preparation is the easy isolation of the intermediate HCl salt. RAFT has allowed the efficient preparation of the first well-defined block copolymers of this monomer class, although the close proximity of the trithiocarbonate end-group to the tertiary amino substituent made control/living character for the piperidine monomer difficult unless the heterocyclic pendant was ionized. In contrast the morpholine-containing monomer did not require acidic conditions in order to achieve control/living character with high conversion obtained, as shown with the poly(**1a**)-*b*-(TBAM) in comparison with poly(**1a**)-*b*-(**1b**)-*b*-(TBAM). Self-assembly gave large rod-like vesicles for amphiphilic morpholine-containing diblock copolymers. For the triblock of similar hydrophobic monomer content, but incorporating the piperidine monomer very different aggregation was observed with pH-expandable nanoparticle spheres observed. These new monomers undoubtedly have further synthetic potential and applications, including for the preparation of pH-responsive smart polymersomes for targeted delivery of therapeutics.

^{1}H NMR (400 MHz) of *N*-[(morpholin-4-yl)methyl]prop-2-enamide hydrochloride in $(CD_3)_2SO$

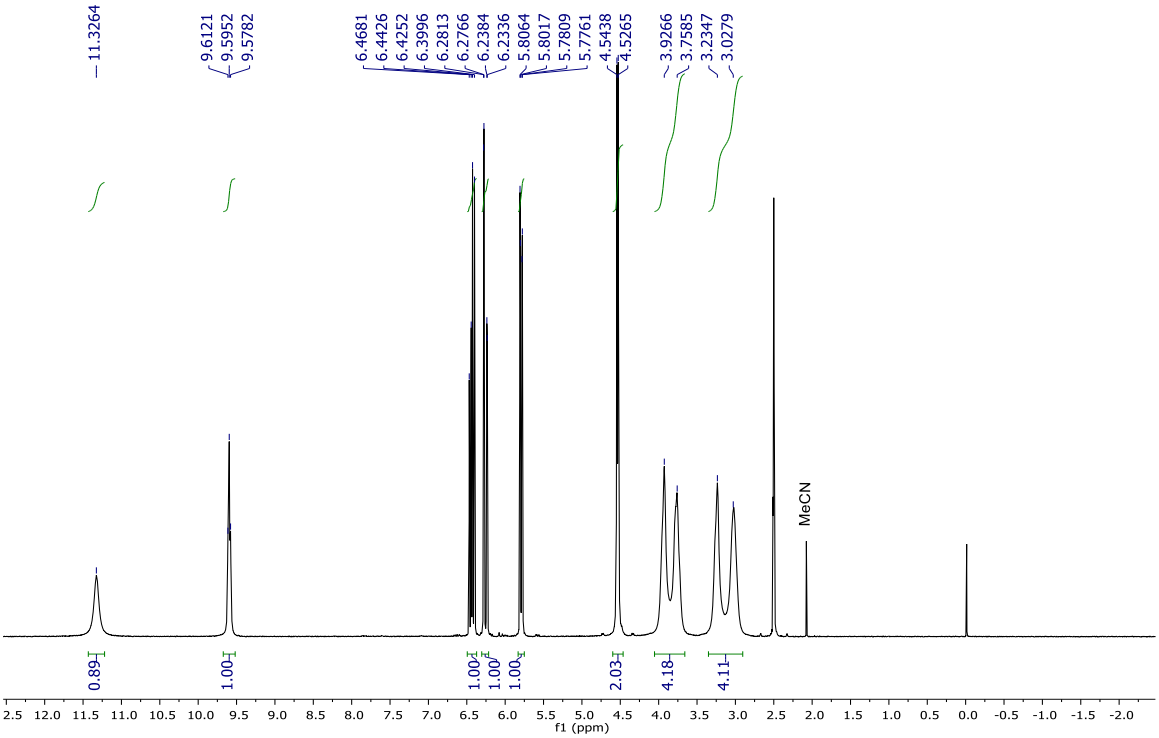

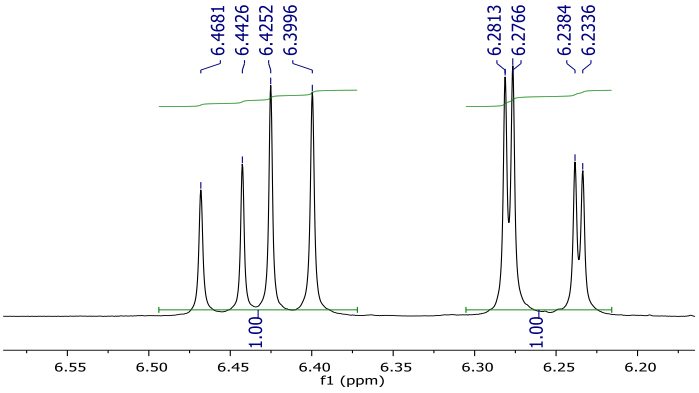

$(CH_3)_2SO$: 2.50 ppm

^{13}C NMR (100 MHz) of *N*-[(morpholin-4-yl)methyl]prop-2-enamide hydrochloride in $(CD_3)_2SO$

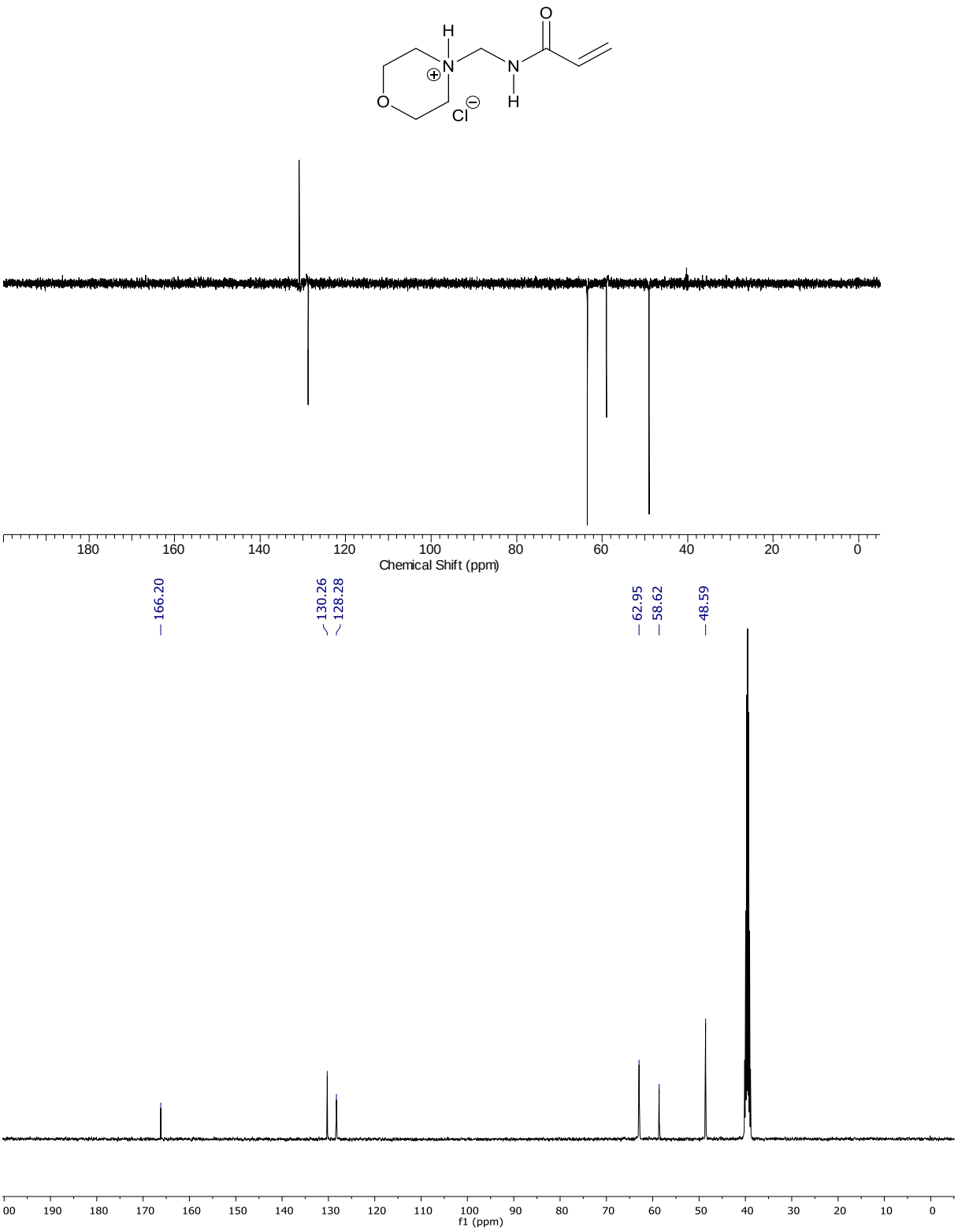

^{1}H NMR (400 MHz) of *N*-[(morpholin-4-yl)methyl]prop-2-enamide in $CDCl_3$

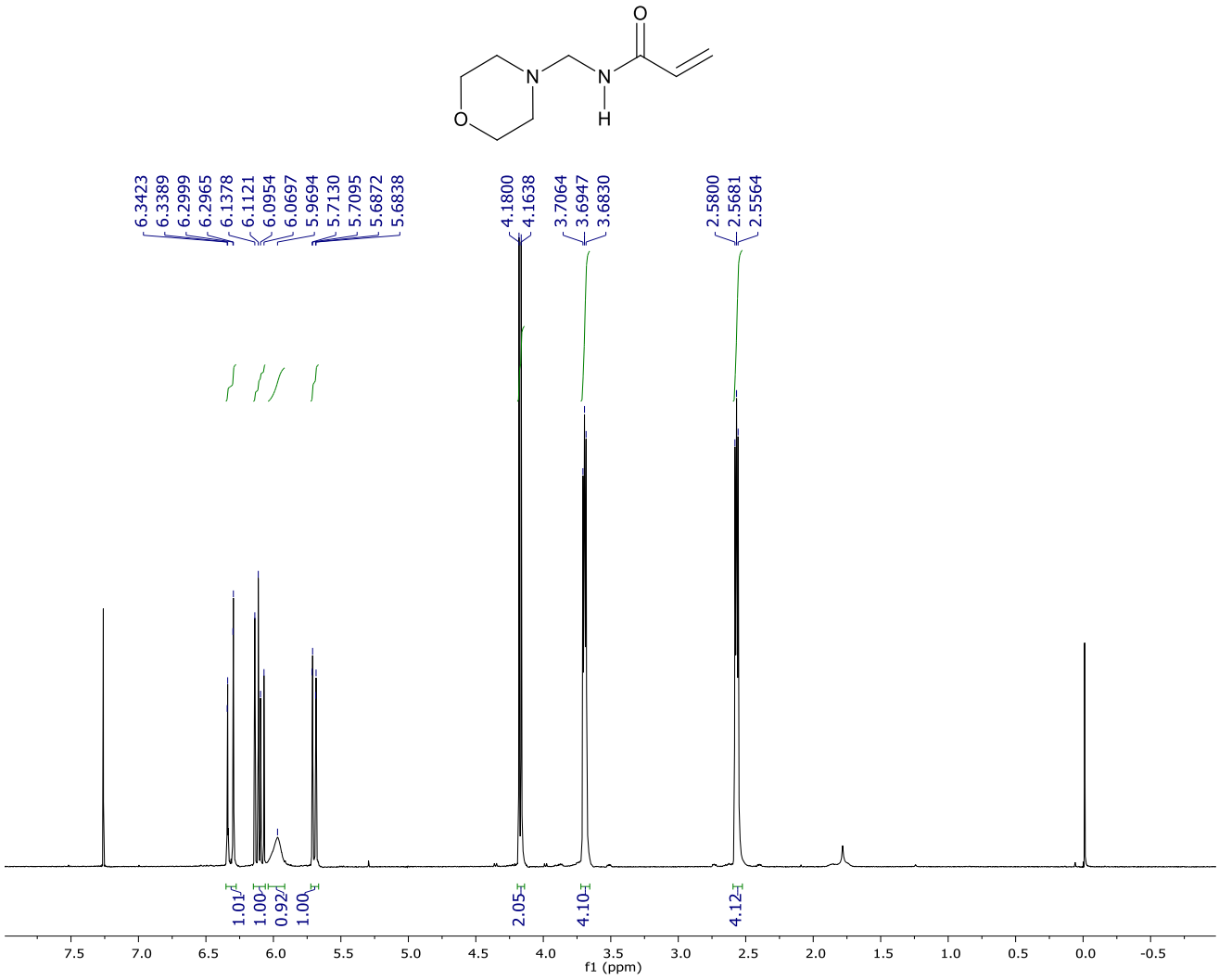

^{13}C NMR (100 MHz) of *N*-[(morpholin-4-yl)methyl]prop-2-enamide in $CDCl_3$

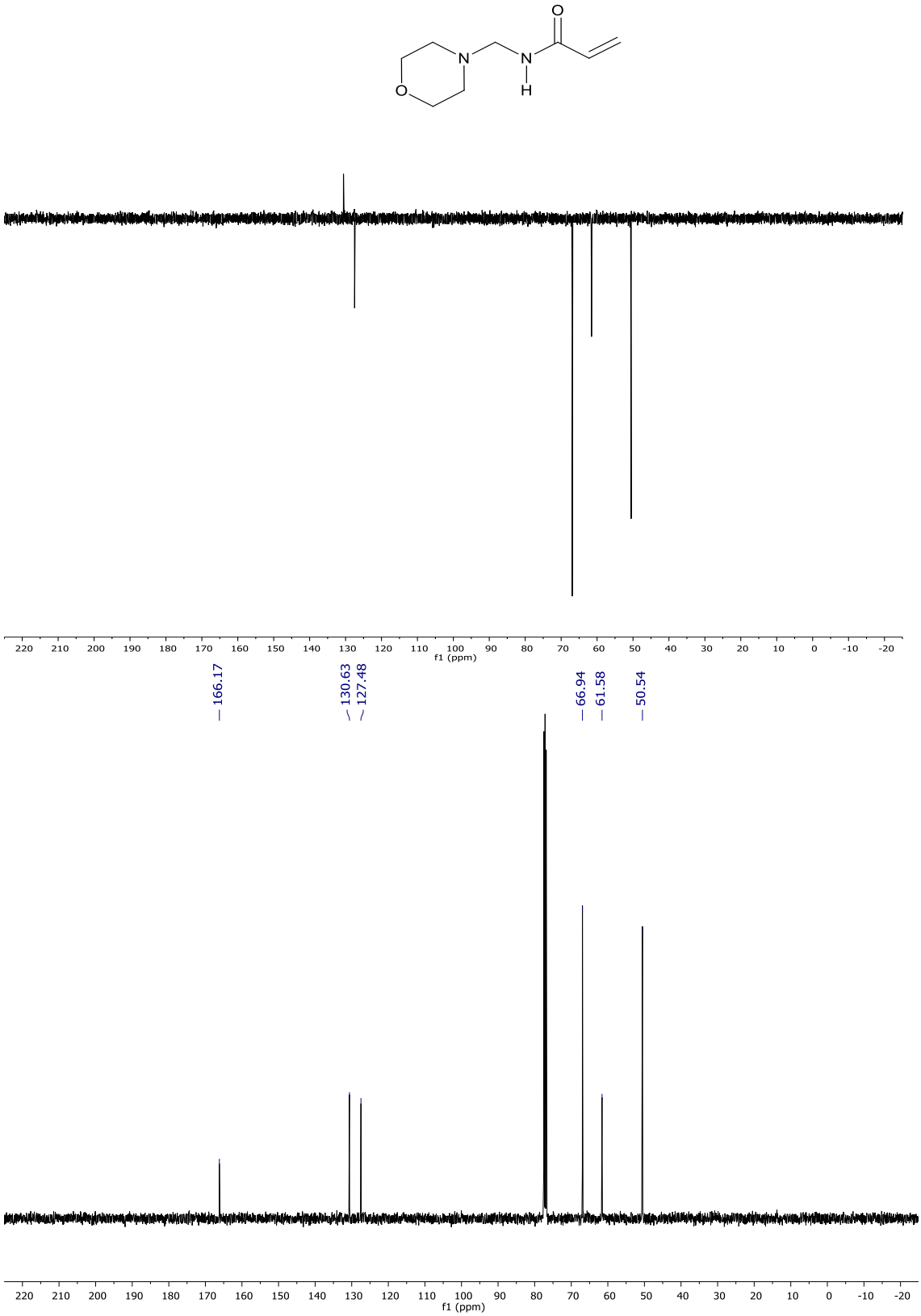

^{1}H NMR (400 MHz) of *N*-[(piperidin-1-yl)methyl]prop-2-enamide hydrochloride in $(CD_3)_2SO$

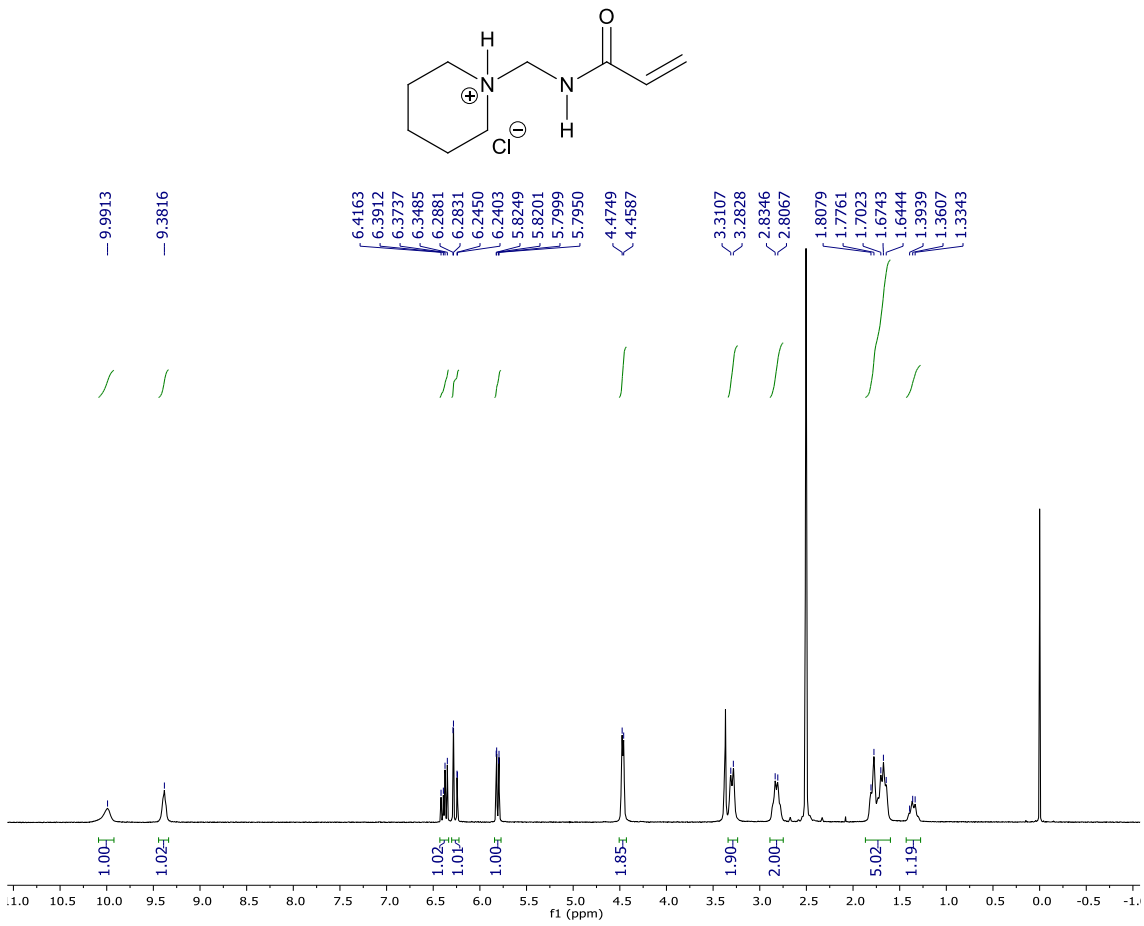

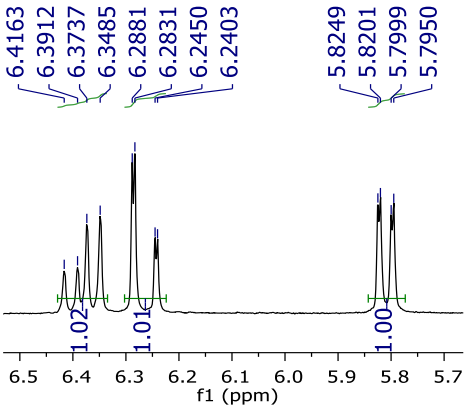

$(CH_3)_2SO$: 2.50 ppm
H_2O in $(CD_3)_2SO$: 3.35-3.39 ppm

^{13}C NMR (100 MHz) of *N*-[(piperidin-1-yl)methyl]prop-2-enamide hydrochloride in $(CD_3)_2SO$

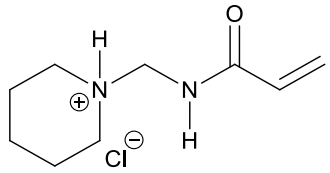

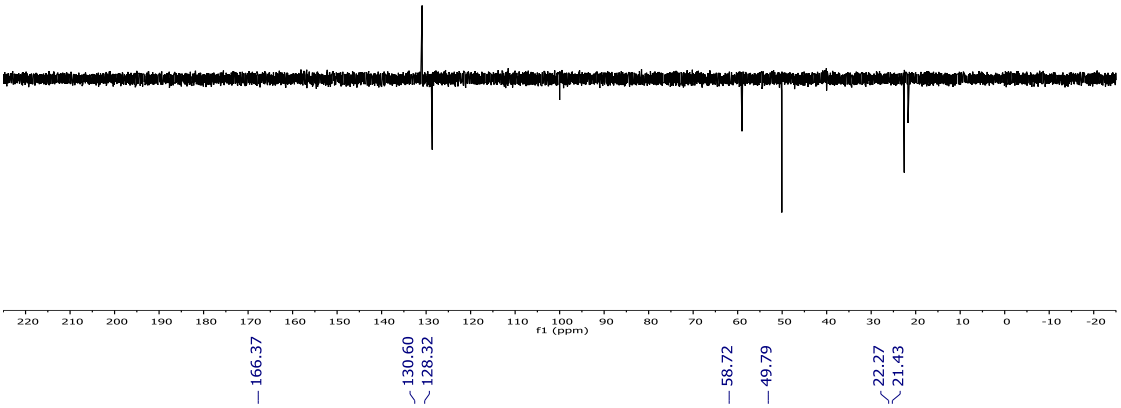

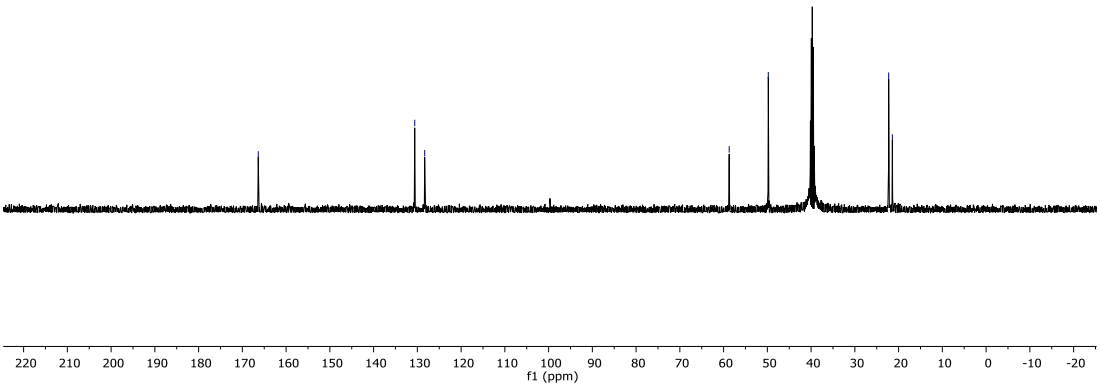

^{1}H NMR (400 MHz) of *N*-[(piperidin-1-yl)methyl]prop-2-enamide in $CDCl_3$

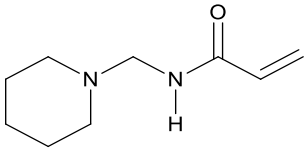

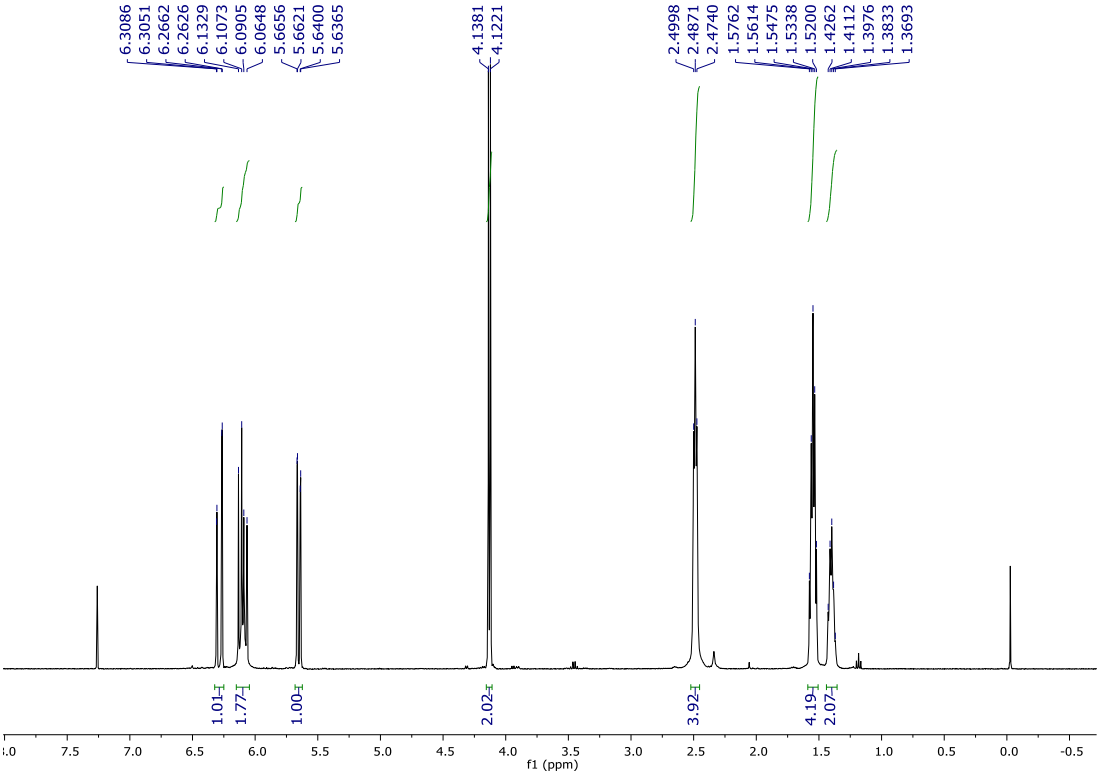

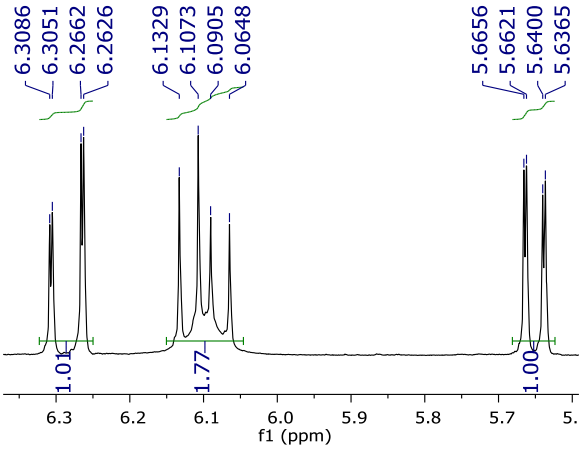

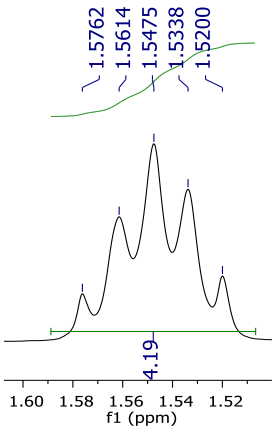

^{13}C NMR (100 MHz) of *N*-[(piperidin-1-yl)methyl]prop-2-enamide in $CDCl_3$

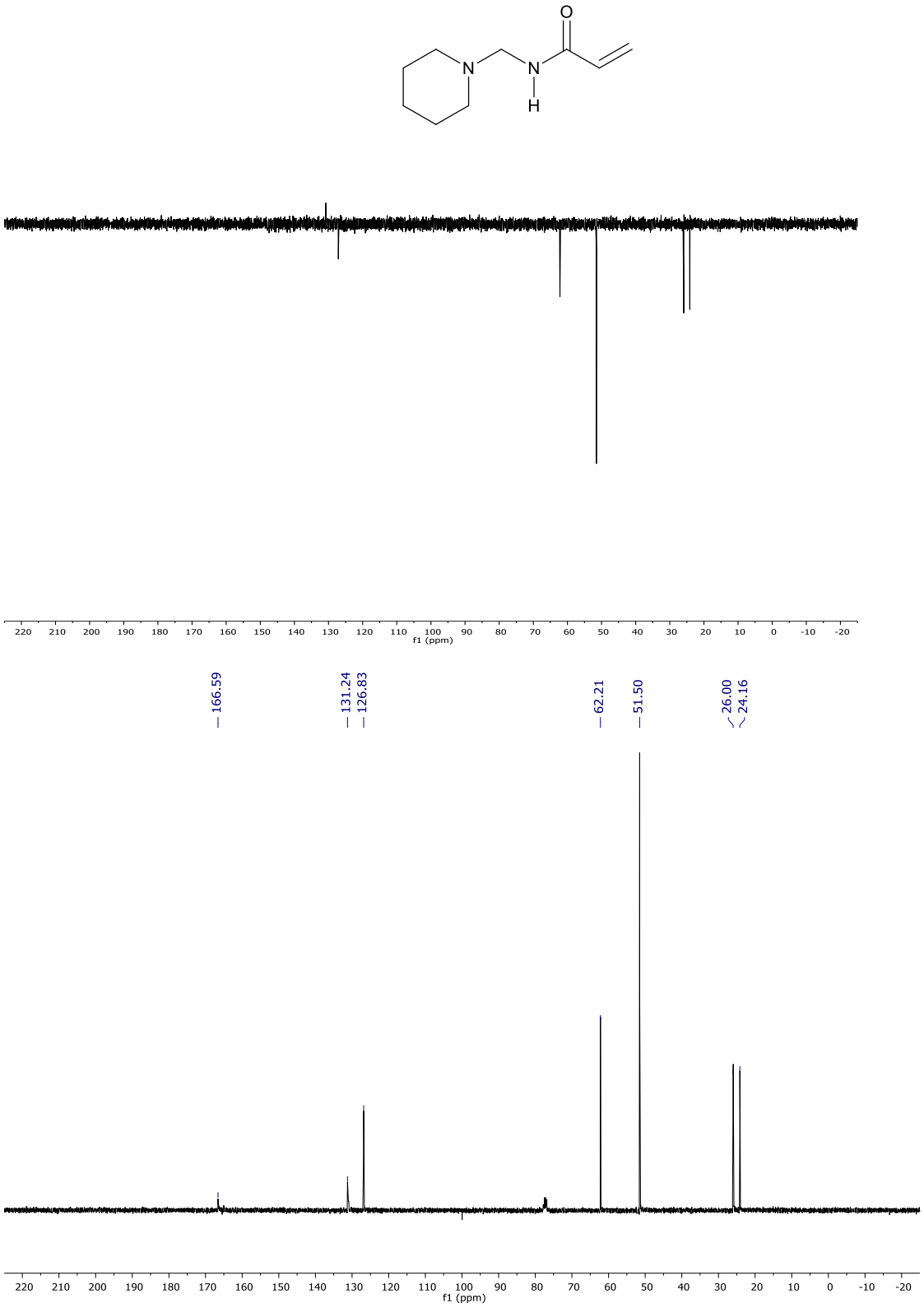

^{1}H NMR (400 MHz) of *N*-[(pyrrolidin-1-yl)methyl]prop-2-enamide hydrochloride in $(CD_3)_2SO$

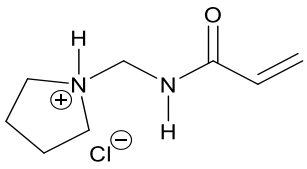

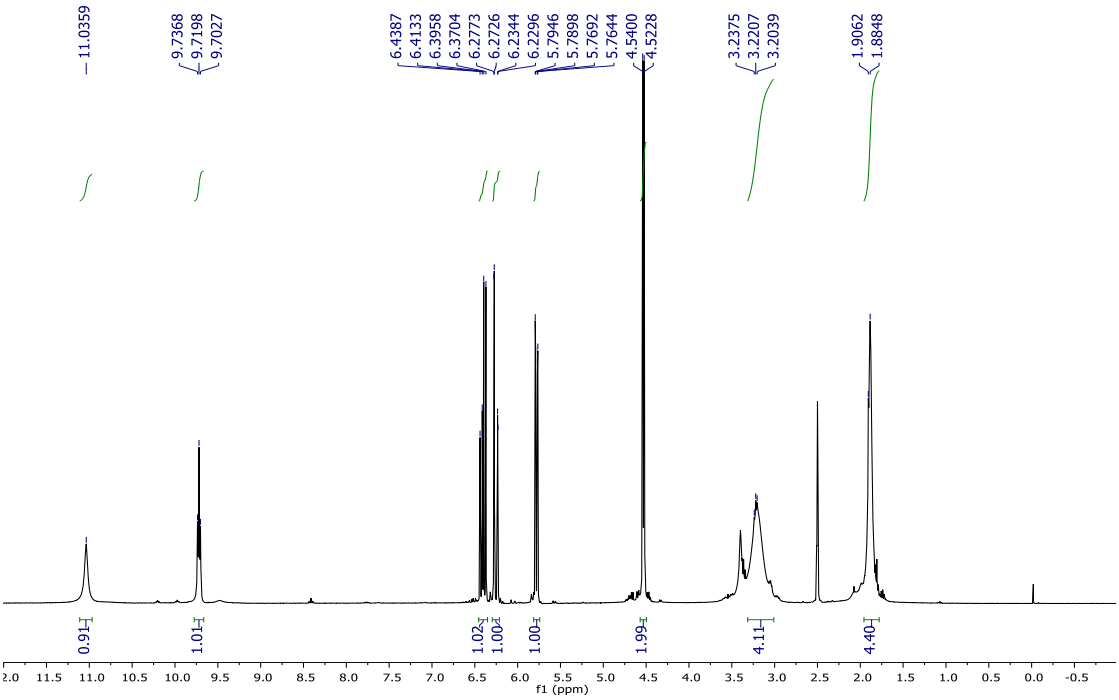

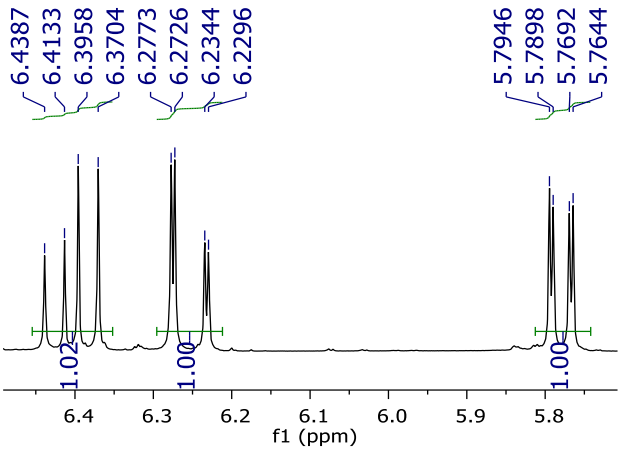

$(CH_3)_2SO$: 2.50 ppm
H_2O in $(CD_3)_2SO$: 3.33-3.45 ppm

^{13}C NMR (100 MHz) of *N*-[(pyrrolidin-1-yl)methyl]prop-2-enamide hydrochloride in $(CD_3)_2SO$

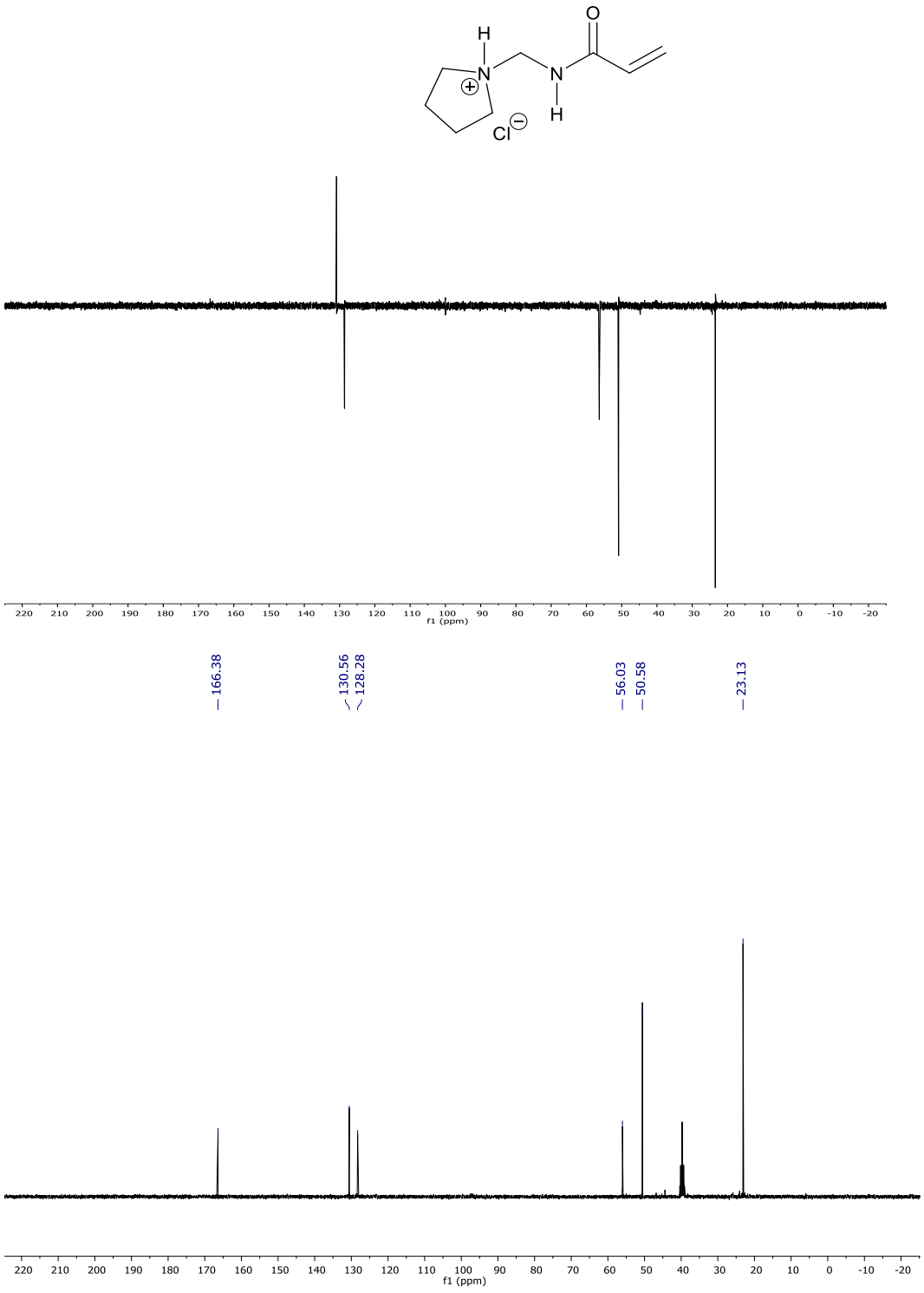

^{1}H NMR (400 MHz) of *N*-[(pyrrolidin-1-yl)methyl]prop-2-enamide in $CDCl_3$

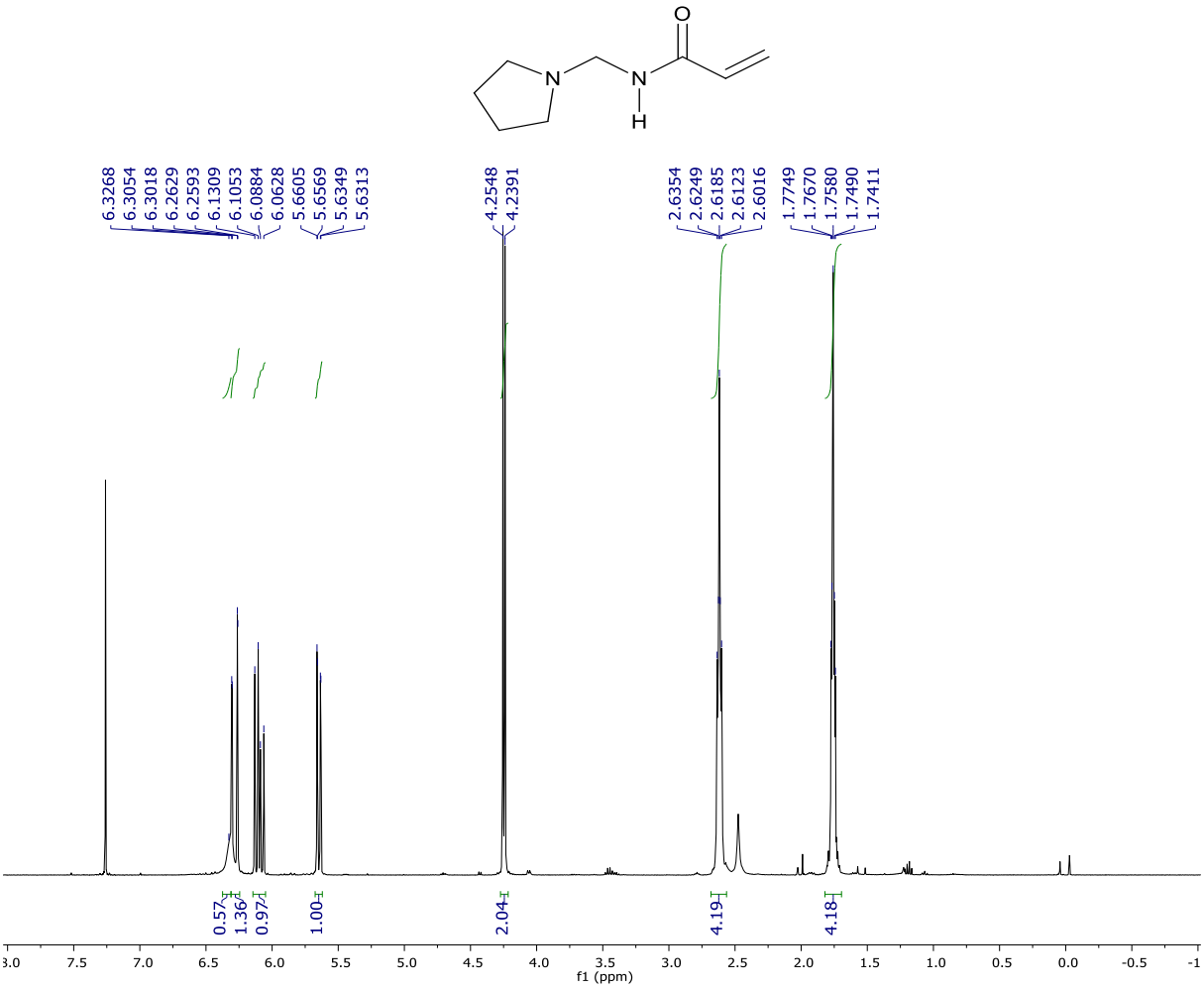

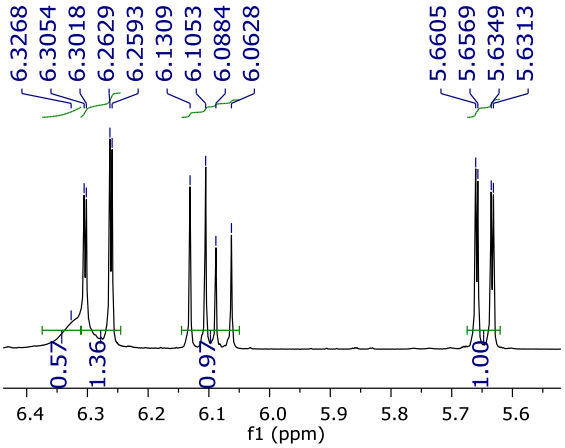

^{13}C NMR (100 MHz) of *N*-[(pyrrolidin-1-yl)methyl]prop-2-enamide in $CDCl_3$

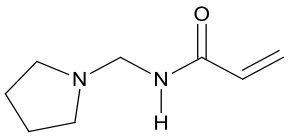

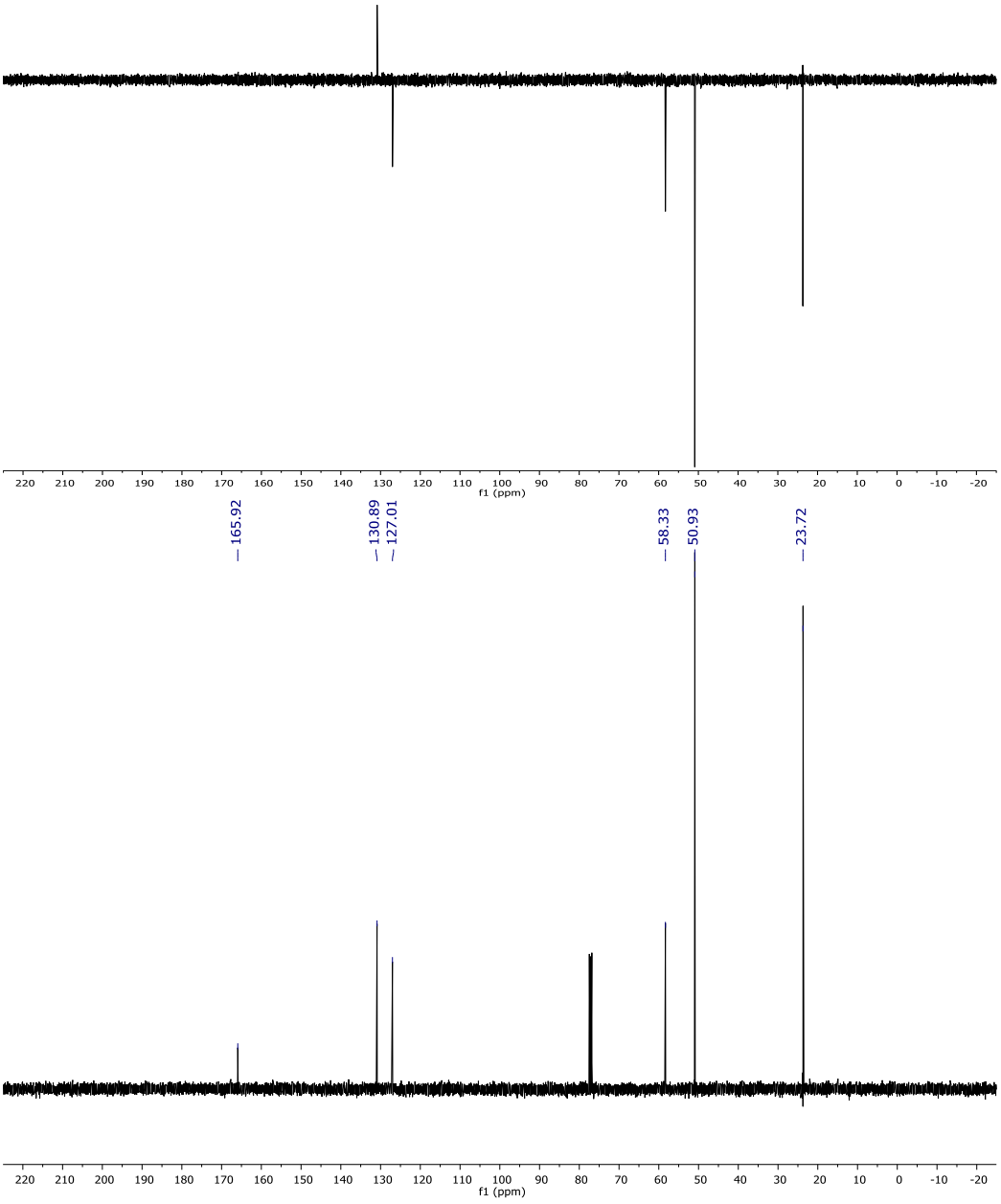

REFERENCES

1. Moad, G.; Solomon, D. H., *The Chemistry of Radical Polymerization*. 2006.
2. Quirk, R. P.; Ocampo, M., *Material Matters* **2006**, *1*, 10-11.
3. Szwarc, M., *Nature* **1956**, *178*, 1168-1169.
4. Szwarc, M.; Levy, M.; Milkovich, R., *J. Am. Chem. Soc.* **1956**, *78*, 2656-2657.
5. Aoshima, S.; Kanaoka, S., *Chem. Rev.* **2009**, *109*, 5245-5287.
6. Aldabbagh, F.; Gibbons, O., Product Class 18: Polystyrenes. In *Science of Synthesis, Houben-Weyl Methods of Molecular Transformations*, Thieme: 2010; Vol. 45b, pp 723-744.
7. Braunecker, W. A.; Matyjaszewski, K., *Prog. Polym. Sci.* **2007**, *32*, 93-146.
8. Yamada, B.; Zetterlund, P. B., General Chemistry of Radical Polymerization. In *Handbook of Radical Polymerization*, Matyjaszewski, K.; Davis, T. P., Eds. John Wiley & Sons: Hoboken, 2002; p 117.
9. Buback, M.; Gilbert, R. G.; Hutchinson, R. A.; Klumperman, B.; Kuchta, F.-D.; Manders, B. G.; O'Driscoll, K. F.; Russell, G. T.; Schweer, J., *Macromol. Chem. Phys.* **1995**, *196*, 3267-3280.
10. Lessard, B.; Tervo, C.; Marić, M., *Macromol. React. Eng.* **2009**, *3*, 245-256.
11. Beuermann, S.; Buback, M.; Davis, T. P.; Gilbert, R. G.; Hutchinson, R. A.; Olaj, O. F.; Russell, G. T.; Schweer, J.; van Herk, A. M., *Macromol. Chem. Phys.* **1997**, *198*, 1545-1560.
12. Kamachi, M.; Yamada, B., Propagation and Termination Constants in Free Radical Polymerization. In *Polymer Handbook 4th Edition*, Brandup, J.; Immergut, E. H.; Grulke, E. A., Eds. John Wiley & Sons: New York, 1999; Vol. 1, p 77.
13. Zetterlund, P. B.; Saka, Y.; McHale, R.; Nakamura, T.; Aldabbagh, F.; Okubo, M., *Polymer* **2006**, *47*, 7900-7908.
14. Magee, C.; Sugihara, Y.; Zetterlund, P. B.; Aldabbagh, F., *Polym. Chem.* **2014**, *5*, 2259-2265.
15. Solomon, D. H.; Rizzardo, E.; Cacioli, P. Polymerization process and polymers produced thereby. US4581429, 1986.
16. Georges, M. K.; Veregin, R. P. N.; Kazmaier, P. M.; Hamer, G. K., *Macromolecules* **1993**, *26*, 2987-2988.

17. Wang, J.-S.; Matyjaszewski, K., *J. Am. Chem. Soc.* **1995**, *117*, 5614.
18. Kato, M.; Kamigaito, M.; Sawamoto, M.; Higashimura, T., *Macromolecules* **1995**, *28*, 1721.
19. Chiefari, J.; Chong, Y. K.; Ercole, F.; Krstina, J.; Jeffery, J.; Le, T. P. T.; Mayadunne, R. T. A.; Meijs, G. F.; Moad, G.; Rizzardo, E.; Thang, S. H., *Macromolecules* **1998**, *31*, 5559.
20. Corpart, P.; Charmot, D.; Biadatti, T.; Zard, S.; Michelet, D. Method for block polymer synthesis by controlled radical polymerisation. WO9858974A1, 1998.
21. Jenkins, A. D.; Jones, R. G.; Moad, G., *Pure Appl. Chem.* **2009**, *82*, 483-491.
22. Fukuda, T.; Terauchi, T.; Goto, A.; Ohno, K.; Tsujii, Y.; Miyamoto, T.; Kobatake, S.; Yamada, B., *Macromolecules* **1996**, *29*, 6393-6398.
23. Benoit, D.; Chaplinski, V.; Braslau, R.; Hawker, C. J., *J. Am. Chem. Soc.* **1999**, *121*, 3904-3920.
24. Gibbons, O.; Carroll, W. M.; Aldabbagh, F.; Yamada, B., *J. Polym. Sci. A Polym. Chem.* **2006**, *44*, 6410-6418.
25. Gibbons, O.; Carroll, W. M.; Aldabbagh, F.; Zetterlund, P. B.; Yamada, B., *Macromol. Chem. Phys.* **2008**, *209*, 2434-2444.
26. Couvreur, L.; Lefay, C.; Belleney, J.; Charleux, B.; Guerret, O.; Magnet, S., *Macromolecules* **2003**, *36*, 8260-8267.
27. McHale, R.; Aldabbagh, F.; Zetterlund, P. B., *J. Polym. Sci. A Polym. Chem.* **2007**, *45*, 2194-2203.
28. Nicolas, J.; Dire, C.; Mueller, L.; Belleney, J.; Charleux, B.; Marque, S. R. A.; Bertin, D.; Magnet, S.; Couvreur, L., *Macromolecules* **2006**, *39*, 8274-8282.
29. Nicolas, J.; Brusseau, S.; Charleux, B., *J. Polym. Sci. A Polym. Chem.* **2010**, *48*, 34-47.
30. Matyjaszewski, K.; Xia, J., *Chem. Rev.* **2001**, *101*, 2921-2990.
31. Mazzotti, G.; Benelli, T.; Lanzi, M.; Mazzocchetti, L.; Giorgini, L., *Eur. Polym. J.* **2016**, *77*, 75-87.
32. Perrier, S.; Takolpuckdee, P., *J. Polym. Sci. A Polym. Chem.* **2005**, *43*, 5347-5393.
33. Tang, C.; Kowalewski, T.; Matyjaszewski, K., *Macromolecules* **2003**, *36*, 8587-8589.
34. Zetterlund, P. B.; Gody, G.; Perrier, S., *Macromol. Theory Simul.* **2014**, *23*, 331-339.
35. Moad, G.; Rizzardo, E.; Thang, S. H., *Material Matters* **2010**, *5*, 2-8.

36. Moad, G.; Rizzardo, E.; Thang, S. H., *Chem. Asian J.* **2013**, *8*, 1634-44.
37. Levere, M. E.; Chambon, P.; Rannard, S. P.; McDonald, T. O., *J. Polym. Sci. A Polym. Chem.* **2017**, *55*, 2427-2431.
38. Van Nieuwenhove, I.; Maji, S.; Dash, M.; Van Vlierberghe, S.; Hoogenboom, R.; Dubruel, P., *Polym. Chem.* **2017**, *8*, 2433-2437.
39. Xiang, Y.; Cong, H.; Li, L.; Zheng, S., *J. Polym. Sci. A Polym. Chem.* **2016**, *54*, 1852-1863.
40. Span, R.; Wagner, W., *J. Phys. Chem. Ref. Data* **1996**, *25*, 1509-1596.
41. Ajzenberg, N.; Trabelsi, F.; Recasens, F., *Chem. Eng. Technol.* **2000**, *23*, 829-839.
42. O'Connor, P.; Zetterlund, P. B.; Aldabbagh, F., *Macromolecules* **2010**, *43*, 914-919.
43. Zetterlund, P. B.; Aldabbagh, F.; Okubo, M., *J. Polym. Sci. A Polym. Chem.* **2009**, *47*, 3711-3728.
44. DeSimone, J. M.; Guan, Z.; Elsbernd, C. S., *Science* **1992**, *257*, 945-947.
45. Guan, Z.; Combes, J. R.; Menceloglu, Y. Z.; DeSimone, J. M., *Macromolecules* **1993**, *26*, 2663-2669.
46. Ryan, J.; Aldabbagh, F.; Zetterlund, P. B.; Okubo, M., *Polymer* **2005**, *46*, 9769-9777.
47. McHale, R.; Aldabbagh, F.; Zetterlund, P. B.; Okubo, M., *Macromol. Rapid. Commun.* **2006**, *27*, 1465-1471.
48. McHale, R.; Aldabbagh, F.; Zetterlund, P. B.; Minami, H.; Okubo, M., *Macromolecules* **2006**, *39*, 6853-6860.
49. McHale, R.; Aldabbagh, F.; Zetterlund, P. B.; Okubo, M., *Macromol. Chem. Phys.* **2007**, *208*, 1813-1822.
50. Aldabbagh, F.; Zetterlund, P. B.; Okubo, M., *Macromolecules* **2008**, *41*, 2732-2734.
51. Aldabbagh, F.; Zetterlund, P. B.; Okubo, M., *Eur. Polym. J.* **2008**, *44*, 4037-4046.
52. O'Connor, P.; Yang, R.; Carroll, W. M.; Rochev, Y.; Aldabbagh, F., *Eur. Polym. J.* **2012**, *48*, 1279-1288.
53. O'Connor, P.; Zetterlund, P. B.; Aldabbagh, F., *J. Polym. Sci. A Polym. Chem.* **2011**, *49*, 1719-1723.
54. Thurecht, K. J.; Gregory, A. M.; Villarroya, S.; Zhou, J.; Heise, A.; Howdle, S. M., *Chem. Commun.* **2006**, *42*, 4383-4385.

55. Thurecht, K. J.; Gregory, A. M.; Wang, W.; Howdle, S. M., *Macromolecules* **2007**, *40*, 2965-2967.
56. Lee, H.; Terry, E.; Zong, M.; Arrowsmith, N.; Perrier, S.; Thurecht, K. J.; Howdle, S. M., *J. Am. Chem. Soc.* **2008**, *130*, 12242-12243.
57. Zong, M.; Thurecht, K. J.; Howdle, S. M., *Chem. Commun.* **2008**, *45*, 5942-5944.
58. Hasell, T.; Thurecht, K. J.; Jones, R. D. W.; Brown, P. D.; Howdle, S. M., *Chem. Commun.* **2007**, *38*, 3933-3935.
59. Sugihara, Y.; O'Connor, P.; Zetterlund, P. B.; Aldabbagh, F., *J. Polym. Sci. A Polym. Chem.* **2011**, *49*, 1856-1864.
60. Thurecht, K. J.; Howdle, S. M., *Aust. J. Chem.* **2009**, *62*, 786-789.
61. Boyere, C.; Jerome, C.; Debuigne, A., *Eur. Polym. J.* **2014**, *61*, 45-63.
62. Magee, C.; Earla, A.; Petraitis, J.; Higa, C.; Braslau, R.; Zetterlund, P. B.; Aldabbagh, F., *Polym. Chem.* **2014**, *5*, 5725-5733.
63. Grignard, B.; Calberg, C.; Jerome, C.; Detrembleur, C., *J. Supercrit. Fluids* **2010**, *53*, 151-155.
64. Minami, H.; Tanaka, A.; Kagawa, Y.; Okubo, M., *J. Polym. Sci. A Polym. Chem.* **2012**, *50*, 2578-2584.
65. Jennings, J.; Beija, M.; Richez, A. P.; Cooper, S. D.; Mignot, P. E.; Thurecht, K. J.; Jack, K. S.; Howdle, S. M., *J. Am. Chem. Soc.* **2012**, *134*, 4772-4781.
66. Jaramillo-Soto, G.; Villa-Avila, C. M.; Vivaldo-Lima, E., *J. Macromol. Sci. A* **2013**, *50*, 281-286.
67. Jennings, J.; Beija, M.; Kennon, J. T.; Willcock, H.; O'Reilly, R. K.; Rimmer, S.; Howdle, S. M., *Macromolecules* **2013**, *46*, 6843-6851.
68. Kuroda, T.; Tanaka, A.; Taniyama, T.; Minami, H.; Goto, A.; Fukuda, T.; Okubo, M., *Polymer* **2012**, *53*, 1212-1218.
69. Taniyama, T.; Kuroda, T.; Minami, H.; Okubo, M., *Polym. J.* **2012**, *44*, 1082-1086.
70. Hawkins, G.; Zetterlund, P. B.; Aldabbagh, F., *J. Polym. Sci. A Polym. Chem.* **2015**, *53*, 2351-2356.
71. Pu, D. W.; Lucien, F. P.; Zetterlund, P. B., *J. Polym. Sci. A Polym. Chem.* **2011**, *49*, 4307-4311.
72. Pu, D. W.; Soh, M.; Zetterlund, P. B.; Lucien, F. P., *J. Supercrit. Fluids* **2013**, *78*, 89-94.

73. Roy, D.; Brooks, W. L. A.; Sumerlin, B. S., *Chem. Soc. Rev.* **2013**, *42*, 7214-7243.
74. Suzuki, K.; Kanematsu, Y.; Miura, T.; Minami, M.; Satoh, S.; Tobita, H., *Macromol. Theory Simul.* **2014**, *23*, 136-146.
75. Zetterlund, P. B.; Kagawa, Y.; Okubo, M., *Chem. Rev.* **2008**, *108*, 3747-3794.
76. Warren, N. J.; Armes, S. P., *J. Am. Chem. Soc.* **2014**, *136*, 10174-85.
77. Zheng, G. H.; Pan, C. Y., *Macromolecules* **2006**, *39*, 95-102.
78. Gody, G.; Maschmeyer, T.; Zetterlund, P. B.; Perrier, S., *Macromolecules* **2014**, *47*, 3451-3460.
79. Compañ, V.; Tiemblo, P.; García, F.; García, J. M.; Guzmán, J.; Riande, E., *Biomaterials* **2005**, *26*, 3783-3791.
80. Pedley, D. G.; Skelly, P. J.; Tighe, B. J., *Brit. Polym. J.* **1980**, *12*, 99-110.
81. Gould, F. E.; Shephered, T. H. Zero order release constant elution rate drug dosage. US 3641237 A, 1972.
82. Efe, H.; Bicen, M.; Kahraman, M. V.; Kayaman-Apohan, N., *J. Braz. Chem. Soc.* **2013**, *24*, 814-820.
83. Bennour, S.; Louzri, F., *Adv. Chem.* **2014**, *2014*, 10.
84. Bencini, M.; Ranucci, E.; Ferruti, P.; Manfredi, A.; Trotta, F.; Cavalli, R., *J. Polym. Sci. A Polym. Chem.* **2008**, *46*, 1607-1617.
85. Zhang, L.; Eisenberg, A., *Science* **1995**, *268*, 1728-1731.
86. Jain, S.; Bates, F. S., *Science* **2003**, *300*, 460-464.
87. Canning, S. L.; Smith, G. N.; Armes, S. P., *Macromolecules* **2016**, *49*, 1985-2001.
88. Pei, Y.; Lowe, A. B.; Roth, P. J., *Macromol. Rapid. Commun.* **2017**, *38*, 1600528-n/a.
89. Delaittre, G.; Nicolas, J.; Lefay, C.; Save, M.; Charleux, B., *Chem. Commun.* **2005**, *5*, 614-6.
90. Rieger, J.; Osterwinter, G.; Bui, C.; Stoffelbach, F.; Charleux, B., *Macromolecules* **2009**, *42*, 5518-5525.
91. Katchalsky, A.; Eisenberg, H., *J. Polym. Sci.* **1951**, *6*, 145-154.
92. An, Z.; Shi, Q.; Tang, W.; Tsung, C.-K.; Hawker, C. J.; Stucky, G. D., *J. Am. Chem. Soc.* **2007**, *129*, 14493-14499.
93. Semsarilar, M.; Jones, E. R.; Blanazs, A.; Armes, S. P., *Adv. Mater.* **2012**, *24*, 3378-82.

94. Boissé, S.; Rieger, J.; Pembouong, G.; Beaunier, P.; Charleux, B., *J. Polym. Sci. A Polym. Chem.* **2011**, *49*, 3346-3354.
95. Gonzato, C.; Semsarilar, M.; Jones, E. R.; Li, F.; Krooshof, G. J.; Wyman, P.; Mykhaylyk, O. O.; Tuinier, R.; Armes, S. P., *J. Am. Chem. Soc.* **2014**, *136*, 11100-6.
96. Semsarilar, M.; Ladmiral, V.; Blanazs, A.; Armes, S. P., *Polym. Chem.* **2014**, *5*, 3466.
97. Wan, W.-M.; Pan, C.-Y., *Macromolecules* **2007**, *40*, 8897-8905.
98. Wang, G.; Schmitt, M.; Wang, Z.; Lee, B.; Pan, X.; Fu, L.; Yan, J.; Li, S.; Xie, G.; Bockstaller, M. R.; Matyjaszewski, K., *Macromolecules* **2016**, *49*, 8605-8615.
99. Konkolewicz, D.; Magenau, A. J. D.; Averick, S. E.; Simakova, A.; He, H.; Matyjaszewski, K., *Macromolecules* **2012**, *45*, 4461-4468.
100. Jakubowski, W.; Min, K.; Matyjaszewski, K., *Macromolecules* **2006**, *39*, 39-45.
101. Magenau, A. J. D.; Strandwitz, N. C.; Gennaro, A.; Matyjaszewski, K., *Science* **2011**, *332*, 81-84.
102. Minami, H.; Kagawa, Y.; Kuwahara, S.; Shigematsu, J.; Fujii, S.; Okubo, M., *Des. Monomers Polym.* **2004**, *7*, 553-562.
103. Barrett, K. E. J., *Dispersion Polymerization in Organic Media*. Wiley: London: 1975.
104. McAllister, T. D.; Farrand, L. D.; Howdle, S. M., *Macromol. Chem. Phys.* **2016**, *217*, 2294-2301.
105. Andrews, R. J.; Grulke, E. A., Glass Transition Temperatures of Polymers. In *Polymer Handbook Fourth Edition*, Brandup, J.; Immergut, E. H.; Grulke, E. A., Eds. 1999; Vol. 1, p 193.
106. Cai, W.; Wan, W.; Hong, C.; Huang, C.; Pan, C., *Soft Matter* **2010**, *6*, 5554.
107. Wan, W.-M.; Pan, C.-Y., *Polym. Chem.* **2010**, *1*, 1475.
108. Wan, W. M.; Sun, X. L.; Pan, C. Y., *Macromol. Rapid Commun.* **2010**, *31*, 399-404.
109. He, W.-D.; Sun, X.-L.; Wan, W.-M.; Pan, C.-Y., *Macromolecules* **2011**, *44*, 3358-3365.
110. Keller, R. N.; Wycoff, H. D.; Marchi, L. E., Copper(I) Chloride. In *Inorganic Syntheses*, John Wiley & Sons, Inc.: 2007; pp 1-4.
111. Huan, K.; Bes, L.; Haddleton, D. M.; Khoshdel, E., *J. Polym. Sci. A Polym. Chem.* **2001**, *39*, 1833-1842.
112. Zhang, X.; Matyjaszewski, K., *Polym. Prepr.* **1999**, *40*, 440-441.

113. Zhou, K.; Wang, Y.; Huang, X.; Luby-Phelps, K.; Sumer, B. D.; Gao, J., *Angew. Chem. Int. Ed.* **2011**, *50*, 6109-6114.
114. Li, H.-J.; Du, J.-Z.; Liu, J.; Du, X.-J.; Shen, S.; Zhu, Y.-H.; Wang, X.; Ye, X.; Nie, S.; Wang, J., *ACS Nano* **2016**, *10*, 6753-6761.
115. Li, Y.; Wang, Z.; Wei, Q.; Luo, M.; Huang, G.; Sumer, B. D.; Gao, J., *Polym. Chem.* **2016**, *7*, 5949-5956.
116. Zhu, L.; Powell, S.; Boyes, S. G., *J. Polym. Sci. A Polym. Chem.* **2015**, *53*, 1010-1022.
117. Wang, K.; Song, Z.; Liu, C.; Zhang, W., *Polym. Chem.* **2016**, *7*, 3423-3433.
118. Chalmers, B. A.; Magee, C.; Aldabbagh, F., Unpublished results.
119. Müller, V. E.; Dinges, K.; Graulich, W., *Makromol. Chem.* **1962**, *57*, 27-51.
120. Müller, V. E.; Thomas, H., *Angew. Makromol. Chem.* **1973**, *34*, 111-133.
121. Eritsyan, M. L.; Barsegyan, Z. B.; Karamyan, R. A.; Manukyan, S. M.; Karapetyan, T. D.; Martirosyan, K. A., *Russ. J. Appl. Chem.* **2011**, *84*, 1257.
122. Baltieri, R. C.; Innocentini-Mei, L. H.; Tamashiro, W. M. S. C.; Peres, L.; Bittencourt, E., *Eur. Polym. J.* **2002**, *38*, 57-62.
123. Böhme, H.; Hartke, K., *Chem. Ber.* **1960**, *93*, 1305-1309.
124. Böhme, H.; Backhaus, P., *Liebigs Ann.* **1975**, *1975*, 1790-1796.
125. Chalmers, B. A.; Alzahrani, A.; Hawkins, G.; Aldabbagh, F., *J. Polym. Sci. A Polym. Chem.* **2017**, *55*, 2123-2128.
126. Porzelle, A.; Williams, C. M., *Synthesis (Stuttg)* **2006**, *18*, 3025-3030.
127. Heaney, H.; Papageorgiou, G.; Wilkins, R. F., *Tetrahedron* **1997**, *53*, 2941-2958.
128. Gody, G.; Maschmeyer, T.; Zetterlund, P. B.; Perrier, S., *Macromolecules* **2014**, *47*, 639-649.
129. Vandenbergh, J.; Junkers, T., *Macromolecules* **2014**, *47*, 5051-5059.
130. Du, J.; Willcock, H.; Patterson, J. P.; Portman, I.; O'Reilly, R. K., *Small* **2011**, *7*, 2070-2080.
131. Valade, D.; Jeon, Y.; Kessel, S.; Monteiro, M. J., *J. Polym. Sci. A Polym. Chem.* **2012**, *50*, 4762-4771.
132. Abel, B. A.; McCormick, C. L., *Macromolecules* **2016**, *49*, 465-474.
133. Abel, B. A.; McCormick, C. L., *Macromolecules* **2016**, *49*, 6193-6202.
134. Blanazs, A.; Armes, S. P.; Ryan, A. J., *Macromol. Rapid Commun.* **2009**, *30*, 267-277.

135. Mai, Y.; Eisenberg, A., *Chem. Soc. Rev.* **2012**, *41*, 5969-5985.

136. Dan, N.; Safran, S. A., *Adv. Colloid Interface Sci.* **2006**, *123*, 323-331.

Publications

RAFT Polymerization in Supercritical Carbon Dioxide Based on an Induced Precipitation Approach: Synthesis of 2-Ethoxyethyl Methacrylate/Acrylamide Block Copolymers

Gerard Hawkins, Per. B. Zetterlund, Fawaz Aldabbagh,

Journal of Polymer Science Part A: Polymer Chemistry, **2015**, *53*, 2351-2356.

Efficient Synthesis and RAFT Polymerization of the Previously Elusive *N*-[(Cycloalkylamino)methyl]acrylamide Monomer Class

Benjamin A. Chalmers, Abdullah Alzahrani, Gerard Hawkins, Fawaz Aldabbagh

Journal of Polymer Science Part A: Polymer Chemistry, **2017**, *55*, 2123-2128.

Conference Proceedings

RAFT Polymerization of *N*-[(Cycloalkylamino)methyl]Acrylamides giving pH-Responsive Polyacrylamide Block Copolymer Vesicles

XVIIth International Conference on Heterocycles in Bioorganic Chemistry, Galway, Ireland, May 28-31, 2017. **Best Student Poster Award** P.O 16

Gerard Hawkins, Benjamin A. Chalmers, Abdullah Alzahrani, Fawaz Aldabbagh.

RAFT Polymerizations of *N*-[(Cycloalkylamino)methyl]Acrylamides giving pH-Responsive Polyacrylamide Block Copolymer Vesicles

Gerard Hawkins, Benjamin A. Chalmers, Abdullah Alzahrani, Fawaz Aldabbagh*

School of Chemistry, National University of Ireland, Galway, Ireland

G.Hawkins1@nuigalway.ie; *Fawaz.Aldabbagh@nuigalway.ie

NUI Galway
OÉ Gaillimh

Monomer Synthesis

Methylene Schiff base salts allow the facile preparation of *N*-[(cycloalkylamino)methyl]acrylamides (where cycloalkylamino are the saturated nitrogen heterocycles (SNHs): morpholine, piperidine and pyrrolidine).[1] The aminal is quarternized using acetyl chloride, forming the Schiff base salt *in situ*. Nucleophilic addition of acrylamide forms the monomer HCl salt, which is then basified to give the monomer.

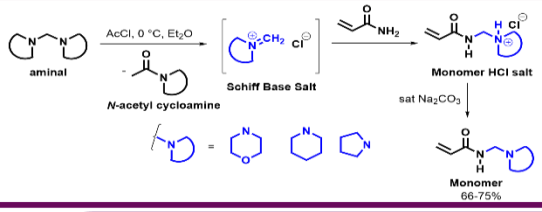

Reversible Addition Fragmentation Chain Transfer (RAFT)

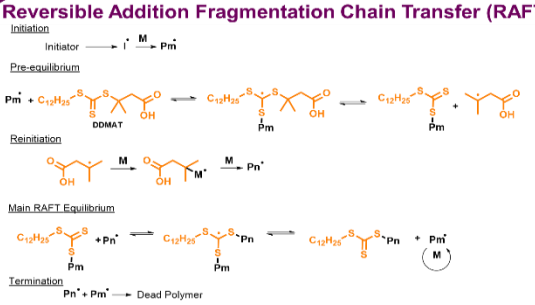

Reversible addition-fragmentation chain transfer (RAFT) is one of the most versatile methods for controlling radical polymerization.[2] The RAFT process follows a degenerative transfer mechanism, where a source of radicals (a radical initiator) is required. It is advantageous to use small amounts of initiator and short polymerization times, since bimolecular termination directly corresponds to the number of radicals generated from the decomposition of the initiator during the polymerization. Termination leads to an unwanted broadening in molecular weight distributions (MWDs), but does not lead to a loss of "living" chains. The number of living chains (substituted by the trithiocarbonate end group) remains constant throughout the polymerization. Ideally, superior controlling character and efficient block copolymer sythesis is achieved when the vast majority of chains originate from the RAFT agent rather than the initiator.

Synthesis of Amphiphilic Diblock Copolymers

The morpholine monomer was polymerized using DDMAT and AIBN as RAFT agent and intiator respectively to give macroRAFT. The macroRAFT was chain extended with further morpholine monomer and *tert*-butyl acrylamide to give amphiphilic block copolymer that self-assembled into large rod-like vesicles of ~13 μm in length.

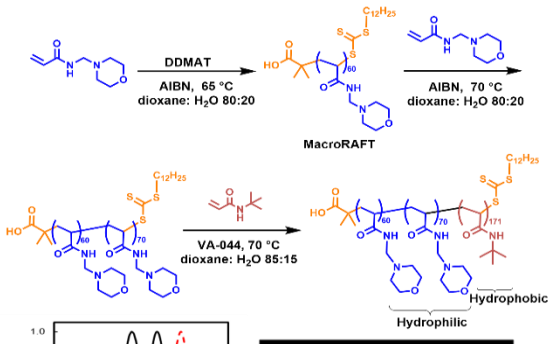

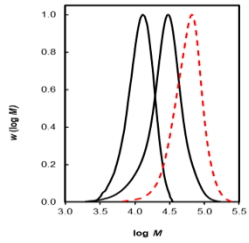

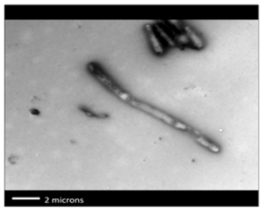

GPC MWDs of morpholine-containing blocks (black solid lines) and *tert*-butyl acrylamide (red dashed line) diblock copolymer prior to precipitation and TEM of corresponding precipitated and dialysed block copolymer.

pH-Expandable Nanoparticles

The triblock was prepared by sequential chain extensions of the macroRAFT with the piperidine monomer and *tert*-butyl acrylamide. This led to the formation of spherical particles of uniform size. These particles can be expanded with the addition of acid, which protonates the SNHs, making the particles less hydrophobic.

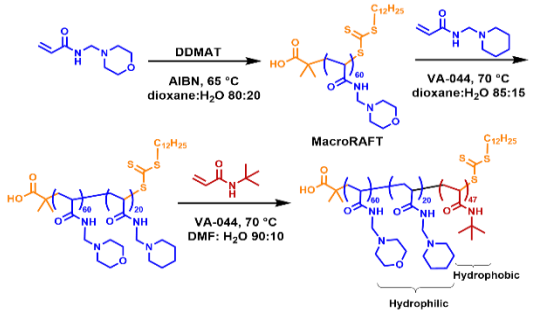

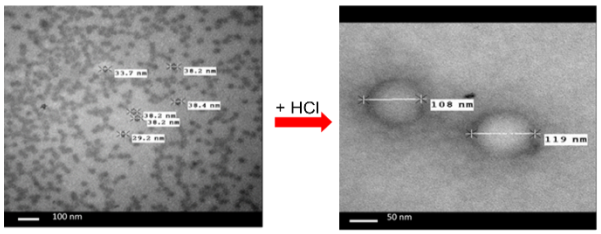

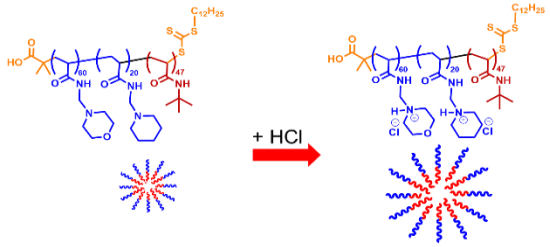

Average Size = 30 nm
Uniform Particle Distribution

Average Size = 115 nm
Expanded Particles

Conclusions

- RAFT has allowed the efficient preparation of the first well-defined block copolymers of this monomer class.
- Self-assembly gave large rod-like vesicles for amphiphilic morpholine-containing diblock copolymers.
- For the triblock containing the piperidine monomer very different aggregation was obtained with pH-expandable nanoparticle spheres observed.

References

1. B. A. Chalmers, A. Alzahrani, G. Hawkins, and F. Aldabbagh, *J. Polym. Sci., Part A: Polym. Chem.*, **2017**, *55*, 2123-2128
2. J. Chieftari, Y. K. Chong, G. Ercole, J. Krstina, J. Jeffery, T. P. T. Le, R. T. A. Mayadunne, G. F. Meijs, C. L. Moad, G. Moad, E. Rizzardio, and S. H. Thang, *Macromolecules*, **1998**, *31*, 5559-5562

XVIIth International Conference on Heterocycles in Bioorganic Chemistry
Galway, Ireland, May 28-31, 2017

Bioheterocycles

Best Student Poster Award

is hereby granted to:

Gerard Hawkins

In recognition of a first prize in the poster competition as judged by representatives named by the Bioheterocycles Organizing Committee.

This Award is made possible by Royal Society of Chemistry.

NUI Galway
OÉ Gaillimh

ROYAL SOCIETY OF CHEMISTRY

Dr. Tawaz Aldabbagh, National University of Ireland Galway
Chairman of Bioheterocycles 2017

Prof. Jan Bergman, Karolinska Institutet
Chairman of the Scientific Committee